REGULATION OF *P. AERUGINOSA* TWITCHING MOTILITY

cAMP-INDEPENDENT AND DEPENDENT REGULATION OF *PSEUDOMONAS AERUGINOSA* TWITCHING MOTILITY

By

RYAN NICHOLAS CARLOS BUENSUCESO, B.Sc., M.Sc.

A Thesis Submitted to the School of Graduate Studies in Partial Fulfillment of the Requirements for the Degree

Doctor of Philosophy

McMaster University DOCTOR OF PHILOSOPHY (2016)
Hamilton, Ontario (Biochemistry and Biomedical Sciences)

TITLE: cAMP-independent and dependent regulation of *Pseudomonas aeruginosa* twitching motility

AUTHOR: Ryan N.C. Buensuceso, B.Sc. (McGill University), M.Sc. (The University of Western Ontario)

SUPERVISOR: Dr. Lori L. Burrows

NUMBER OF PAGES: xvii, 197

LAY ABSTRACT

Pseudomonas aeruginosa is a bacterium that causes infection in people with weakened immune systems. One key factor it uses to cause infection is the type IVa pilus (T4aP), a filamentous appendage displayed on the cell surface. T4aP can repeatedly extend and retract, and are involved in attachment to host cells, and movement along surfaces. When T4aP cannot extend or retract, the bacteria cannot cause infection. Many proteins work together to control T4aP function – this study focuses on two of them. They have one overlapping function, controlling levels of a signalling molecule needed to make T4aP. We also show that they have a second, non-overlapping function. One is involved in controlling the extension/retraction balance, possibly by marking the front of a cell, while the other may localize pilus-related proteins within a cell. This work helps us understand how *P. aeruginosa* makes T4aP, and provides information helpful to understanding control of virulence.

ABSTRACT

Type IVa pili (T4aP) are long, retractile, filamentous, surface appendages involved in cellular surface adhesion, biofilm formation, DNA uptake, and a unique form of motility called 'twitching'. They are a critical virulence factor in a number of bacteria, including the opportunistic pathogen *Pseudomonas aeruginosa,* a major cause of hospital-acquired infections. T4aP function is controlled by a number of different regulatory proteins and systems. A putative chemosensory system termed 'Chp', controls levels of the second messenger molecule cyclic adenosine monophosphate (cAMP). cAMP works with a cAMP receptor protein called Vfr to control expression of ~200 virulence genes, including those that are required to make T4aP. cAMP levels are regulated by proteins outside the Chp system, including the bitopic inner membrane protein, FimV. This study examines the role of the Chp system and FimV in T4aP regulation. Both proteins are required for regulation of cAMP levels, while the Chp system also has a cAMP-independent role in regulating twitching. FimV has been shown to regulate cAMP levels, possibly connecting to the Chp system through a scaffold protein, FimL. We present the structure of a conserved cytoplasmic region of FimV, and show that this region is required for connecting FimV to the Chp system. We also characterize the cAMP-independent role of FimV, confirming that it is distinct from that of the Chp system, and is involved in localizing T4P regulatory proteins. We

also provide evidence that the cAMP-independent role of the Chp system is to mediate the balance between T4P extension and retraction, possibly through denoting the 'front' of a motile cell. Together, these data help to resolve the cAMP-independent and –dependent pathways controlling twitching motility.

ACKNOWLEDGEMENTS

I would like to thank my supervisor Dr. Lori Burrows for everything over all these years. You've been more supportive than I probably deserved, and given me confidence to keep going when I had none. Without the faith you've shown in me, I would never have been able to make it here. It's easy to say that you've helped me grow as a scientist, but the lessons I've learned in the lab have helped me grow as a person too. I could never thank you enough for being such a wonderful mentor. The lessons I've learned in the lab are ones that I'll carry with me forever.

I would also like to thank my committee members Dr. Brian Coombes and Dr. Lynne Howell, who have pushed me to get this far. You've always helped me to find what I thought were my limits, and given me that extra nudge to get over them. Thank you for challenging me and helping me change the way I think.

This whole experience wouldn't have been the same without the amazing people I've had the utmost pleasure of working with in the Burrows lab. You're all such a wonderful, talented, smart, and hilarious bunch of people. As tough as the grad school life could get, you all made it so much fun, brightening up every day. Hanjeong, Ryan, Tiff, Sara, Uyen, Ylan, Tyson, and Tori, we've spent so many years together, I look at you all like family, and your support has meant everything. We've all shared so many laughs, adventures, and amazing times, I couldn't even begin to list

them all. Thanks for all the memories, and I wish all of you the very best for your (most certainly) bright futures. And a special shout-out to my lab fish Petri… we did it!

To all my friends who've helped me get to here, from Montreal, to London, to Hamilton, you made it all possible. My former labmates from the Koromilas lab at McGill: you trained me when I was an undergrad and got me started on this journey. To my dear friend Elaine Ngan, you've always been there to listen to my rants and given me support when I needed it. We made that pact in CEGEP to always help each other through the tough times – thanks so much for seeing it through. To Jake Dougherty-St. Arnaud, you were one of the best of us – your memory will keep living on. My friends from London: Arthur Lau, Monty McKillop, and Sonali de Chickera, thanks for always keeping my spirits up. Thanks for being amazing friends, even after we've all gone our separate ways.

Of course there are countless friends I've made at McMaster, far too many to list here. From the coffee houses, the wine days, Phoenix trips, and everything in between, you've all helped make my time here loads of fun. Thanks for all the laughs over the years! To the many teammates I've had from McMaster Ultimate Frisbee, thanks for somehow at the same time making me feel young, but always reminding me how much older I was. Everything, from being on the fields, cheering from the

sidelines, the road trips, the bus trips, the hotels, and the “who dats”, it was a blast!

To my family – my amazing parents, brother, and all my cousins, aunts, uncles, and grandparents – you’ve been amazing over all these years. It’s been through your patience, love, and support, that I’ve been able to come this far. You’ve been the best cheering section, and even if I don’t say it often enough, I love you all so much. Lastly, I couldn’t imagine going through all of this without the amazing Jennifer Lau. I can’t believe how lucky I was to meet you so early on in my time at McMaster. You’ve been my rock every step of the way, and an unending source of support. Thanks for being there to celebrate all the highs, and putting up with me through all the lows. I couldn’t have done this without you, so everything in here is just as much yours as it is mine.

TABLE OF CONTENTS

LIST OF FIGURES

CHAPTER FIVE – Conclusions and future directions

LIST OF TABLES

LIST OF ABBREVIATIONS

°C	degree Celsius
A	alanine
ATP	adenosine triphosphate
ATPase	adenosinetriphosphatase
BCIP	5-bromo-4-chloro-3-indolylphosphate
C-terminal	carboxy-terminal
cAMP	cyclic adenosine monophosphate
cdG	cyclic di-guanosine monophposphate
crp	cAMP receptor protein
D	aspartic acid
DGC	diguanylate cyclase
DNA	deoxyribonucleic acid
E	glutamic acid
eYFP	enhanced yellow fluorescent protein
g	gravity
GFP	green fluorescent protein
h	hour(s)
IPTG	isopropyl-β-D-thiogalactopyranoside
kb	kilobases
LB	lysogeny broth
LED	light emitting diode
MASE2	membrane associated sensor 2
MCP	methyl-accepting chemotaxis protein
mg	milligrams
min	minute(s)
mm	millimeters
N	asparagine
N-terminal	amino-terminal
NBT	nitro-blue tetrazolium
NIH	National Institutes of Health
OD	optical density
P/A	proline/alanine
PAGE	polyacrylamide gel electrophoresis
PAK	*Pseudomonas aeruginosa* strain K
PBS	phosphate buffered saline
PCR	polymerase chain reaction
PDB	protein databank
PDE	Phosphodiesterase
PEG	polyethylene glycol
pH	power of hydrogen
s	second(s)
SAD	single wavelength anomalous dispersion

SDS	sodium dodecyl sulfate
SeMet	selenomethionine
T2S	type II secretion
T2SS	type II secretion system
T4aP	type IVa pilus/pili
T4bP	type Ivb pilus/pili
T4P	type IV pilus/pili
TEV	tobacco etch virus
TM	transmembrane
TPR	tetratricopeptide repeat
Vfr	virulence factor regulator
w/v	weight by volume
µm	micrometers

CHAPTER ONE

Introduction

Preface:

Chapter One includes text adapted from the following publication:

Leighton TL*, Buensuceso RNC*, Howell PL, Burrows LL. 2015. Biogenesis of *Pseudomonas aeruginosa* type IV pili and regulation of their function. Environ. Microbiol. 17:4148-4163.

*authors contributed equally.

Sections included here were written primarily by R.N.C.B, P.L.H., and L.L.B.

Introduction

Type IV pili

Type IV pili (T4P) are long, filamentous protein polymers expressed by a broad range of gram positive and gram negative bacteria and archaea (1) (Figure 1.1). They are involved in surface attachment, biofilm formation, DNA uptake, and twitching motility (2-8). T4P are critical virulence factors, as mutants lacking T4P are impaired in pathogenicity (9, 10). Structurally, T4P are large, polar, multi-protein complexes that in gram-negative bacteria, have components in the outer membrane, periplasm, inner membane, and cytoplasm.

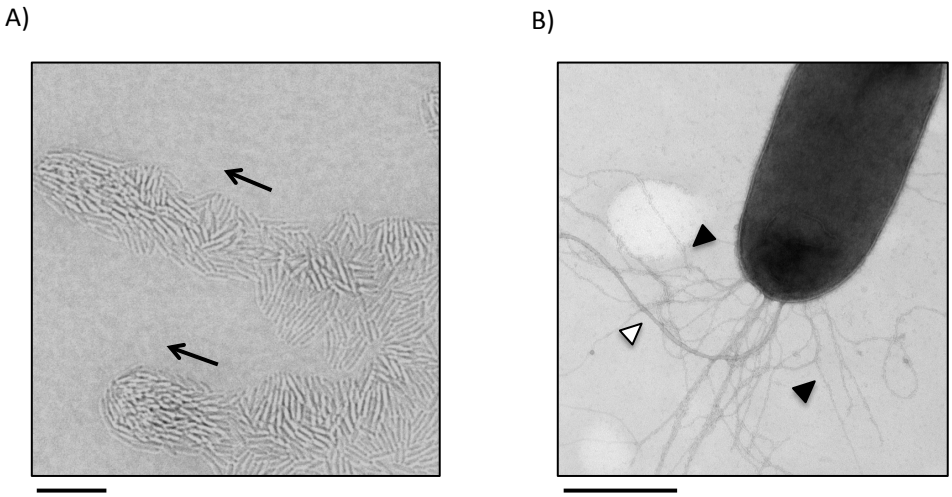

Figure 1.1 – T4aP are polar surface appendages. (A) Representative image of a twitching raft moving away form the point of inoculation. Arrows indicate direction of movement. Scale bar = 10μm. (B) The pole of a *P. aeruginosa pilT* mutant was visualized by transmission electron microscopy. The single, polar flagellum (open arrowhead) is thicker than the numerous T4aP (closed arrowhead). Scale bar = 500 nm.

T4P are important virulence factors in the opportunistic pathogen, *P. aeruginosa*, one of the model organisms for study of T4P biology (11). *P. aeruginosa* is a common cause of nosocomial infection (12, 13). Chronic infection of the lungs with *P. aeruginosa* is common in cystic fibrosis patients, and a major cause of morbidity and mortality in this population (13). T4P play a critical role in the *P. aeruginosa* infection cycle, mediating the initial attachment to biotic surfaces, and are thus integral to biofilm formation (8). Mutants lacking T4P have decreased virulence and are impaired in their ability to adhere to epithelial cells in culture (9).

T4P can be divided into two major subfamilies based on the composition of the pilus fiber and the assembly system: type IVa pili (T4aP) and type IVb pili (T4bP). T4aP are typically associated with twitching motility (7, 14, 15). They can undergo repeated cycles of extension (assembly), adhesion, and retraction (disassembly) to pull a cell along a surface, similar to a molecular grappling hook. T4aP are broadly expressed, and have been well-studied in a number of model organisms including *P. aeruginosa* (11), *Neisseria* spp., and *Myxococcus xanthus,* where species-specific differences in the regulation of twitching motility have been reported (16). In contrast, T4bP are more commonly found in enteric bacteria. Unlike T4aP, they are not usually associated with motility, and often lack a retraction ATPase (7).

Proper T4aP function requires correct assembly of the T4aP structural components, and regulatory input controlling transcription of T4aP assembly proteins, and subcellular asymmetry in protein distribution to promote directional twitching. This thesis describes critical regulators of T4P function and their modes of action.

Overview of twitching motility

T4aP are associated with a flagellar-independent form of movement termed twitching motility, or 'twitching'. Twitching typically occurs on moist, viscous surfaces (7). T4aP on twitching cells undergo repeated cycles of extension (assembly), adherence to a surface, and retraction (disassembly). Although individual cells can twitch, it is generally a social form of motility, in which groups of cells aligned along their long axis move outward at the edge of a colony in projections called 'rafts' (Figure 1.1A) (17). Importantly, not all of the cells within a raft are actively extending and retracting pili simultaneously, and nonmotile strains or even inanimate particles can be transported by twitching rafts (Burrows and Dutcher labs, unpublished data).

The twitching motility function of T4aP has been shown to play an important role in virulence. *P. aeruginosa* retraction-deficient mutants exhibit less cytotoxicity towards epithelial cells (9, 18). Furthermore, *P. aeruginosa* strains bearing mutations in twitching motility signalling

pathways are less lethal in *Drosophila* models (19). The importance of functional T4aP in virulence was further highlighted in *Dichelobacter nodosus*, where it was shown that loss-of-function mutations that abrogated pilus function without affecting piliation resulted in avirulence (20). These data suggest that it is the presence of a functional pilus that imparts virulence, rather than the presence of a pilus in general (20), emphasizing the need to better understand regulators of T4P function.

The T4aP assembly system

The T4aP assembly system of *P. aeruginosa* is composed of four subcomplexes spanning the inner and outer membrane (IM and OM; Figure 1.2). The OM secretin is composed of 14 subunits of PilQ (21) and its pilotin protein PilF. PilF is an outer membrane lipoprotein responsible for localization of PilQ to the OM (22). The pore formed by multimeric PilQ forms a gated channel through which the pilus exits the cell (23). The IM motor subcomplex is composed of a dimer of the platform protein PilC (24), the site of T4P assembly and disassembly, and three cytoplasmic ATPases PilB, PilT, and PilU, which drive extension (PilB) and retraction (PilT and PilU) of the pilus fiber (25-27). The alignment subcomplex, composed of PilMNOP (28, 29), spans the cytoplasm, IM, and periplasm, connecting the IM components and the secretin. The final subcomplex is the pilus fiber itself, composed primarily of the major pilin subunit, PilA.

Prior to incorporation into the fiber, PilA monomers are processed into the mature form by the prepilin peptidase, PilD (30). A subcomplex composed of the minor pilins, PilVWXE and FimU plus the non-pilin protein adhesin PilY1, prime T4P assembly and promote PilY1 exposure on the cell surface (31).

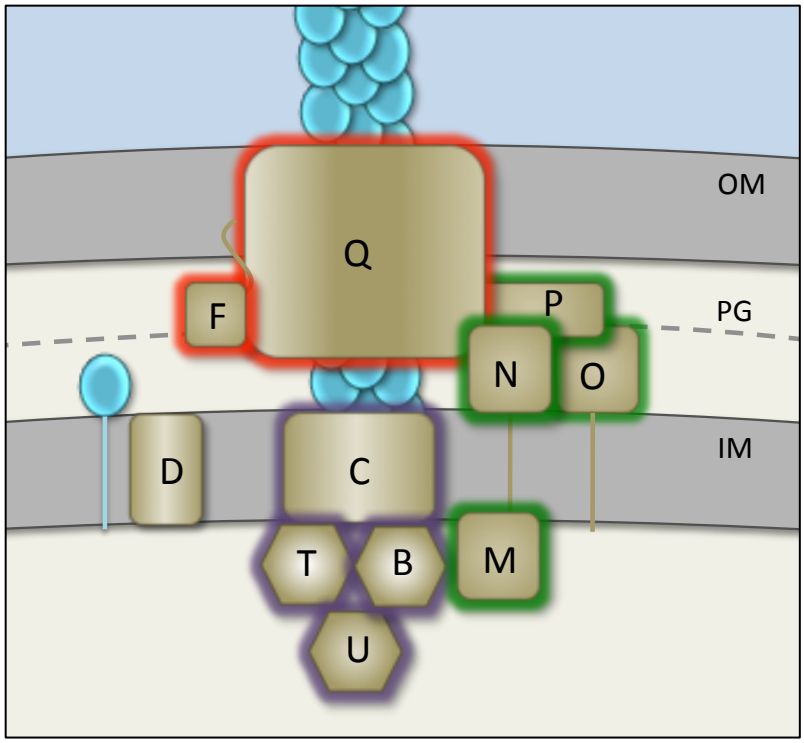

Figure 1.2 – The *P. aeruginosa* T4aP assembly complex. The P aeruginosa T4aP assembly complex can be divided into 4 subcomplexes. The pilus fiber (teal) is composed of major and minor pilin subunits arranged in a helical fashion. The leader sequence at the N-terminus of pilin subunits is cleaved at the cytoplasmic face by the prepilin peptidase PilD. The inner membrane motor subcomplex (purple outline) provides energy for T4P extension and retraction, adding/removing pilins from the fiber. The pilus fiber exits the cell through the outer membrane secretin (red outline). The alignment subcomplex (green outline) connects the

outer membrane and inner membrane components. Abbreviations: OM, outer membrane; PG, peptidoglycan; IM, inner membrane.

The outer membrane secretin

The OM pore is a channel formed by a 14-mer of the secretin monomer, PilQ (21). Like other proteins of the secretin family, PilQ has a periplasmic N-terminal domain, and a C-terminal membrane-embedded secretin domain that forms the IM pore. The periplasmic domain has four distinct subdomains, two tandem species-specific domains that are structurally related to the peptidoglycan-binding AMIN domain of peptidoglycan amidases, followed by N0 and N1 subdomains. PilQ is connected to the alignment complex through an interaction between its N0 domain and the C-terminal β-sandwich domain of PilP. The AMIN domains are likely involved in targeting PilQ to septal PG (32, 33) (Carter et al in preparation). PilQ is shuttled to the OM by its pilotin lipoprotein, PilF (22).

In *Myxococcus xanthus*, multimeric OM secretin was proposed to initiate assembly of the T4aP system. Multimerized secretin recruits alignment sub-complexes, which then recruit the IM motor sub-complex (34). Whether this assembly cascade occurs in *P. aeruginosa* has not yet been shown. However, Carter et al (in preparation) showed that deletion of *pilQ* – but not *pilM* – mislocalizes PilO, confirming that PilQ controls placement of the system at the poles of the cell.

The inner membrane motor complex

Energy for T4aP extension and retraction is provided by hydrolysis of ATP by cytoplasmic ATPases arranged in a homohexamer. The T4P motor ATPases belong to the Additional Strand Catalytic E (ASCE) superfamily of ATPases. ASCE ATPase monomers are two domain proteins, separated by a linker region. The C-terminal domain contains the Walker A and Walker B motifs associated with ATP binding and hydrolysis and the N-terminal domain of PilT and PilU are associated with ATPase localization (35).

Most T4aP systems have two ATPases, but *P. aeruginosa* has 3 ATPases that are all required for twitching – PilB, PilT, and PilU (25-27). All three ATPases interact directly with PilC (24, 36), although deletion of *pilC* mislocalized PilB but not PilT or PilU (35). PilB and PilT function in extension and retraction respectively, evidenced by surface piliation levels reflective of extension deficient (non-piliated) and retraction deficient (hyperpiliated) states (25, 26).

Two models for ATPase function have been recently proposed. Mancl et al. solved the crystal structure of *Thermus thermophilus* PilB bound to ATP (37). Monomers worked in tandem with the monomer on the opposite side of the hexamer. Hydrolysis of ATP leads to structural changes that appear to push pilin monomers into the growing fiber. McCallum and colleagues also recently solved the crystal structure of PilB

from *Geobacter metalloreducens* bound to either ADP or the non-hydrolyzable ATP analogue, AMP-PNP (McCallum el al. submitted). They propose an alternate model, where ATP hydrolysis rotates PilC while inserting or removing pilins from the filament.

The role of PilU is currently unknown. Unlike *pilB* and *pilT*, *pilU* mutants have near wild-type levels of surface pili and are sensitive to killing by pilus-specific bacteriophage, which requires functional pili (27). Interestingly, PilU is the only one of the ATPases that has unipolar localization – PilB and PilT are both bipolar (35). The asymmetry created by PilU may allow the cell to distinguish between leading and lagging poles, to impart directionality for movement.

The alignment subcomplex

The T4P alignment subcomplex spans the cytoplasm, inner membrane, and periplasm, and connects the OM secretin to the inner membrane motor subcomplex. It is comprised of the cytoplasmic protein PilM, the bitopic inner membrane proteins PilN and PilO (38), and the lipoprotein PilP, all encoded in a polycistronic operon with *pilQ* (29). The alignment complex components are hypothesized to be in a 1:1:1:1 ratio with monomers of the PilQ 14-mer (39). PilN and PilO are predicted to be structurally similar, with their core domains in the periplasm, a single transmembrane segment, and a short N-terminal cytoplasmic domain (38).

Leighton et al. recently showed simultaneous formation of PilN and PilO hetero- and homodimerization, arranged as a heterodimer of homodimers (40). Cytoplasmic PilM binds to the N-terminus of PilN (41), while the N-terminus of PilO has no known binding partners. PilM also interacts with both PilB and PilT, further suggesting a connection between the alignment complex and T4aP extension and retraction (36).

Several roles have been proposed for the alignment subcomplex. It may align the IM and OM components of the T4aP assembly complex, allowing for efficient extension of the T4aP from the motor subcomplex to the secretin (39). It may also function as a 'cage' at the IM, locally concentrating pilin subunits that have either not yet been assembled into the pilus fiber, or have been disassembled from the fiber following T4aP retraction to improve the efficiency of polymerization (39). Recently, Leighton et al. showed using disulfide bond analysis, perturbation of specific interaction interfaces within the PilN and PilO heterodimer of homodimers could impair pilus assembly and twitching (40, 42). It was proposed that domain movements in PilM are transduced through PilN and PIlO, ultimately leading to a movement in PilO.

The pilus fiber

The pilus fiber is a ~6nm diameter helical protein filament extending from the pole(s) of a cell, through the OM PilQ secretin. It is composed of

thousands of copies of the major pilin subunit, PilA. The pilins are characterized by their hydrophobic N-terminal alpha helix, and a globular C-terminal head group. The hydrophobic N-terminus is preceded by a short leader sequence containing a unique cleavage site for the dedicated PilD pre-pilin peptidase, which removes the leader at the cytoplasmic face of the inner membrane to produce mature pilins (30).

At the tip of the pilus fiber is a complex of pilin-like proteins termed the ‘minor’ pilins which are encoded in a polycistronic operon, *fimUpilVWXE*, with the non-pilin protein, PilY1 (43-45). The minor pilins are proposed to form a complex that primes T4aP assembly (31): PilVWX and PilY1 form an initial complex that recruits PilE, which together with FimU, connects the minor pilin complex to the major pilin, PilA. Additional PilA subunits are then incorporated into the fiber at its base, producing a helical filament several microns in length.

Several functions have been ascribed to PilY1. It has been proposed to be an adhesin (46), contributing to T4P-mediated surface attachment; a calcium-dependent anti-retraction factor (47), and more recently, a surface sensor (48). PilY1 contains a mechanically sensitive von Willebrand Factor A (vWFa) domain near its amino terminus (48), whose deformation of the vWFa domain upon surface binding has been proposed to initiate a surface-activated virulence program.

Regulation of twitching motility

In addition to the T4P assembly system, other proteins have been identified that contribute to T4P dynamics in *P. aeruginosa* through other regulatory or structural means. Transcription of the genes encoding the alignment complex proteins PilMNOP, the OM secretin PilQ, and the ATPases, are all dependent on a transcriptional regulator called Vfr (virulence factor regulator), which binds the second messenger molecule, cyclic adenosine monophosphate (cAMP) (49). Levels of cAMP are in turn regulated by signalling through a putative chemosensory system related to the *E. coli* Che system, termed 'Chp' (50-52), but also through other cAMP-regulatory proteins, including the inner membrane protein FimV (53), and the cytoplasmic protein FimL (54). All these proteins appear to control the activity of the major adenylate cyclase, CyaB (55, 56). In addition to these systems are regulatory proteins such as two-component system (TCS), PilSR, that regulates pilin gene expression in response to pilin levels in the membrane (57), and the cyclic-di-GMP regulatory pathway that controls the switch between motility and sessility. Twitching motility is thus controlled by a complex regulatory network; however, how these systems intersect is still unclear.

Response regulator networks

At the core of most bacterial chemotactic pathways is the two-component histidine kinase-response regulator relationship. Activity of the kinase in these systems is controlled in response to environmental signals, which regulate its autophosphorylation. In its simplest form, the kinase then transfers the phosphate group to its cognate response regulator, leading to the output of the signalling system (58, 59).

Response regulators typically have a receiver (REC) domain containing a conserved aspartate residue that is phosphorylated by the histidine kinase, although phosphorylation at alternative sites is possible (60, 61). Phosphorylation leads to a change in conformation and the signalling response. While most response regulators have a dedicated output domain (62), single domain response regulators that mediate chemotactic responses often do not. For example, the *E. coli* chemotaxis response regulator, CheY, interacts with the flagellar switch complex to change the direction of flagellum rotation (63).

Signal termination is an important component of TCS that allows control over the signalling response. Phosphorylated response regulators can undergo a basal level of auto-dephosphorylation. However, given the slow rate of dephosphorylation, other proteins are involved in signal termination. Dedicated phosphatases such as CheZ of the *E. coli* Che system (64), or histidine kinases with phosphatase activity such as PilS of the PilSR system controlling *pilA* transcription (65), can actively remove

the phosphate group from the response regulator, and are the most common forms of signalling control. Some systems lack a dedicated phosphatase and instead use a second response regulator-like protein as a phosphate sink (66, 67). Data from the *S. meliloti* system shows that in addition to response regulator dephosphorylation, there is also reverse phosphorylation from the response regulator to the histidine kinase (67). The phosphate sink is characterized by a high phosphorylation rate and low reverse phosphorylation rate (67, 68).

Chemotactic regulation of motility

Chemotactic clusters represent a more complex form of the two-component system. While a histidine kinase-response regulator system is at its core, the chemotaxis system builds on this by adding ligand sensors, adaptation proteins, adapters, and movement-based signalling output. Taxis sytems allow bacteria to respond to different environmental cues through movement (69-71). This allows to cell to move towards favorable, or away from unfavorable conditions.

One of the best studied taxis systems is the Che chemotaxis system of *E. coli*. This system allows the cell to sense changes in the cell's chemical environment, and respond by altering the direction of flagellar rotation. It consists of methyl-accepting chemotaxis proteins (MCPs) that sample the cell's chemical environment. MCPs are inner membrane

proteins arranged as trimers of dimers (72-74), with large periplasmic loops for sensing specific chemical ligands, and a large cytoplasmic domain. The cytoplasmic domain can be divided into 4 functional domains (75): a histidine kinase, adenylyl cyclase, methyl-binding protein and phosphatase (HAMP) domain, a methylation helix, a signaling domain, and a second methylation helix. The *E. coli* system has 5 well-known MCPs that respond to different signals, Tar, Tsr, Trg, Tap, and Aer (76). In response to the appropriate signal, changes in conformation in the cytoplasmic domain are transmitted through an adapter protein, CheW, to a histidine kinase, CheA (73, 77-79). CheA phosphorylates the response regulator CheY (80), which then interacts with the flagellar switch complex protein, FliM, to reverse the direction of flagellar rotation (81). Levels of phosphorylated CheY are controlled by the phosphatase CheZ (82). As the cell moves along the concentration gradient, adaptation of the system is mediated by differential methylation of the MCP by the CheR methyltransferase, and CheB methylesterase (83-85).

The Chp cluster

The Pil-Chp cluster (Chp) is one of four putative chemotactic clusters in *P. aeruginosa*, and the only one that controls twitching motility (50, 51). The Chp system encodes components homologous to those of the well-studied *E. coli* Che system that controls flagellar rotation

(reviewed by (86); Figure 1.3). By analogy, the Chp system of *P. aeruginosa* encodes one MCP, PilJ, whose ligand(s) is unknown but may include phosphatidylethanolamine or PilA (87, 88). PilK and ChpB are homologous to CheR and CheB, respectively, and are thus predicted to be responsible for methylation and demethylation (50, 51, 89). PilI and ChpC are both CheW homologs, although the role of ChpC is unclear. Only deletion of PilI impairs twitching motility; however, ChpC has been hypothesized to function as an adaptor that might couple other MCPs to the Chp system (50). ChpA is a large, complex ortholog of CheA containing nine potential sites of phosphorylation, although only two have been experimentally demonstrated to participate in the majority of phosphotransfer to PilG and PilH (90, 91).

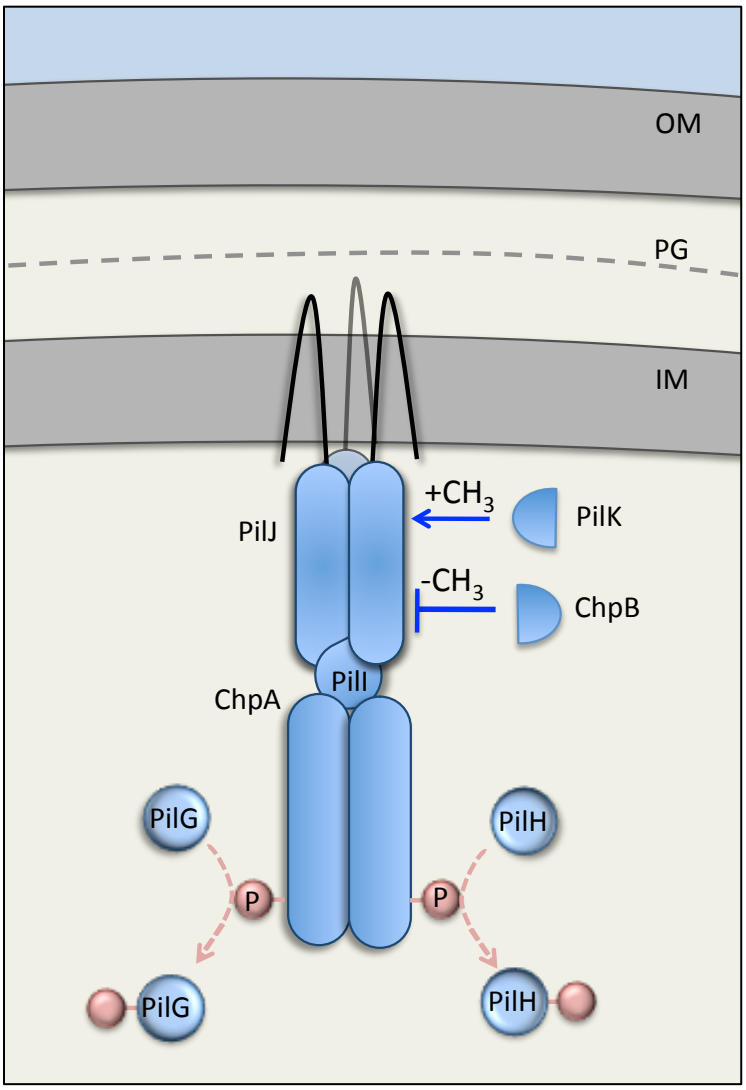

Figure 1.3 – Schematic of the *P. aeruginosa* Chp system. The Chp system encodes one putative MCP, PilJ (shown as a trimer based on it being a predicted MCP (51, 74)). It is connected to the histidine kinase, ChpA, via the PilI adapter. Upon stimulation, ChpA undergoes autophosphorylation, ultimately transferring the phosphate group to response regulators, PilG or PilH. PilK and ChpB methylate and demethylate PilJ to adapt to changes in concentration along a chemical gradient. Abbreviations: OM, outer membrane; PG, peptidoglycan; IM, inner membrane.

One major difference between the Chp system and the canonical Che system comes at the level of the response regulator. Instead of a single CheY-like response regulator and a CheZ-like phosphatase, the *chp* cluster encodes two CheY-like single domain response regulators, PilG and PilH, both of which can be phosphorylated by ChpA (51, 92), although phosphotransfer to PilH appears to be favoured (91). The two response regulator configuration mirrors that of the CheY system of *Sinorhizobium meliloti,* which also lacks a CheZ-like phosphatase (63). Two possible modes of action for the PilG/PilH system have been proposed. Inclan et al. (93) hypothesized that PilG and PilH control extension and retraction by regulating activity of PilB and PilT, respectively. Alternatively, PilH has been proposed to be a phosphate sink that could attenuate Chp signaling in lieu of a phosphatase (55). Signaling through the Chp pathway is required for twitching motility and surface piliation. Notably, deletion of *pilG, pilJ*, *chpA*, or *pilI* results in significantly reduced levels of surface pili, suggesting that all are involved in pilus biogenesis (51, 90, 92, 94). However, signaling output from the Chp system is not absolutely required for T4aP extension and retraction, as *pilG* and *pilH* mutants are both susceptible to lysis by pilus-specific phage (93), although deletion of either leads to impaired twitching (51, 92, 93).

The Chp system was hypothesized to be similar to the Frz system controlling T4aP-dependent social motility in *Myxococcus xanthus* (50, 95).

The FrzZ response regulator is a fusion of two CheY domains, and was hypothesized to mirror the PilG/PilH system (50, 96). The remainder of the upstream Frz chemotaxis machinery is similar to the Chp and Che systems (50, 97). The Frz system controls cellular reversals (98), switching the localization of the GTPases MglA and MglB, causing the ATPases to switch poles as well. However, unlike *P. aeruginosa*, *M. xanthus* only encodes two ATPases, PilB and PilT, and lacks a functional PilU analog (99). Unlike the bipolar localization of extension and retraction ATPases in *P. aeruginosa* (35), *M. xanthus* PilB and PilT are localized to the leading and lagging poles, respectively (100). Whether the Chp system is also involved in cellular reversals is unclear, however, the only unipolar ATPase of *P. aeruginosa,* PilU, does not switch poles following cellular reversals (Cynthia Whitchurch, personal communication).

In addition to its role in regulating twitching, the Chp system is also a key regulator of cAMP through activation of the major adenylyl cyclase, CyaB (described in section 1.3.5.1) (55). It also plays a role in a proposed mechanosensory pathway controlling virulence (described in section 1.5) (88, 89).

Small molecule messenger-based regulation of twitching

In *P. aeruginosa*, twitching motility and T4aP function are regulated by a number of different signalling inputs. Both cAMP and c-di-GMP

regulate motility, as well as virulence and biofilm formation (49, 101). In turn, levels of cAMP and c-di-GMP are regulated by the coordinated signaling input from a number of proteins (55, 102, 103). Small molecule signalling is central to the proposed models of T4aP-based mechanosensing that control virulence (89), with c-di-GMP promoting the switch from motile to sessile lifestyles, and cAMP activating the *P. aeruginosa* virulence program (55).

Cyclic AMP

cAMP is a critical second messenger molecule that plays important roles in signal transduction in many organisms, from prokaryotes to eukaryotes (104). Intracellular cAMP levels are maintained by adenylyl cyclases, which generate cAMP from adenosine triphosphate (ATP). Conversely, cAMP is degraded into AMP by phosphodiesterases (PDEs). Intracellular cAMP exerts its effects through cAMP receptor proteins (CRPs). CRPs are often transcription factors, which upon cAMP binding, undergo a conformational change and bind to specific DNA sequences.

P. aeruginosa encodes 3 adenylyl cyclases, ExoY, CyaA, and CyaB (49, 105). ExoY is a class II exotoxin secreted by the type 3 secretion system. In contrast, CyaA and CyaB are membrane-bound adenylyl cyclases that maintain the intracellular cAMP pool (55, 106). CyaA belongs to class I, which is typically associated with bacterial regulation of

nutrient utilization, although its specific role in *P. aeruginosa* is unclear (49, 107). CyaB is the major contributor to the cAMP pool (49, 55). It is a class IIIb adenylyl cyclase (107). Class III adenylyl cyclases have at least one regulatory domain fused to the catalytic domain (108). CyaB has a 6 transmembrane segment associated sensor 2 (MASE2) domain (109) that is required for CyaB function, which likely tethers it to the cell pole although its role is unknown (107, 109). Intracellular cAMP in *P. aeruginosa* binds to the CRP, Vfr (virulence factor regulator) (110). cAMP-Vfr alters the transcription of ~200 virulence-related genes, including the the T4P alignment subcomplex and secretin (*pilMNOPQ*), and the minor pilin (*fimU-pilVWXY1Y2E*) operons. Intracellular cAMP levels are also controlled by the cAMP phosphodiesterase, CpdA (111).

Fulcher et al. (55) described a cAMP regulatory circuit controlled by the Chp system (Figure 1.4). The levels of intracellular cAMP were proposed to control pilus extension, as mutants with low levels of cAMP (e.g. *cyaAB*, *pilG*) had little or no recoverable surface pili (55). Supplementation of the growth medium with exogenous cAMP restored wild-type levels of surface pili but not twitching to a *pilG* mutant, suggesting an additional cAMP-independent role of the Chp pathway in twitching motility, likely in pilus retraction (55). Surface pili were also required for cAMP production, as both *pilA* and *pilB* mutants had decreased intracellular cAMP. However, *pilT* mutants did not have

decreased cAMP, suggesting that the pili did not have to be functional for CyaB activation. Interestingly, other components of the T4P assembly complex were not identified in the screen, suggesting that T4P-mediated cAMP regulation is not simply related to pilus assembly.

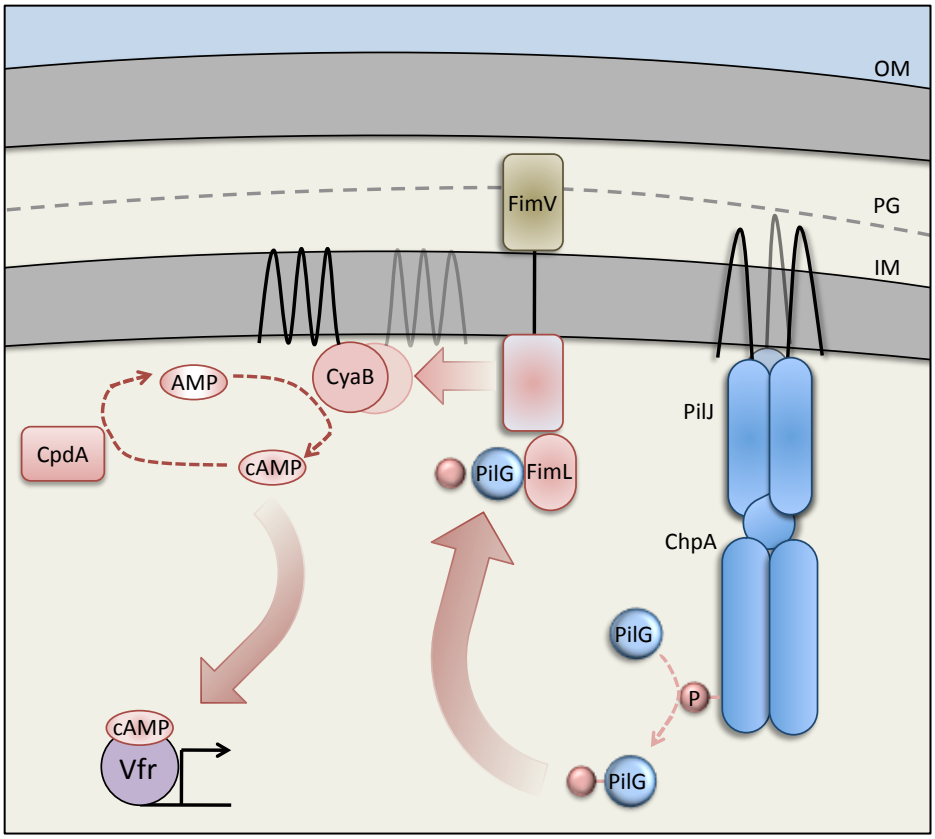

Figure 1.4 – The cAMP regulatory circuit. FimV, FimL, and the Chp system work in concert to regulate CyaB activity. CyaB functions as a dimer to convert ATP into cAMP, which is bound by Vfr. The cAMP-Vfr complex differentially regulates ~200 genes, including many involved in virulence. The cAMP phosphodiesterase (CpdA) degrades cAMP to AMP to regulate cAMP-Vfr activity. Abbreviations: OM, outer membrane; PG, peptidoglycan; IM, inner membrane.

Other proteins in addition to T4P assembly components and the Chp system have been identified as regulators of CyaB. Mutants lacking *fimL* and *fimV* (described below) both have decreased cAMP (55, 56). Interestingly, *fimL* deletion can be rescued by secondary mutations that map outside the previously identified *cpdA*, *cyaB*, *cyaB*, *vfr*, *pilG*, or *pilH* loci, suggesting that there are other cAMP regulators that have yet to be been identified.

Cyclic-di-GMP

The messenger c-di-GMP plays a key role in the transition between motile and sessile states (112). At high c-di-GMP concentrations, *P. aeruginosa* transitions to sessile growth, leading to the formation of adherent biofilms (113). The intracellular c-di-GMP pool is maintained through the activity of diguanylate cyclases (DGCs) and cyclic diguanylate c-di-GMP phosphodiesterases (PDEs) that synthesize and degrade c-di-GMP, respectively. DGCs contain a characteristic GGDEF motif, while PDEs have EAL or HD-GYP motifs (114, 115).

P. aeruginosa also encodes a number of GGDEF and EAL domain-containing regulatory proteins without enzymatic function. Two have been identified as T4aP regulators – PilZ and FimX. PilZ is required for pilus extension (116). *P. aeruginosa* PilZ is the original member of the ‘PilZ

domain' family – a large and diverse family of c-di-GMP binding proteins (116, 117) – despite the fact that PilZ itself does not bind c-di-GMP. How PilZ functions remains unknown; however, in *Xanthomonas axonopodis* pv. Citri, PilZ interacts with PilB and FimX (118). FimX is required for T4P assembly at low concentrations of c-di-GMP (119). It was originally characterized as a sensor of environmental signals and their transduction to T4P (120). *fimX* mutants are retraction competent, but have low levels of surface pili, suggesting impaired pilus extension (120). Contrary to the original report, FimX was subsequently suggested to be catalytically inactive but capable of binding c-di-GMP with high affinity (121, 122).

While c-di-GMP levels can affect pilus function, the T4P protein PilY1 and the minor pilins PilW and PilX have been implicated in regulation of c-di-GMP-mediated control of swarming motility and biofilm formation (123, 124). Impaired swarming in a mutant lacking the PDE BifA (which has high levels of c-di-GMP) was rescued by suppressor mutations in *pilY1*, *pilX*, or *pilW,* consistent with the recent finding that the products of those genes likely form a subcomplex with PilV (31), although interestingly, loss of the latter had no effect on swarming (123). The effect of those mutations involved regulation of the activity of the DGC, SadC. Surprisingly, PilWXY1 exert this regulatory effect independently of their T4P-related functions; mutation of the leader sequence of PilX to prevent processing by the prepilin peptidase PilD, required for extraction from the

inner membrane, blocked twitching but did not affect PilX's ability to modulate swarming. Further elaboration of the regulatory circuitry that connects the cAMP and c-di-GMP regulons will help to shed light on the ancillary functions of the PilWXY1 proteins.

Other relevant regulatory components

FimV

FimV was identified in a transposon screen for mutants deficient in twitching motility (53). It is a large protein with an N-terminal periplasmic region containing a peptidoglycan-binding LysM motif and coiled coil region, a single TMS, and a highly acidic C-terminal cytoplasmic domain predicted to contain three tetratricopeptide repeat (TPR) motifs separated by a long, highly acidic, unstructured region – two located proximal to the IM, and one at the C-terminus (125). The C-terminal region also contains the conserved 'FimV C-terminal domain' (TIGR03504), which contains the predicted C-terminal TPR motif.

TPR motifs are composed of ~34 amino acid sequences that form two antiparallel α-helices joined by a short loop. TPR proteins consist of 3-16 tandem repeats of TPR motifs that associate to form a superhelical protein-protein interaction surface which can be accessible on either convex or concave faces. The sequences of TPRs are highly variable, but a core consensus sequence W_4-L_7-G_8-Y_{11}-A_{20}-F_{24}-A_{27}-P_{32} was identified

(126). Variation is still observed within the core sequence, but the basic content of large and small hydrophobic residues is conserved (127). It is hypothesized that the core hydrophobic residues are involved in forming the TPR itself, while other residues impart specificity for TPR interaction partners. TPR motifs often have a terminal 'capping' helix; although its function is unknown, it is believed to aid in solubility (127).

A number of FimV homologs, while lacking significant sequence identity with FimV, share similar domain organization (128-131). One of the variable features is the unstructured region between the membrane proximal TPRs and the C-terminal TPR. The linker regions of *Legionella pneumophila* FimV, *N. meningitidis* TspA, and *V. cholerae* HubP each contain different sets of tandem repeats (128, 132, 133). The number of repeats affects function of the protein, influencing pigmentation, cell length, and twitching in *Legionella*, and protein-protein interactions in *V. cholerae*. In *P. aeruginosa*, the linker region lacks repeats or are very degenerate; this may reflect differences in function.

Some of the FimV homologs – HubP from *Vibrio cholerae*, *V. alginolyticus*, and *Shewanella refaciens* – regulate flagellar function through interactions with FlhF and FlhG. In *V. cholerae* and *S. putrefaciens*, are also involved in correct positioning of the chromosomal origin of replication (128, 129). However, deletion of *N. meningitidis tspA*

does not affect twitching, suggesting that the role of the FimV family is not limited to motility.

Together, these features suggest that FimV is involved in a number of protein-protein interactions. Its exact role in twitching motility remains unclear, although in-frame deletion of FimV's peptidoglycan-binding LysM motif reduced motility and secretin levels, raising the possibility that it helps to integrate the PilQ secretin into the cell wall (125). Both its periplasmic and cytoplasmic domains are required for twitching, although they can be provided as physically separated fragments and still complement a *fimV* mutant (125), suggesting their functions may be independent of one another.

In addition to twitching motility, FimV is required for type II secretion of elastase on solid media (134) and positively regulates levels of intracellular cAMP (55). Therefore, FimV could be indirectly involved in pilus assembly via cAMP-dependent transcriptional regulation of T4aP assembly components. Although not formally tested, the reported deficiencies in T2S in the *fimV* background were likely due to reduced levels of cAMP, as T2SS expression is Vfr-dependent (49). FimV's role in CyaB activation suggests that it may interact with the adenylate cyclase, either directly or through other cAMP-regulatory proteins.

FimV has recently been shown to affect localization of the cAMP regulatory protein FimL (detailed in section 1.4.2), PilG (135), and the

T4aP assembly complex proteins PilQ and PilO (Carter et al., in preparation). The FimV-FimL-PilG interaction is particularly important in the CyaB activation pathway (135).

FimL

FimL was originally identified as a gene product required for T4aP biogenesis and function that intersected with the Vfr pathway (54). Impaired twitching in a *fimL* mutant could be rescued by a compensatory mutation in *cpdA*, the cAMP phosphodiesterase responsible for breakdown of cAMP into AMP (56, 136). Mutants lacking *fimL* are phenotypically similar to those lacking *cyaAB* – with decreased levels of intracellular cAMP, and reduced twitching motility (54, 56). Since the compensatory mutation in *cpdA* rescues the *fimL* phenotype, FimL likely functions exclusively in regulating CyaB activity and cAMP production, and not in any other T4P-specific behavior.

FimL is homologous to the N terminus of the histidine kinase, ChpA, with two phosphotransfer-like domains. However, while ChpA has His and Thr phosphoacceptor residues in those domains, they are replaced in FimL with Gln (54). Thus, it is unlikely that FimL plays a direct role in a phosphorelay. Instead, FimL may control CyaB function in a complex with other cAMP-regulatory proteins. Inclan et al. (135) showed recently that FimL interacts directly with FimV and PilG, and that FimV was epistatic to

the Chp pathway. Their model suggests that FimL functions as a scaffold protein to bridge FimV and the Chp system, as polar localization of FimL and PilG is dependent on FimV. However, unidentified suppressor mutations which map outside the *cpdA, pilG*, *pilH*, *vfr*, *cyaA* and *cyaB* loci and rescue twitching and intracellular cAMP levels in the *fimL* background suggest that there is at least one more component in the FimL branch of the regulatory pathway (136).

Mechanosensory of T4P regulation

Many of the aforementioned systems were independently found to regulate T4aP function. Only recently have links been drawn between the Chp system, small-molecule signalling, FimV, and FimL, pointing to a mechanosensing/surface sensing model that relies on PilY1 (48, 88, 89).

The mechanosensory model suggests that there is parallel signalling through both the Chp system and the pilus fiber, activating CyaB and the diguanylate cyclase, SadC, respectively (89). PilY1-mediated surface sensing leads to increased c-di-GMP levels via SadC activity, promoting biofilm formation. In parallel, activation of the Chp system leads to increased levels of cAMP and activation of the cAMP-Vfr pathway. cAMP-Vfr and the transcriptional regulator AlgR promote transcription of the minor pilin operon, which in turn negatively regulate their own transcription through PilJ, Vfr, and AlgR (49, 89, 137).

Surface-dependent activation of cAMP synthesis and biofilm formation allows the bacterium to employ a context-dependent 'on switch' for expression of virulence genes and biofilm-related genes. However, the mechanosensory model does not account for cAMP-independent roles of PilG or FimV, both of which are critical for normal pilus function.

Hypothesis and research aims

The critical role of twitching motility and the cAMP-Vfr pathway in regulating virulence makes them important topics of study. A number of different systems and proteins contribute to regulation of both systems, including the Chp system and FimV, both of which have cAMP-dependent and independent roles in regulating twitching. A better understanding of these systems is crucial for understanding how *P. aeruginosa* regulates virulence. The overarching goal of this work is to deepen our understanding of regulation of T4aP assembly and extension, focusing on resolving the cAMP-dependent and independent roles of the Chp system and FimV. The aims of the project are as follows:

1. **Investigate the roles of FimV controlling twitching motility**

   FimV is a regulator of CyaB activity (55) and is required for twitching motility, although its role relative to the Chp system and other cAMP regulators is unclear. Given that all other identified

cAMP regulators are cytoplasmic (55, 56, 111), we hypothesized that the cytoplasmic domain of FimV is critical for its cAMP-regulatory function. We examined the role of its cytoplasmic domain, in particular the conserved 'FimV C-terminal domain' in Chapter 2.

While FimV is responsible for maintaining PilMNOP levels and multimerization of PilQ, its role in CyaB activation makes it unclear which of those phenotypes are cAMP-dependent and which are not. In Chapter 3, we resolve the cAMP-dependent and independent roles of FimV, and distinguish its cAMP-independent role from that of PilG.

2. **Characterize the cAMP-dependent and independent roles of PilG in motility**

PilG, the response regulator of the Chp system, has both cAMP-dependent and independent roles in regulating twitching (55). The cAMP-dependent pathway promotes assembly, while the cAMP-independent pathway is related to retraction. In Chapter 4, we investigate the role of PilG in regulation of twitching and distinguish the outputs of the cAMP-dependent and independent pathways.

CHAPTER TWO

The conserved TPR-containing C-terminal domain of *Pseudomonas aeruginosa* FimV is required for its cAMP-dependent and independent functions

Preface

Chapter Two consists of the following publication:

Buensuceso RNC, Nguyen Y, Zhang K, Daniel-Ivad M, Sugiman-Marangos SN, Fleetwood AD, Zhulin IB, Junop MS, Howell PL, Burrows LL. 2016. The conserved tetratricopeptide repeat-containing C-terminal domain of *Pseudomonas aeruginosa* FimV is required for its cyclic AMP-dependent and -independent functions. J Bacteriol 198:2263–2274

Attributions: R.N.C.B. cloned plasmids, generated mutants, performed twitching assays, sheared surface protein preparations and SDS-PAGE, protease secretion assays, and protein interaction assays. K.Z. and M.D.I Cloned and expressed the protein. S.S.M. and M.S.J. collected diffraction data. Y.N. and S.S.M. solved the structure. A.D.F. and I.B.Z. performed bioinformatics analysis. R.N.C.B. and L.L.B. designed the experiments. R.N.C.B., P.L.H., and L.L.B. wrote the manuscript with help from I.B.Z. (Bioinformatics sections) and Y.N. (protein expression and purification methods).

The conserved tetratricopeptide repeat-containing C-terminal domain of *Pseudomonas aeruginosa* FimV is required for its cAMP-dependent and independent functions

Ryan N.C. Buensuceso[a], Ylan Nguyen[a], Kun Zhang[a,c], Martin Daniel-Ivad[a], Seiji N. Sugiman-Marangos[a], Aaron D. Fleetwood[d], Igor B. Zhulin[d], Murray S. Junop[a,c], P. Lynne Howell[b]*, and Lori L. Burrows[a]* #

Department of Biochemistry and Biomedical Sciences, and the Michael G. DeGroote Institute for Infectious Diseases Research, McMaster University, Hamilton, ON[a]; Program in Molecular Structure and Function, Hospital for Sick Children, Toronto, ON and Department of Biochemistry, University of Toronto, Toronto, ON[b;] Department of Biochemistry, Western University, London, ON[c]; Computer Science and Mathematics Division, Oak Ridge National Laboratory, Oak Ridge, TN, USA and Department of Microbiology, University of Tennessee, Knoxville, TN, USA[d]

Running Head: Role of the C-terminal domain of *P. aeruginosa* FimV

*Corresponding authors:

L.L. Burrows,

Tel: 905-525-9140 x22029 Fax: 905-522-9033 Email:

burrowl@mcmaster.ca

P.L. Howell,

Tel: 416-813-5378 Fax: 416-813-5379 Email: howell@sickkids.ca

ABSTRACT

FimV is a *Pseudomonas aeruginosa* inner membrane protein that regulates intracellular cyclic AMP (cAMP) levels, and thus type IV pilus (T4P)-mediated twitching motility and type II secretion (T2S) of toxins, by activating the adenylate cyclase CyaB. Its cytoplasmic domain contains three predicted tetratricopeptide repeat (TPR) motifs separated by an unstructured region – two proximal to the inner membrane, and one within the 'FimV C-terminal domain', which is highly conserved across diverse homologs. Here, we present the crystal structure of the FimV C-terminus, $FimV_{861-919}$, containing a TPR motif decorated with solvent-exposed, charged side chains, plus a C-terminal capping helix. $FimV_{689}$ – a truncated form lacking this C-terminal motif – did not restore wild-type levels of twitching or surface piliation compared with the full-length protein. $FimV_{689}$ failed to restore wild type levels of the T4P motor ATPase PilU or T2S, suggesting that it was unable to activate cAMP synthesis. Bacterial two-hybrid analysis showed that TPR3 interacts directly with the CyaB activator, FimL. However, $FimV_{689}$ failed to restore wild type motility in a *fimV* mutant expressing a constitutively active CyaB (*fimV cyaB-R456L)*, suggesting that the C-terminal motif is also involved in cAMP-independent functions of FimV. The data show that the highly conserved TPR-containing C-terminal domain of FimV is critical for its cAMP-dependent and independent functions.

IMPORTANCE

FimV is important for twitching motility and cAMP-dependent virulence gene expression in *P. aeruginosa*. FimV homologs have been identified in a number of human pathogens, and their functions are not limited to T4P expression. The C-terminus of FimV is remarkably conserved among otherwise very diverse family members, but its role is unknown. Here we provide biological evidence for the importance of the C-terminal domain in both cAMP-dependent (through FimL) and independent functions of FimV. We present X-ray crystal structures of the conserved C-terminal domain and identify a consensus sequence for the C-terminal TPR within the conserved domain. Our data extend knowledge of FimV's functionally important domains, and the structures and consensus sequences provide a foundation for functional studies of FimV and its homologs.

INTRODUCTION

Type IV pili (T4P) are filamentous surface appendages produced by a wide range of bacteria and archaea (2, 5), where they assist in DNA uptake, surface attachment, and twitching motility (3, 4, 6). There are two major subfamilies of T4P, T4aP and T4bP. T4aP are typically associated with twitching (5), a process in which the pili undergo repeated cycles of

extension, adhesion, and retraction, thus acting as molecular grappling hooks to pull cells along a surface.

The T4aP machinery is composed of four structural subcomplexes (7). In the model bacterium *P. aeruginosa*, an inner membrane motor subcomplex consisting of the platform protein PilC and three hexameric ATPases, PilB, PilT, and PilU, provide energy for T4aP extension and retraction (25, 27, 138). A second inner membrane alignment subcomplex composed of PilMNOP connects the motor subcomplex with an outer membrane secretin composed of multimeric PilQ (5, 36, 38, 139, 140). Finally, the pilus fiber is composed of the major pilus subunit PilA, and a set of minor pilins that prime pilus assembly and export the adhesin PilY1 to the cell surface (31). These proteins comprise the physical T4aP machinery, but its synthesis and function are further regulated by a number of components. A chemotaxis-like system called Chp controls T4aP function in part by regulating function of the major adenylate cyclase, CyaB, and thus levels of the second messenger molecule cyclic adenosine monophosphate (cAMP) (55). The transcriptional activator Vfr (virulence factor regulator) binds cAMP and controls the expression of over 200 gene products – many involved in pathogenicity – including members of the T4aP alignment subcomplex, and the minor pilins (49).

Also implicated in regulation of T4aP assembly and function is the inner membrane protein, FimV (53, 125). FimV is involved in a number of

virulence mechanisms, including twitching motility, type II secretion (T2S) of lipases and proteases, and regulation of cAMP production, and thus Vfr function (53, 55, 134). FimV is a 919 residue protein consisting of a large periplasmic domain with a peptidoglycan (PG)-binding lysin motif (LysM) (141), a single transmembrane segment, and a highly acidic cytoplasmic domain that is predicted to contain three discontinuous tetratricopeptide repeat (TPR) protein-protein interaction motifs (142, 143). TPR motifs are typically composed of 3-16 tandem repeats of a ~34-residue α-helical hairpin. Individual pairs of helices associate to form a superhelical structure that mediates protein-protein interactions (144). TPR protein sequences are highly variable, although a core consensus sequence, W_4-L_7-G_8-Y_{11}-A_{20}-F_{24}-A_{27}-P_{32} was identified 2 decades ago (126). None of the positions of the consensus are invariable, although hydrophobic residues are commonly observed at those positions (126, 127, 145). Of the three predicted TPR motifs in *P. aeruginosa* FimV, two are organized in tandem, proximal to the inner membrane (TPR1 and TPR2, residues 544 to 611), while the third (TPR3, residues 873 to 906) is at the C-terminus, separated from TPR1 and TPR2 by a long, highly acidic region predicted to lack regular secondary structure (53).

In addition to controlling cAMP production and related phenotypes, FimV functions in a cAMP-independent manner, promoting multimerization of the PilQ secretin (125). Based on recent work in other species, FimV

may be a hub protein – similar to HubP of *Vibrio cholerae* and *Shewanella putrefaciens* – that coordinates interactions of a number of landmark proteins involved in motility and chromosome segregation at the poles of rod-shaped bacteria (128, 129). These large proteins have very limited sequence identity aside from their LysM motifs, single transmembrane segment, and a highly conserved "FimV C-terminal sequence" of approximately ~50 residues (NCBI Conserved Domain Database designation, TIGR03504) (125) predicted to include a single TPR motif. FimV's domain architecture and C-terminal sequence are shown in Figure 2.1.

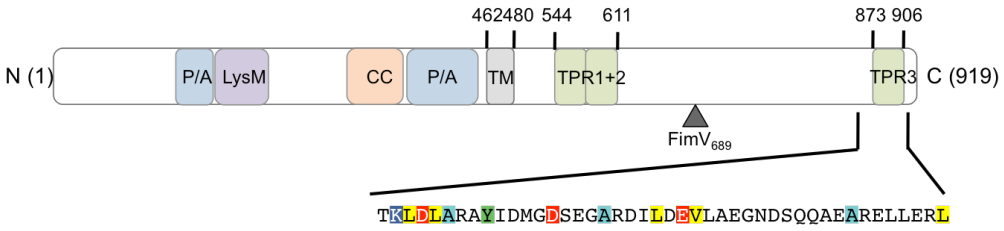

Figure 2.1. Schematic of FimV domain organization. FimV has a peptidoglycan-binding LysM motif, two proline/alanine rich regions (P/A), and a coiled-coil (CC) motif in its periplasmic domain (residues 1-462), followed by a single transmembrane segment (TM) (125). The cytoplasmic domain (residues 480-919) has three predicted TPR motifs (143), two in tandem (residues 544-611), and a third at the C-terminus (residues 873-906). The 'FimV C-terminal domain' (TIGR03504) is highly conserved among orthologs. The amino acid sequence of the conserved C-terminal domain is shown. Domains are drawn to scale. The boundary of the truncated $FimV_{689}$ is shown with an arrowhead.

The way in which FimV regulates cAMP production by the major *P. aeruginosa* adenylate cyclase CyaB is unclear. While other regulators of cAMP levels have been identified, including the Chp chemotaxis-like system, the CyaB activator FimL, and the phosphodiesterase CpdA (55, 56, 111), only FimL interacts with FimV (135). All the regulators identified so far are cytoplasmic, suggesting that interactions with FimV are likely to occur with its cytoplasmic domain. Here, we present the X-ray crystal structure of the highly conserved TPR3-containing C-terminal domain at 2.05 Å, and provide evidence that it plays a key functional role in regulation of motility and cAMP production, and therefore production of many *P. aeruginosa* virulence factors.

MATERIALS AND METHODS

Bacterial growth conditions

Bacterial strains and plasmids are listed in Table 1. Unless otherwise stated, *P. aeruginosa* strains were grown on LB agar at 37 °C on media containing 30 μg ml^{-1} gentamicin. *E. coli* BL21 (DE3) and B834 (DE3) strains were grown in media containing 100 μg ml^{-1} ampicillin.

Sequence analysis

The CDvist server, which uses an array of protein sequence analysis tools and protein feature databases (146), was used to delineate complete domain architectures of FimV and orthologous sequences that were downloaded from the EggNOG database (147). A multiple sequence alignment was constructed using MAFFT-LINSI with the legacygappenalty option (148). A maximum likelihood tree was built using MEGA with pairwise deletion and the JTT substitution (149).

Twitching motility assay

Twitching motility was tested as previously described (150) with some modifications. In brief, cells from an overnight culture were stab inoculated to the interface between LB 1% agar polystyrene petri dish, and incubated at 37 °C for 16 h (Thermo Fisher). Media was supplemented with 0.1% (wt/vol) arabinose to induce expression of FimV, and petri dishes were tissue culture treated to promote twitching. Twitching zones were visualized by removing the agar and staining cells on the petri dish with 1% (wt/vol) crystal violet and washing with water to remove unbound dye. Twitching zones were measured by analyzing the diameter of each twitching zone in pixels using ImageJ software (NIH). Twitching zones were normalized to the twitching diameter of wild type PAK in each individual experiment. Data are representative of n = 3 independent experiments.

Sheared surface protein preparation

Surface pili were analyzed as previously described (150). In brief, strains of interest were streaked in a grid-like pattern onto LB 1.5% agar supplemented with 0.1% (wt/vol) arabinose and grown overnight at 37 °C. Cells were gently scraped from the plates using a sterile coverslip and resuspended in 4.5 ml PBS (pH 7.4). Surface appendages were sheared by vortexing the cells for 30 s. The OD_{600} for each strain was measured, and an amount of cells equivalent to 4.5 ml of the sample with the lowest OD_{600} was pelleted by centrifugation at 16,100 × g for 5 min. When necessary, PBS was added to samples to a final volume of 4.5 ml prior to centrifugation. Supernatants were removed and centrifuged again at 16,100 × g for 20 min to remove remaining cells. Supernatants were collected and mixed with 5 M NaCl and 30% (wt/vol) polyethylene glycol (Sigma; molecular weight range ~8000) to a final concentration of 0.5 M NaCl and 3% (wt/vol) polyethylene glycol, and incubated on ice for 30 min. Precipitated surface proteins were collected by centrifugation at 16,100 × g for 30 min. Supernatants were discarded and samples were centrifuged again at 16,100 × g for 2 min. Pellets were resuspended in 150 μl of 1× SDS-PAGE sample buffer (80 mM Tris, pH 6.8, 5.3% (vol/vol) 2-mercaptoethanol, 10% (vol/vol) glycerol, 0.02% (wt/vol) bromophenol blue, 2% (wt/vol) SDS). Samples were boiled for 10 min and resolved by 15%

SDS-PAGE. Bands were visualized by staining with Coomassie brilliant blue (Sigma). Data are representative of n = 3 independent experiments.

Western blotting

Western blotting of whole cell lysates was performed as previously described with some modifications (28). In brief, whole cell lysates prepared from strains grown overnight on LB 1.5% agar supplemented with 0.1% (wt/vol) arabinose. Cell growth was resuspended in 1× PBS and normalized to an OD_{600} of 0.6. Cells were pelleted by centrifugation at 2,300 × g for 5min. Pellets were then resuspended in 175 μl of 1× SDS-PAGE loading dye. Cell lysates were resolved on 15% SDS-PAGE gels and transferred to nitrocellulose membranes. Membranes were blocked in 5% skim milk dissolved in PBS (pH 7.4) for 1 h, washed in PBS, and incubated with antisera raised against the FimV periplasmic domain (125) or PilU (24), diluted in PBS (anti-$FimV_{peri}$ 1:1000; anti-PilU 1:5000) for 1 h, washed, incubated with alkaline phosphatase-conjugated goat-anti-rabbit secondary antibody (1:3000, Bio-Rad) for 1 h, and washed. Blots were developed using 5-bromo-4-chloro-3-indolylphosphate (BCIP) and nitro blue tetrazolium (NBT). Data are representative of n = 3 independent experiments.

Densitometric analysis

Pixel density of the band corresponding to PilU and a non-specific loading control band were determined using ImageJ software (NIH) (151) . Pixel density of the PilU band was normalized to the pixel density of the loading control band, expressed as a percentage of the normalized PilU levels in wildtype PAK. Data are representative of the average of n = 3 independent experiments. Pairwise student's t-test was performed using GraphPad Prism 5 Software (GraphPad Software) to determine statistical significance. Results were considered significantly different if $p < 0.05$.

Type II secretion assay

Overnight cultures grown on LB 1.5% agar were resuspended in PBS and diluted to an OD_{600} of 0.6. Two μl of the normalized suspension were spot inoculated onto trypticase soy agar supplemented with 2% (wt/vol) skim milk and 0.1% arabinose (wt/vol), and incubated for 40 h at 30 °C. Secretion of the type II secretion substrate elastase was visualized as a zone of clearance (degradation of casein) around the colony. Secretion was quantified by calculating the difference between the diameter of the zone of clearance and the diameter of the bacterial growth, and expressed as a percentage of wild type PAK. Data are representative of n = 3 independent experiments.

Bacterial two-hybrid assay

E. coli BTH101 cells were cotransformed with TPR1 and 2 ($FimV_{488-618}$), TPR3 ($FimV_{811-919}$), TPR1-3 including the linker region ($FimV_{488-919}$), or FimL, fused to either the T18 or T25 fragments of *Bordetella pertussis* CyaB (152) by heat shock. Single colonies were resuspended in 5ml LB supplemented with 100ug/ml ampicilin and 50ug/ml kanamycin and grown overnight.A 5ml subculture using 100ul of the overnight culture was grown to OD_{600} of 0.6. Five ul of each strain was then spot plated onto MacConkey agar supplemented with 100ug/ml ampicilin and 50ug/ml kanamycin, 1% (w/v) maltose, and 0.5mM isopropyl b-D-thiogalactopyranoside (IPTG), and LB/1.5% agar (w/v) supplemented with 100ul of 20mg/ml 5-bromo-4-chloro-3-indolyl-β-D-galactopyranoside (X-gal) spread and allowed to dry onto the surface of the plate, and incubated at 30°C for 24h. Positive interactions were visualized by pink bacterial growth representing fermentation of maltose on MacConkey agar, or blue growth on LB/1.5% agar supplemented with X-gal representing X-gal cleavage.

Protein overexpression and purification

TEV protease was expressed from plasmid pRK793 (Addgene plasmid #8827) (153). *E. coli* BL21 transformed with pRK793 was grown overnight at 37 °C in 10 ml LB supplemented with ampicillin. The overnight culture was subcultured into 1 L of fresh media and grown at 37 °C until

OD_{600} = 0.6. Expression was induced with 1mM IPTG and the cells grown at 30 °C for 4h. Cells were harvested and the pellet resuspended in 20 mM Tris pH 8, 500mM NaCl, 10% glycerol, 25 mM imidazole for lysis by sonication and centrifugation as above. TEV protease was purified by nickel affinity chromatography on an AKTA FPLC as above where the protein was eluted in 220 mM imidazole following washes with 25 mM, 40 mM, 50 mM and 65 mM imidazole. The elution fraction was diluted up to 50 ml with 50 mM Tris pH 8, 1 mM EDTA, 5mM DTT and 10% glycerol. TEV protease was further purified by cation exchange chromatography using a 5 ml HiTrap SP HP column (GE Healthcare) on an AKTA FPLC. The protein was eluted a gradient of 150 mM – 500 mM KCl, fractions were analyzed by SDS-PAGE and those with TEV protease were pooled. TEV protease was concentrated to 1mg/ml, flash frozen with liquid nitrogen and stored at -80°C until used.

The DNA fragment encoding $FimV_{862\text{-}919}$ was amplified using forward 5'CACCGATGACTTCGACTTCCTCTCCGGTGC3' and reverse 5'TCAGGCCAGGCGCTCCAGCAACTC3' primers and cloned into pET151/D-TOPO for expression with a cleavable His_6-V5 tag. *E. coli* BL21 (DE3) transformed with pET151::*$fimV_{862\text{-}919}$* was grown in LB supplemented with ampicillin for 6 h at 37 °C , and subcultured into Terrific Broth (TB) with ampicillin for 72 h at 20 ºC. Cells were harvested and the pellet resuspended in 20 mM Tris pH 7.5, 500 mM NaCl for lysis by

sonication on ice for 2 min in 10 sec pulses with 10 sec cooling in between using a Sonicator 3000 (Misonix) at power level 3. The cell lysate was centrifuged at 8,891 × g for 1 h at 4 °C and DNase I was added to the supernatant (1 μg ml^{-1}) before purification. His_6-V5-$FimV_{862-919}$ was purified with Ni-NTA agarose (Qiagen) where the protein was collected in 20 mM, 40 mM and 80 mM imidazole elution fractions. These fractions were pooled and diluted with 20 mM Tris pH 7.5 to lower the salt concentration to 100 mM NaCl for anion exchange chromatography where a gradient of 100mM – 500 mM KCl was used to elute His_6-V5-$FimV_{862-919.}$ The protein eluted at ~250 mM KCl, and was dialyzed into 20 mM Tris pH 7.5, 100 mM NaCl overnight and the tags removed by TEV protease cleavage. A second nickel affinity purification step was performed to purify $FimV_{862-919}$ without the His_6-V5 tag. The flow-through fraction containing purified $FimV_{862-919}$ in 20 mM Tris pH 7.5, 100 mM NaCl was concentrated to 2 mg ml^{-1} using a Vivaspin 20 concentrator.

For SAD phasing, selenomethionine (SeMet) labeled proteins were expressed from *E. coli* B834 (DE3) in M9 SeMet high-yield growth media (Shanghai Medicilon) supplemented with ampicillin (100 μg ml^{-1}). A 10 ml starter culture was grown for 7.5 h at 37 °C and subcultured into a 100 ml of fresh media and grown overnight at 37 °C. The overnight culture was subcultured into 1 L of fresh media and grown at 37 °C until OD_{600} = 0.6. SeMet-labeled His_{6-}V5-$FimV_{862-919}$ expression was induced with 1 mM

isopropyl b-D-thiogalactopyranoside (IPTG) and the cells grown overnight at 20 °C. Purification was performed as above except for nickel affinity chromatography, a 1 ml HiTrap chelating HP column (GE Healthcare) pre-charged with 100 mM $NiCl_2$ was used on an AKTA FPLC system where the protein eluted in 300 m*M* imidazole. An additional buffer exchange step into 20 m*M* Tris pH 7.5, 100 mM NaCl was also added following the second round of nickel affinity purification. SeMet labeled proteins were concentrated to 2.87 mg ml^{-1} using a Vivaspin 20 concentrator.

Crystallization

Broad crystallization screening was performed using the hanging drop method with commercially available crystallization screens. Native $FimV_{862-919}$ crystals grew in a 1:1 ratio of protein (2 mg/ml) and precipitant solution (1 M $NH_4H_2PO_4$, 100 mM tri-sodium citrate pH 5.6) and equilibrated over 1.5 M ammonium sulfate at 18 °C. SeMet $FimV_{862-919}$ (2.87 mg ml^{-1}) was mixed in a 1:1 ratio with buffer containing 1.6 M NaH_2PO_4, 0.4 M KH_2PO_4, 0.1 M phosphate citrate (pH 4.2) and equilibrated over 1.5 M ammonium sulfate at 18 °C overnight. Crystallization was seeded with native $FimV_{862-919}$ microcrystals grown in the same buffer. Small SeMet $FimV_{862-919}$ crystals grew within 10-25 days. Additional growth was achieved by further incubation at 4°C for 7-10 days.

Structure determination

Diffraction data were collected at beamline X29 of the National Synchrotron Light Source (Brookhaven, NY) at a wavelength of 1.075 Å for native FimV and 0.9791 Å for SeMet FimV. Datasets were processed using the HKL-2000 program suite (154). SAD phasing, density modification, auto model building, and refinement were performed using the PHENIX suite of programs (155, 156). Manual model building and refinement were performed using Coot (157) until R and R_{free} values could no longer be improved. The refined $FimV_{862-919}$ -SeMet structure (PDB 4MAL) was used as an initial search model for structure determination of native $FimV_{862-919}$ by molecular replacement in PHENIX (155, 156). Model refinement was performed using PHENIX (155, 156). The stereochemical quality of the models was verified using MolProbity (158). Data collection and model refinement statistics are listed in Table 3.

Data deposit

The structures of native and SeMet derivatized FimV TPR3 can be accessed through the RCSB Protein Database using accession codes 4MBQ and 4MAL, respectively.

Results and Discussion

The C-terminal TPR sequence of FimV is highly conserved among diverse homologs

We downloaded all FimV ortholog sequences from the EggNOG database, which generates orthologous groups of proteins from complete genomes (147). The set of FimV ortholog sequences (COG3170) contained 235 sequences, including the previously characterized proteins FimV from *Legionella pneumophila* (132), TspA from *Neisseria meningitidis* (130) and HubP from *V. cholerae* and *S. putrefaciens* (128, 129). A multiple sequence alignment was constructed based on the full-length sequence of FimV orthologs and the resulting phylogenetic tree revealed three major clades, exemplified by FimV from *P. aeruginosa*, HubP, and TspA, respectively (Figure 2.2A). The functions of FimV orthologs in the context of T4P vary. Although they are in the same clade, deletion of *N. meningitidis tspA* had no effect on twitching motility or surface piliation (130), while *L. pneumophila fimV* mutants have reduced motility (132). Representative sequences from all three major clades (selected from smaller subgroups to avoid bias) were subjected to in-depth domain architecture analysis using the CDvist tool (146), revealing that only two domains are strongly conserved: the periplasmic LysM domain and the C-terminal TPR-containing domain, designated TIGR03504 in the TIGRFAM database of protein families. Multiple sequence alignment revealed a dozen highly conserved residues within the C-terminal TPR-

containing domain (Figure 2.2B) that were further analyzed in the context of the corresponding structure (below).

A)

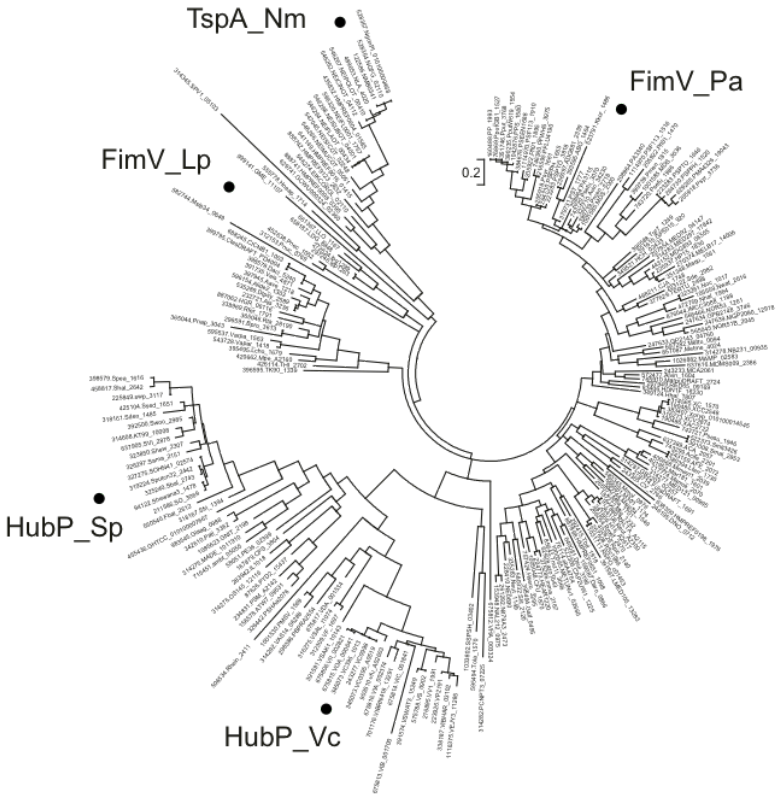

B)

```
2D structure              .hhhhhhhhhhhhhhhh....hhhhhhhhhhhhh...hhhhhhhhhhhhh....
PA3115 (FimV_Pa)          GADEAATKLDLARAYIDMGDSEGARDILDEVLAEGNDSQQAEARELLERLA---   919
MDS_2000                  GTDETATKLDLARAYIDMGDTEGARDILDEVVAEGNDAQQQEAREMISKLV---   946
Pput_3768                 GSDEVATKLDLARAYIDMGDSQGARDILDEVVKDGDDSQRQEAEDMLSRLV---   911
HCH_02433                 DTDEAATKLDLARAYIDMGDREGARDILEEVVEEGNNDQKQEAASLLKRLA---  1012
Sde_2082                  DSDETATKLDLARAYIDMGDAEGARDIIEEIKKEGNDQQKEEADKLLSRI----  1245
Lcho_1679                 GSDPLARKLELAEEFNQIGDYEGARDLLQEVIENADGALKAKAQAMLDGLA---   883
Daci_5240                 PEDPLATKLALAQEFNAIGDSDGARTLIEEVIAEAHGDLKAKAQRLLAEID---   964
Reut_A2309                GGRDMQIKLDLARAYIEIGDKEGARELLQEVVEQSQDDLQAEARSLLLEVV---   952
Tmz1t_3066                MNEEAETKLELARAYEEMGDKEGALELLEEVVAEGTPRQQTTARDMIARLG---  1027
CV_2766                   MDDPLATKLDLAKVYLDMGDREGAREVLQDLLSEAKGALKDEAQALFDKIST--   755
Kkor_1486                 SEDEVQTKLELAKAYIEMGDEESAKDILQEVQKEGNAKQSEEAGKLLAKH----   767
Noc_1017                  DLDEMEVKLDLARAYMDMGDADGARGLLEEVVAEGTEQQRDTGEGLLAELAKAS   888
Mettu_0094                DMDELETKLDLAKAYVDMGDAEAAKDIAKEVLEQGTAEQKKAAKALLDELD---  1012
XC_1570                   QQDAGRDRLELAVAYMDLGDKDTARGLLLEVAATGDAATRAEAADLLDRLA---   685
lpg1299 (FimV_Lp)         SKKALDTLLDLAKTYISMGDIETARSSLEEVIEHGSANQKEQARQLLEQLK---   813
NMB0341 (TspA_NM)         SDAPSEAKYDLAEMYLEIGDRDAAAETVQKLLEEAEGDVLKRAQALAQELGI--   875
VC0998 (HubP_VC)          SGAEAAGKLDLAKIYIEMNDEKGAIKLLEEAIVDGDDEIRQQAKRLIDVLNGRV  1621
Tola_1570                 DDGGVGAKLDLARAYLEIDDKANAKVLLLEVQAMGSSEQIKEAEKLLSRIV---   697
Sputcn32_2442 (HubP_Sp)   EENSVSAKLDLARAYIEIDDSDSAKALLKEVQIDGNEHQQDEAGRLLKEIS---  1097
CPS_3804                  EDGSMSSKLDLAKMYIEMNDEENAQVILQEVISKGDKTQRAEAQALLDSL----  1162
Consensus 90%             ..t.htsplpLAp.a.phsD.psAhthlp-l..tup.t..tpAtthhttl....
Consensus 80%             tts.htsKL-LAphYh-hsD.cuAptlLpElhtpustt.ptpApthltpl....
```

Figure 2.2. The C-terminal domain is highly conserved across FimV homologs. (A) Maximum-likelihood phylogenetic tree based on full-length FimV homolog sequences (COG3170 from the EggNOG database). Experimentally studied proteins are indicated: Pa, *P. aeruginosa* (53); Vc, *V. cholerae* (128); Sp, *S. putrefaciens* (129); Lp, *L. pneumophila* (132); Nm, *N. meningitidis* (130). (B) Conservation of the C-terminal TPR3-containing domain in representative FimV proteins. Locus tags are shown as sequence identifiers. Conserved positions are highlighted: positively charged (blue), negatively charged (red), aromatic (green), aliphatic (yellow), and alanine (cyan). Consensus was calculated for the complete set of homologs shown in panel A. Secondary structure elements (h, alpha-helix) corresponding to the TPR motif (first two alpha-helices) and the C-terminal capping helix are shown above the alignment.

The C-terminus is required for FimV function

The high level of conservation of FimV's C-terminus implies a key functional role, supported by early observations (17) that transposon insertion at a position ~230 nucleotides from the 3' end of *fimV* markedly decreased twitching motility. To determine if this region was required for FimV's functions, we generated an arabinose-inducible expression construct ($FimV_{689}$) encoding FimV 1-689 (of 919), lacking the region encompassing predicted TPR3. The boundaries selected for the $FimV_{689}$ construct were based on the phenotype of a previously characterized transposon mutant, *fimV2091,* which expresses a stable fragment of FimV lacking the C-terminal region encompassing TPR3 (125, 159). The

truncated construct or full-length *fimV* was used to complement a *fimV* deletion mutant. To examine cAMP-independent phenotypes controlled by FimV, a *fimV* mutant encoding a constitutively active point mutant of the adenylate cyclase CyaB (*fimV cyaB-R456L*) (107) was used to restore cAMP biogenesis in the *fimV* background. Both full length and truncated proteins were stable and expressed to levels comparable to those in the wild type control, as determined by western blot with FimV-specific antisera (Figure 2.3). It is worth noting that FimV exhibits anomalous migration on SDS-PAGE (125) so it is not possible to accurately gauge its mass using that method.

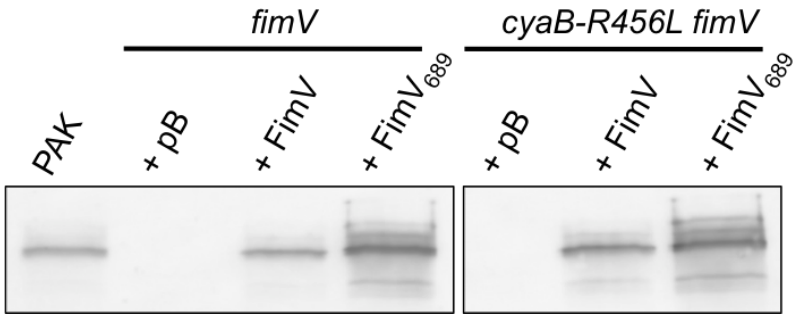

Figure 2.3. FimV$_{689}$ is a stable fragment. *fimV* and *fimV cyaB-R456L* were transformed with arabinose-inducible expression vectors encoding full-length FimV (FimV) or a truncated form lacking TPR3 (FimV$_{689}$). As a control, strains were also transformed with empty vector (pB). Cell lysates prepared as described in the Methods from cells grown on LB 1.5% agar supplemented with 0.1% (wt/vol) arabinose were resolved on 10% SDS-PAGE and transferred to a nitrocellulose membrane. FimV was visualized by immunoblotting with anti-FimV antiserum. The previously reported

anomalous migration pattern of FimV on SDS-PAGE (53, 125) means that the full length and truncated versions appear similar in mass despite their differences in length. Data are representative of n=3 experiments.

To confirm that $FimV_{689}$ was functional, we used it to complement a *fimV* mutant disrupted at nucleotide 1194, $fimV_{1194}$ (125). This mutant expresses the cytoplasmic portion of FimV, and can be complemented in trans with an N-terminal FimV construct expressing residues 1-507, $FimV_{507}$ (125). Expression of $FimV_{689}$ in $fimV_{1194}$ restored twitching to the same degree as full length FimV (Figure S2.1), providing strong evidence that it is correctly folded and inserted into the inner membrane.

As a proxy to assess relative levels of intracellular cAMP, we examined levels of the T4P motor ATPase PilU (Figure 2.4A), which are positively correlated with levels of cAMP (Figure S2.2) (49). The *fimV* mutant complemented with empty vector had low levels of PilU, suggesting low levels of cAMP, while the *fimV cyaB-R456L* mutant had high levels of PilU, confirming that CyaB R456L was active in the absence of *fimV*. Complementation of *fimV* in trans with the full-length *fimV* gene *in trans* restored PilU levels to ~66% of wild type, but expression of $FimV_{689}$ failed to increase PilU levels relative to the empty vector control, suggesting that $FimV_{689}$ was incapable of activating CyaB.

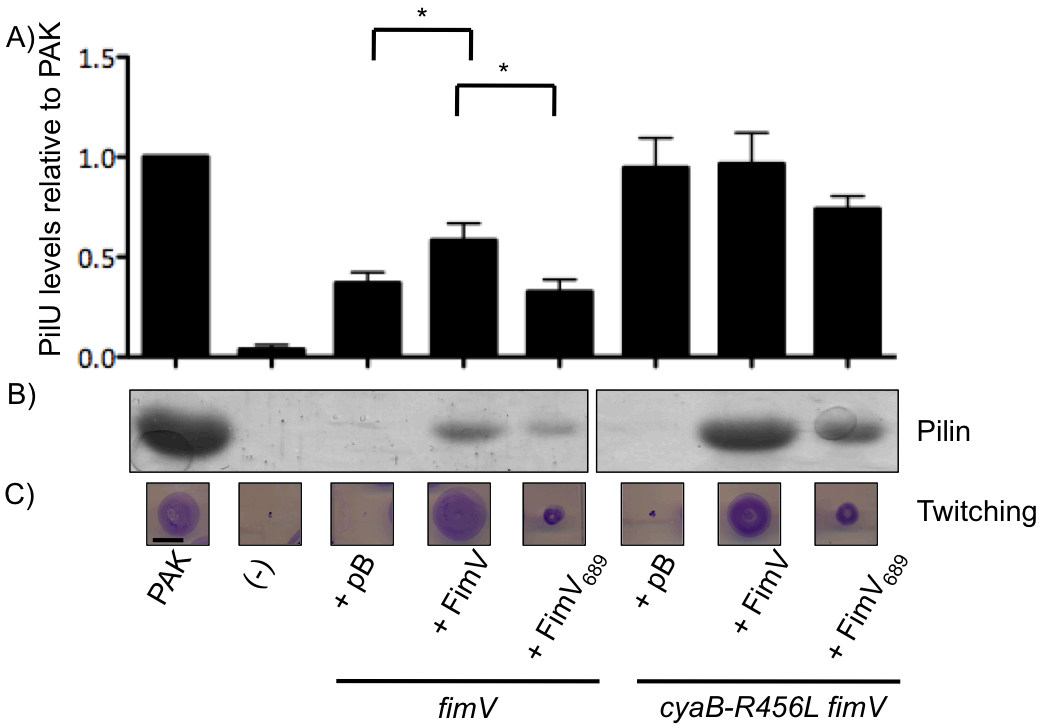

Figure 2.4. FimV TPR3 is critical for FimV function. *fimV* and *fimV cyaB-R456L* were transformed with arabinose-inducible expression constructs encoding full-length FimV (FimV), or a truncation mutant lacking TPR3 ($FimV_{689}$). As controls, strains were also transformed with empty vector (pB) (A) Levels of PilU were determined by preparing cell lysates as described in the Methods, of cells grown overnight on LB 1.5% agar supplemented with 0.1% (wt/vol) arabinose. Samples were resolved by SDS-PAGE and transferred to a nitrocellulose membrane. PilU was visualized by immunoblotting with anti-PilU antiserum. Densitometric analysis (average of n = 3) was carried out using ImageJ, normalizing band intensity of the PilU band to a nonspecific control band, and shown as a percentage of the normalized band intensity of wild type ± standard error. Samples were considered significantly different if a pairwise Student's t-test gave values of *$p < 0.05$. (B) Levels of surface pilins were assessed by sheared surface protein preparation of strains grown on LB

1.5% agar supplemented with 0.1% (wt/vol) arabinose. The surface protein fractions were prepared as described in the Methods, and resolved by SDS-PAGE and visualized by Coomassie blue staining. (C) Twitching motility was determined by stab inoculation of the indicated strains into LB 1% agar supplemented with 0.1% (wt/vol) arabinose. Strains were incubated for 16 h, and twitching zones were visualized by removing the agar layer and staining the bacteria with 1% (wt/vol) crystal violet. Motility was measured as the diameter of the stained twitching zone. Scale bar denotes 1 cm. (-) represents the negative control for each experiment, *pilU* for the anti-PilU immunoblots or a nonpiliated *pilA* strain for surface piliation and twitching motility. Images are representative of n=3 experiments.

Activation of CyaB via FimV is required for transcription of structural components of the T4P machinery, including the PilMNOP alignment subcomplex (49). The periplasmic domain of FimV has a role in promoting multimerization of the PilQ secretin (125) – and thus surface piliation – in a cAMP-independent manner. We characterized levels of surface piliation in *fimV* and *fimV cyaB-R456L* mutants upon complementation with $FimV_{689}$ (Figure 2.4B). *fimV* complemented with empty vector had no recoverable surface pili, but piliation was restored with full-length *fimV* in trans. In contrast, $FimV_{689}$ restored ~65% of surface pilin levels relative to complementation with full-length FimV. The *fimV cyaB-R456L* mutant with empty vector had few recoverable surface pili, but piliation was restored upon complementation with full-length FimV. Complementation of *fimV*

cyaB-R456L with $FimV_{689}$ restored ~50% of piliation relative to complementation with full-length FimV. As $FimV_{689}$ complemented inefficiently compared with the full-length protein in either *fimV* or *fimV cyaB-R456L*, we conclude that the FimV C-terminal domain is required for both cAMP-dependent and independent functions of FimV.

We also examined twitching motility by subsurface stab assay (Figure 2.4C). Consistent with previous reports, mutants lacking FimV – either *fimV* or *fimV cyaB-R456L* – were unable to twitch (53, 125). Twitching was restored in both strains upon complementation with full-length FimV. However, the $FimV_{689}$ construct only restored ~31% of twitching relative to full-length FimV in the *fimV* background, and ~50% in *fimV cyaB-R456L*. The discrepancy between surface pilin levels and twitching likely reflects differences in the balance between pilus extension and retraction in these strains. For example, *cyaAB* mutants have almost no recoverable surface pili, but are motile (15), whereas *pilT* mutants are hyperpiliated but nonmotile. Given that the *fimV cyaB-R456L* mutant had high levels of PilU, and thus cAMP (Figure 2.4A), these data suggest that failure of $FimV_{689}$ to restore twitching is independent of its inability to activate CyaB.

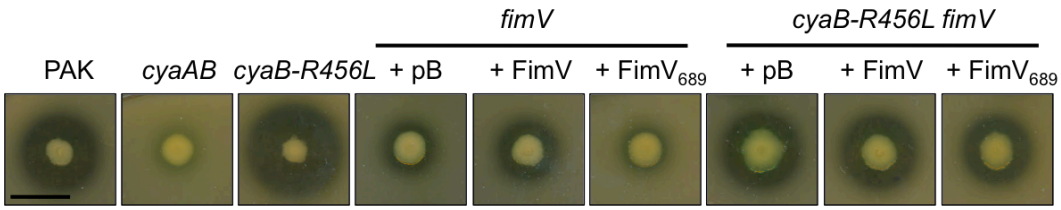

Figure 2.5. FimV TPR3 regulates type II secretion through modulation of cAMP levels. *fimV* and *fimV cyaB-R456L* were transformed with arabinose-inducible expression vectors encoding full-length FimV (FimV) or a truncation mutant lacking TPR3 ($FimV_{689}$). As controls, strains were also transformed with empty vector (pB), and representative high cAMP (*cyaB-R456L*) and low cAMP (*cyaAB*) strains were included. Cells were grown overnight and resuspended in PBS at OD_{600} 0.6. Two µl of resuspended cells were spotted onto trypticase soy broth/1.5% agar supplemented with 0.1% (wt/vol) arabinose and 2% (wt/vol) skim milk, and incubated for 40 h at 30°C. Elastase secretion was visualized as a zone of clearance around the bacterial colony. Secretion for each strain was measured as the difference between the diameter of the zone of clearance and the diameter of the colony (average of n = 3). Image is representative of n=3 experiments. Scale bar denotes 1 cm.

We next examined T2S in *fimV* and *fimV cyaB-R456L* complemented with $FimV_{689}$ (Figure 2.5). Transcription of T2S genes is cAMP-dependent (49), and FimV regulates T2S at least in part through the cAMP-binding protein, Vfr (134). We tested whether $FimV_{689}$ could complement defects in T2S by assessing casein hydrolysis using skim milk agar. *fimV* was defective for protease secretion, consistent with previous findings (134). Complementation with full-length FimV restored

~48% of T2S relative to wild type, while $FimV_{689}$ failed to restore secretion. The *fimV cyaB-R456L* mutant had ~70% of wild type T2S, suggesting that T2S is a mostly cAMP-dependent phenotype and thus likely to be indirectly regulated by FimV. Expression of FimV or $FimV_{689}$ in *fimV cyaB-R456L* did not increase secretion relative to the vector control, confirming that the involvement of FimV in T2S is cAMP-dependent.

FimV TPR3 interacts with FimL

Inclan *et al.* recently reported that the CyaB-activating component FimL interacts with FimV (135), but did not define the specific interaction domain. As FimL is a cytoplasmic protein, we tested if the TPR segments of FimV, TPR1 and 2 ($FimV_{488-618}$) or TPR3 ($FimV_{811-919}$) were sufficient to interact with FimL using a bacterial two-hybrid (BTH) assay. T18 or T25 fragments of *Bordetella pertussis* adenylate cyclase CyaB were fused to the C-termini of the entire cytoplasmic domain of FimV ($FimV_{488-919}$), $FimV_{488-618}$, $FimV_{811-919}$, and FimL, and the constructs expressed pairwise in *E. coli* BTH101 (Figure 2.6). As a positive control, we co-expressed FimL-T18 and PilG-T25 whose interaction was also reported by Inclan and colleagues (135). FimL interacted with $FimV_{488-919}$ and $FimV_{811-919}$ but not with $FimV_{488-618}$, suggesting that TPR3 alone was sufficient. These data provide additional evidence that the C-terminal domain of FimV plays an

important role in regulation of CyaB, via an interaction between TPR3 and FimL.

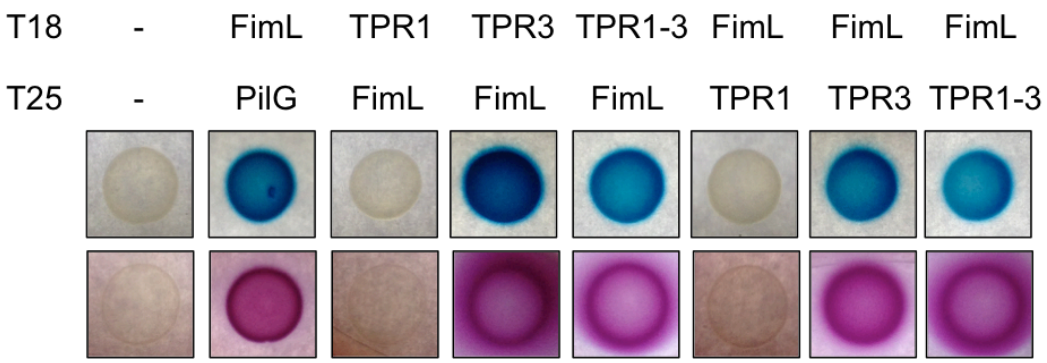

Figure 2.6. TPR3 interacts with FimL. Fusions of $FimV_{488-618}$, $FimV_{811-919}$, $FimV_{488-919}$, or FimL to *B. pertussis* CyaB T18 or T25 fragments were expressed in *E.coli* BTH101 in a pairwise manner. As a positive control, we used FimL-T18 and PilG-T25 (135). Single colonies form the transformations were resuspended in 5ml LB and incubated at 37°C overnight. A 5ml subculture using 100µl of each overnight culture was made the following morning and grown to OD_{600} 0.6. Five µl was then spotted onto MacConkey agar supplemented with 1% maltose and 0.5mM IPTG, and LB/1.5% agar with 100µl of 20mg/ml X-gal spread onto the surface and dried. Plates were incubated at 30°C for 24h. Protein-protein interaction is visualized by pink growth on MacConkey agar, or blue growth on LB + X-gal, indicating protein-protein interaction and reconstitution of *B. pertussis* CyaB function.

Structure of the conserved C-terminal TPR3-containing domain

To gain further insight into FimV function, we initially attempted to solve the structure of the entire cytoplasmic domain; however, its large

predicted unstructured region made the construct highly susceptible to degradation, and smaller fragments – while soluble even at high concentrations – failed to crystallize. Because of its pronounced conservation – and mutant phenotypes that suggested TPR3 plays a key role in FimV's virulence-related functions – we focused on solving the crystal structure of the C-terminal region. Using the predicted boundaries of the TPR3 region, we generated a construct spanning residues 862-919 ($FimV_{862-919}$), for structure determination.

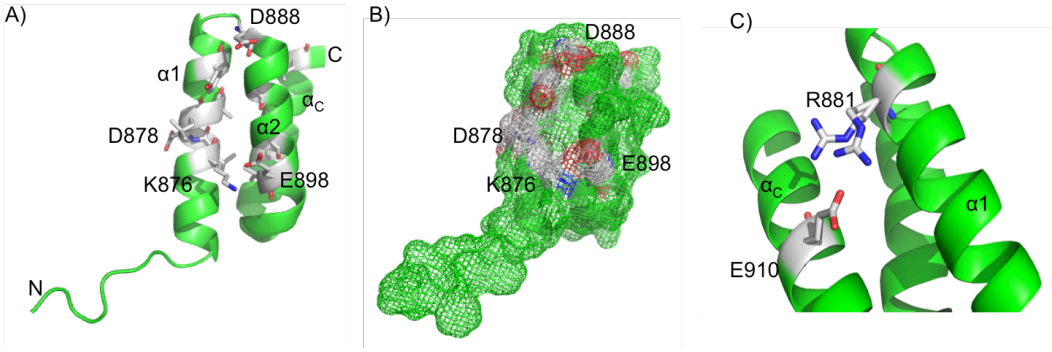

Figure 2.7. X-ray Crystal structure of the FimV C-terminal domain. The X-ray crystal structure of SeMet FimV TPR3 (residues 862-919) was solved to 2.05 Å (PDB ID: 4MAL). (A) Chain A is shown, with identified conserved residues shown as sticks. Conserved charged residues are labeled directly. The two α-helices making up the TPR and the capping helix have been labeled as α1, α2, and α_C. (B) Surface mesh representation of 4MAL Chain A from the same view as panel A. Conserved charged residues are shown as white patches. (C) Residue R881 was observed to occupy two different states. Two-thirds of the time, R881 was in close proximity to E910, likely forming a salt bridge between α1 and α_c.

The structure of $FimV_{862-919}$ was solved by SAD phasing with SeMet-labelled protein. SeMet $FimV_{862-919}$ crystallized as a dimer in the space group $P4_12_12$. The final model was refined to 2.05 Å (PDB ID: 4MAL). Native $FimV_{862-919}$ crystallized in space group $P2_12_12_1$ and contained six copies of the protein in the asymmetric unit, arranged as two trimers. The final model for native $FimV_{862-919}$ was refined to 2.01 Å (PDB ID: 4MBQ). Statistics for data collection and model refinement are presented in Table 2.3.

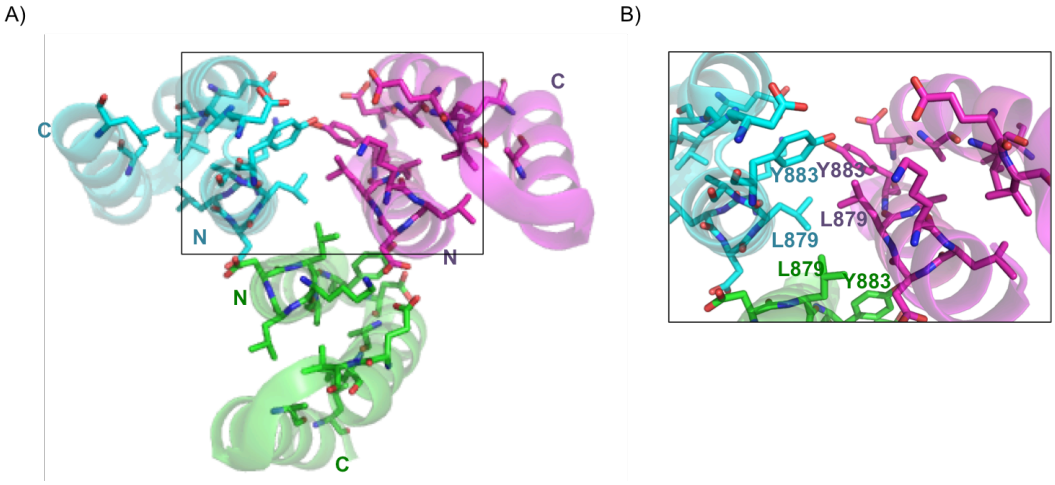

Figure 2.8. X-ray crystal structure of FimV C-terminal domain homotrimer. The X-ray crystal structure of native FimV TPR3 was solved to 2.01 Å (PDB ID: 4MBQ). Individual monomers are colored in cyan, green, or magenta. Highly conserved residues are shown as sticks with side chains colored by monomer. Residues, N-, and C- termini are labeled in cyan, green, or magenta based on the associated monomer. Residues are numbered based on their position in full length FimV. The outlined rectangular area is enlarged in the right panel.

$FimV_{862-919}$ includes the conserved FimV C-terminal domain (TIGR03504), which consists of two antiparallel α-helices forming the predicted TPR motif, followed by a C-terminal capping helix, which may play a role in enhancing solubility (127) (Figure 2.7A). The SeMet labelled structure (PDB ID: 4MAL) contained two biological assembly monomers (Chain A is shown in Fig. 2.7). Each monomer had three α-helices, with hydrophobic residues directed between the three helices and hydrophilic residues extending outwards. Surface representation suggests that conserved charged residues (Figure 2.2B) are located primarily on one face of TPR3 (Figure 2.7B). The side chain of R881 was found in two possible conformations (Figure 2.7C), one of which formed a salt bridge with E910 on the capping helix in two-thirds of monomers.

FimV native crystals contained two similar trimeric assemblies within the asymmetric unit (PDB ID: 4MBQ; Fig. 2.8). Subunits within each trimer associated primarily through helix 1 of neighbouring monomers, and were arranged with helix 1 of each TPR at the center with the capping helix facing outwards (Figure 2.10, right panel). Conserved hydrophobic residues of each TPR motif were arranged in the center of a trimer, with hydrophilic residues from helix 2 and the capping helix facing outwards. Structural comparison of individual protomers from the SeMet and native structures showed that despite differences in crystal and monomer packing, they were very similar, with root mean square deviation

(RMSD) values of 0.64 Å or less (Supplementary Table S1). The closest structural hit to 4MAL and 4MBQ as predicted by DaliLite (160, 161) (RMSD 1.51 Å over 49 residues) was the type III secretion system chaperone, IpgC (PDB ID: 3GZ1), a small, negatively-charged all α-helical protein that escorts partly unfolded *Shigella flexneri* effectors IpaB and IpaC to the base of the secretion apparatus (162).

Our data suggest that FimV plays key roles in both cAMP-dependent and independent regulation of virulence factor function, and that its conserved TPR3 region is critical for both roles. Previously identified cytoplasmic regulators of CyaB, FimL and PilG (55, 56) all require FimV for function (135), connecting FimV to surface mechanosensing through the Chp system. Loss of an indirect FimV-PilG interaction through loss of FimL binding may explain the inability of $FimV_{689}$ to complement either cAMP-dependent and independent phenotypes, as PilG functions in both pathways (55).

FimL failed to interact with TPR1 and 2 (Figure 2.6), but other regulatory components may bind these motifs. Since TPRs typically form superhelical structures composed of 3 or more repeats, it is possible that transient interactions of the region between TPRs 1 and 2 and TPR3 with specific regulatory components might lead to its restructuring, bringing the three into proximity to form a new interface for protein binding. Studies of the $p67^{phox}$ subunit of phagocyte NADPH suggested that the linker region

between TPR motifs can bind target proteins (163). The linker regions in *N. meningitidis* TspA, *V. cholerae* HubP, and *L. pneumophila* FimV each contain different sets of multiple tandem repeats (128, 132, 133) – which are absent or degenerate in *Pseudomonas* – and alteration of repeat numbers influenced pigmentation, cell length, and twitching in *Legionella* (132) and abolished interactions with some partners of *Vibrio* HubP (128). These differences may reflect the individual repertoires of interaction partners in each species.

The conservation of TPR3 among divergent species suggests that it might interact with a component that is widely conserved. Here we showed interactions of TPR3 and FimL, while the C-terminus of *V. cholerae* HubP (which is 45% identical to *P. aeruginosa* TPR3 over 42 residues) interacts with FlhG, a protein responsible for controlling flagellar polar localization (128). This finding raises the possibility that FimV could have a broader role in sub-cellular spatial organization in *P. aeruginosa.* While both *P. aeruginosa* and *L. pneumophila* encode FlhG orthologs called FleN (164, 165), *Neisseria* lacks flagella and thus FlhG/FleN orthologs, arguing against the evolutionarily conserved partner hypothesis. In *V. cholerae*, deletion of HubP's C-terminus failed to mislocalize another of its interaction partners, ParA1, suggesting that like FimV, it has multiple cytoplasmic protein-protein interaction domains specific for different partners.

Self-interactions mediated by hydrophobic residues were observed in TPR3 crystals (Figure 2.8, right panel), but it is not yet clear if those are physiologically relevant. The remarkably well-conserved TPR3 unit could also potentially contribute to intermolecular interactions, promoting the functional oligomerization of FimV monomers. TPR motif-dependent homo-oligomerization has been reported in yeast (166) and bacteria (167). In *Escherichia coli*, trimerization of YbgF – part of the Tol system – is mediated by a single C-terminal TPR motif (167). Involvement in self-interactions might explain why this region is conserved among very diverse FimV/HubP family members. However, we saw no TPR3-TPR3 interactions in a BTH assay (data not shown), arguing against self-interactions as a driver of sequence conservation.

Wehbi et al. (125) showed that the LysM motif of FimV was required for optimal PilQ multimerization, and that the periplasmic and cytoplasmic domains of FimV could reconstitute FimV function when expressed individually. However, our prediction that the periplasmic and cytoplasmic domains had separate structural and regulatory roles was not supported by the phenotype of the $FimV_{689}$ complemented strains. TPR3 is required to promote cAMP synthesis by CyaB, likely through its FimL interaction; however, $FimV_{689}$ only partly restored piliation and motility in the cAMP-replete *fimV cyaB-R456L* background, suggesting that TPR3 is important for cAMP-independent function(s) of FimV as well. Efforts to

define the full repertoire of protein interaction partners of *P. aeruginosa* FimV are ongoing.

ACKNOWLEDGEMENTS

This work was supported by Canadian Institutes of Health Research grant MOP 93585 to LLB and PLH; and MOP 89903 to MSJ and by National Institutes of Health grant R01GM072285 to IBZ. All X-ray diffraction data used in this study were collected at beamline X29 of the National Synchrotron Light Source. NSLS funding came primarily from the Offices of Biological and Environmental Research and of Basic Energy Sciences of the U.S. Department of Energy and from the National Center for Research Resources (Grant P41RR012408) and the National Institute of General Medical Sciences (Grant P41GM103473) of the National Institutes of Health.

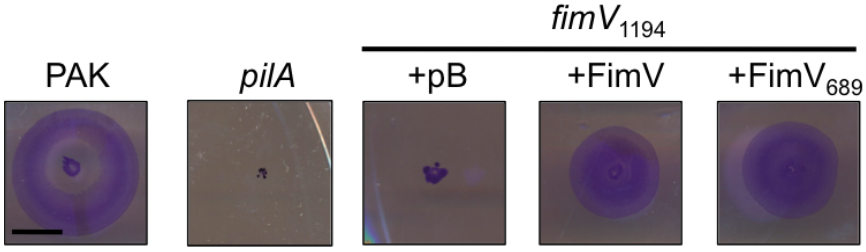

Figure S2.1. FimV$_{689}$ is functional. A mutant of *fimV* that expresses only the cytoplasmic region of the protein (*fimV*$_{1194}$) was transformed with arabinose-inducible expression constructs encoding either full length FimV or a truncation mutant lacking TPR3 (FimV$_{689}$). As a control, *fimV*$_{1194}$ was also transformed with empty vector (pB). Twitching motility was determined by stab inoculation of the strains into LB 1% agar supplemented with 0.1% (wt/vol) arabinose. Strains were incubated for 16 h, and twitching zones were visualized by removing the agar layer and staining the bacteria with 1% (wt/vol) crystal violet. Motility was measured as the diameter of the stained twitching zone. Scale bar denotes 1 cm.

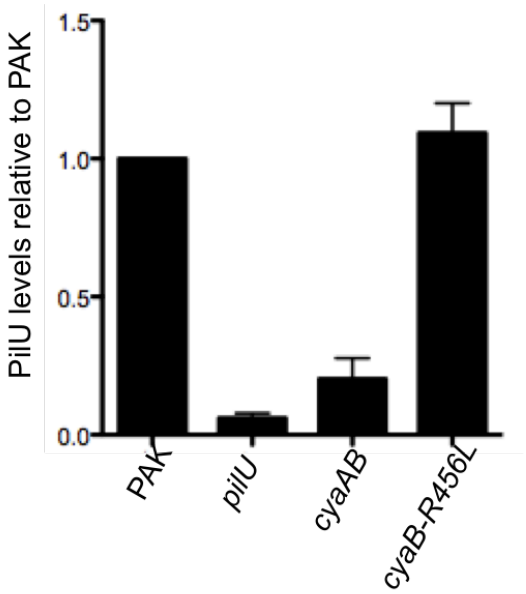

Figure S2.2. PilU levels are positively correlated with intracellular cAMP levels. Levels of PilU were determined by preparing cell lysates as described in the Methods, of wild type PAK, *pilU*, a mutant lacking the major adenylate cyclases (*cyaAB*), and a point mutant encoding a constitutively active adenylate cyclase (*cyaB-R456L*) (107) grown overnight on LB 1.5% agar. Samples were resolved by SDS-PAGE and transferred to a nitrocellulose membrane. PilU was visualized by immunoblotting with anti-PilU antiserum. Densitometric analysis (average of n = 3) was carried out using ImageJ, normalizing band intensity of the PilU band to a nonspecific control band, and shown as a percentage of the normalized band intensity of wild type ± standard error.

Table 2.1. Strains and plasmids used in this study

Strain or Plasmid	Description	Source
P. aeruginosa		
PAK	*Pseudomonas aeruginosa* strain K	(55)
PAK *pilA*	PAK with deletion of *pilA*	(168)
PAK *pilU*	PAK with deletion of *pilU*	Matthew C. Wolgang
PAK *cyaAB*	PAK with deletions of *cyaA* and *cyaB*	(55)
PAK *cyaB-R456L*	PAK with arginine to leucine substitution in *cyaB* at amino acid position 456	This study
PAK *fimV*	PAK with deletion of *fimV*	(55)
PAK *cyaB-R456L fimV*	PAK with deletion of *fimV* and arginine to lysine substitution in *cyaB* at amino acid position 456	This study
PAK $fimV_{1194}$	PAK with an FRT insertion at nucleotide position 1194 of *fimV*	This study
E. coli		
BL21 (DE3)	*E. coli* protein overexpression strain	Invitrogen
B834 (DE3)	Methionine auxotrophic protein expression strain	Invitrogen
BTH101	Bacterial two-hybrid system reporter strain	Euromedex
Plasmids		
pRK793	IPTG-inducible expression vector encoding tobacco etch virus protease	(153)
pBADGr	Arabinose inducible protein expression vector	(169)
pBADGr::*fimV*	Arabinose inducible vector encoding full length FimV	This study
pBADGr::$fimV_{689}$	Arabinose inducible vector encoding FimV from residues 1-689	This study

pET151/D-TOPO::*fimV*$_{862\text{-}919}$	IPTG-inducible protein over-expression vector encoding FimV from residues 862-919	This study
pKNT25	IPTG-inducible expression vector encoding T25 fragment of *B. pertussis* CyaB	Euromedex
pKNT25::*fimV*$_{488\text{-}618}$	IPTG-inducible expression vector encoding T25 fragment of *B. pertussis* CyaB fused to the C-terminus of FimV TPR1+2	This study
pKNT25::fimV$_{811\text{-}919}$	IPTG-inducible expression vector encoding T25 fragment of *B. pertussis* CyaB fused to the C-terminus of FimV TPR3	This study
pKNT25::*fimL*	IPTG-inducible expression vector encoding T25 fragment of *B. pertussis* CyaB fused to the C-terminus of FimL	This study
pKNT25::*pilG*	IPTG-inducible expression vector encoding T25 fragment of *B. pertussis* CyaB fused to the C-terminus of PilG	This study
pUT18	IPTG-inducible expression vector encoding T18 fragment of *B. pertussis* CyaB	Euromedex
pUT18::*fimV*$_{488\text{-}618}$	IPTG-inducible expression vector encoding T18 fragment of *B. pertussis* CyaB fused to the C-terminus of FimV TPR1+2	This study
pUT18::fimV$_{811\text{-}919}$	IPTG-inducible expression vector encoding T18 fragment of *B. pertussis* CyaB fused to the C-terminus of FimV TPR3	This study
pUT18::*fimL*	IPTG-inducible expression vector encoding T18 fragment of *B. pertussis* CyaB fused to the C-terminus of FimL	This study

Table 2.2. Oligonucleotides used in this study

Primer Name	Sequence
cyaB-R456L F1	5' - GCGGGTACCTTCACCGCACTGGTCATCG - 3'
cyaB-R456L R1	5' - GCGTCTAGAAAGTCAACGGAGTCGTCACC - 3'
cyaB-R456L SDM F	5' - TGCAACAGGCCGCCGAGCTCCTGCGCGACAA GGTC - 3'
cyaB-R456L SDM R	5' - GACCTTGTCGCGCAGGAGCTCGGCGGCCTGT TGCA - 3'
$fimV_{862-919}$ F	5’ - CACCGATGACTTCGACTTCCTCTCCGGTGC - 3’
$fimV_{862-919}$ R	5’ - TCAGGCCAGGCGCTCCAGCAACTC - 3’
FimV F	5' - TTAGTACTAAGGGATTACACTATGGTTCGGCT - 3'
FimV R	5' - CAGTTCTAGATCAATGGTGATGGTGATGATGG GCCAGGCGCTCCAGCAACTC - 3'
FimV689 F	5' - TAAGAATTCCAAGGGATTACACTATGGTTCGGC TT - 3'
FimV689 R	5' - AATAAGCTTTCAGAGGTCGGCCTGCACGTCG - 3'
B2H FimV TPR1F	5' - GCGTCTAGAGATGAATGCGCAGAAAGAGAAGG - 3'
B2H FimV TPR1R	5' - GCGGGTACCGCCTTGAGCTGCTCGAC - 3'
B2H FimV TPR3F	5' - GCGTCTAGAGATGGAGAAGGGCGAGGACAG - 3'
B2H FimV TPR3R	5' - GCGGGTACCGCGGCCAGGCGCTCCAG - 3'
B2H FimL-F	5' - GCG TCT AGA GAT GGT CAC AGG AGC CAC GTC CC - 3'

B2H FimL-R	5' - GCG GGT ACC GCG GCG GCC ACC GG - 3'
B2H PilG-F	5' - GCG TCT AGA AAT GGA ACA GCA ATC CGA CGG - 3'
B2H PilG-R	5' - TAA GGT ACC CGG GAA ACG GCG TCC ACC - 3'

Table 2.3. Data collection and refinement statistics

Data Collection	**SeMet-FimV**	**Native-FimV**
Beamline	NSLS X29	NSLS X29
Wavelength (Å)	0.9791	1.075
Space group	$P4_12_12$	$P2_12_12_1$
a, b, c (Å)	42.33, 42.33, 139.48	34.0, 58.5, 136.7
α, β, γ (°)	90.0, 90.0, 90.0	90.0, 90.0, 90.0
Molecules per ASU	2	6
Resolution (Å)	50.0-2.05 (2.09-2.05)	50.0-2.00 (2.07-2.00)
Total Reflections	122397	246901
Unique Reflections	8648 (412)	18054 (1394)
Redundancy	14.2 (11.1)	13.7 (10.6)
Completeness (%)	99.9 (99.3)	94.6 (76.2)
Mean I / σI	33.9 (6.2)	20.8 (2.5)
R_{merge} (%) ∓	7.2 (47.8)	15.1 (78.1)
Refinement		
R_{work} / R_{free} (%) ♯	21.5 / 24.2	20.8 / 25.8
Resolution (Å)	40.50-2.05	44.45-2.01
Reflections ¥	8,314	17,404
Atoms	984	2244
Protein	949	2159
Water	35	85
RMSD		
Bond lengths (Å)	0.013	0.002
Bond angles (°)	1.042	0.541
Average B (Å^2) £	38.8	39.8
Protein	38.8	39.7
Water	40.4	42.2
Coordinate error (Å) €	0.23	0.25
Ramachandran statistics (%)		
Ψ	95.97	99.31
Most Favoured regions	4.03	0.69
Allowed regions	0.00	0.00
Disallowed regions	4MAL	4MBQ
PDB ID		

Note: Values in parentheses correspond to the highest resolution shell.
∓, $R_{merge} = \sum_{hkl} \sum_i | I_i(hkl) - (I(hkl)) | / \sum_{hkl} \sum_i I_i(hkl)$

[♯], $R_{work} = \sum | |F_{obs}| - k|F_{calc}| | / |F_{obs}|$ where F_{obs} and F_{calc} are the observed and calculated structure factors, respectively. R_{free} is the sum extended over a subset of reflections (9.92 and 10.08% for Selmet and Native, respectively) excluded from all stages of the refinement.
[¥], Only reflections with Fobs/σ(Fobs) ≥ 1.34 were used for SeMet-FimV model refinement. All unique reflections in the resolution range 44.45-2.01 Å were included without further cut off criteria for refinement of Native-FimV.
[£] As calculated using Phenix Refine (155, 156).
[€], Maximum-likelihood based Coordinate Error, as determined by PHENIX (170).
[Ψ], As calculated using MolProbity (171)

CHAPTER THREE

cAMP-independent control of twitching motility in *Pseudomonas aeruginosa* by FimV

Preface

Chapter Three consists of the following manuscript for publication:

Buensuceso RNC, Daniel-Ivad M, Kilmury SLN, Harvey H, Howell PL, Burrows LL. 2016. cAMP-independent control of twitching motility in *Pseudomonas aeruginosa* by FimV.

Attributions: R.N.C.B. cloned plasmids, performed western blot and SDS-PAGE analyses, twitching motility assays, swimming assays, and fluorescent microscopy. S.L.N.K. cloned the bacterial two-hybrid and fluorescent fusion constructs. H.H. generated mutants. R.N.C.B. and L.L.B. designed the experiments. R.N.C.B., P.L.H., and L.L.B. wrote the manuscript.

cAMP-independent control of twitching motility in *Pseudomonas aeruginosa* by FimV

Ryan N.C. Buensuceso[1], Martin Daniel-Ivad[1], Sara L.N. Kilmury[1], Hanjeong Harvey[1], P. Lynne Howell[2] and Lori L. Burrows[1]

[1] Department of Biochemistry and Biomedical Sciences, and the Michael G. DeGroote Institute for Infectious Diseases Research, McMaster University, Hamilton, ON

[2] Program in Molecular Structure and Function, Hospital for Sick Children, Toronto, ON and Department of Biochemistry, University of Toronto, Toronto, ON

ABSTRACT

FimV is a *Pseudomonas aeruginosa* inner membrane protein implicated in regulating levels of the important second messenger, cyclic AMP (cAMP), by activating the adenylate cyclase CyaB. FimV mutants lack type IV pilus (T4P)-associated twitching motility; have decreased levels of T4P components PilMNOPQ, and decreased levels of cAMP. FimV is a putative 'hub' protein, containing multiple protein-protein interaction motifs that could bind various partners. Here we show that FimV regulates twitching motility in both cAMP-dependent and –independent ways. Using epistasis analyses, we found that the response regulator of the pilus-associated Chp chemotaxis system, PilG, required both FimV and the CyaB regulator, FimL, to activate CyaB. However, in backgrounds lacking the cAMP phosphodiesterase CpdA, or expressing a constitutively-active CyaB enzyme, *pilG* and *fimV* mutants did not twitch, highlighting their cAMP-independent roles in twitching motility. Unlike the hub proteins characterized in other bacteria, FimV had little effect on swimming motility. The FimV LysM motif, which interacts with peptidoglycan to localize the protein to the poles, was dispensable for CyaB activation but required for wild type levels of twitching. Both cytoplasmic and periplasmic domains of FimV were important for its cAMP-dependent and –independent roles. Lastly, we show that FimV is required for localization of a key regulator of PilA transcription, PilS,

providing evidence that FimV is required for localization of T4P regulatory proteins in addition to those of the Chp pathway.

INTRODUCTION

Type IV pili (T4P) are polar filamentous surface appendages made by a broad range of bacteria and archaea (2, 5). They can be divided into two sub-families, type IVa (T4aP) and type IVb (T4bP), which differ in their pilin subunit architecture, and organization of their assembly systems (5). T4aP are involved in several processes, including DNA uptake, surface attachment, and twitching motility (3, 4, 6). During twitching motility, T4aP undergo repeated cycles of assembly and disassembly, acting as molecular grappling hooks to pull cells along a surface. Well-studied T4aP model species include *Neisseria spp.*, *Myxococcus xanthus*, and *Pseudomonas aeruginosa* (16, 172). Although they share core structural components of the T4P assembly machinery and the pilus fibre, each species has evolved unique regulatory elements that control the function of the assembly machinery in response to specific environmental requirements. Without these regulatory proteins, the bacteria make intact but non-functional T4aP systems.

The Chp system of *P. aeruginosa* is a putative chemosensory system that controls twitching motility and intracellular levels of cyclic adenosine monophosphate (cAMP), and resembles the well-studied Che system of *E. coli* (50, 51, 93). It includes a ligand binding methyl-accepting chemotaxis (MCP) protein, PilJ; an adaptation methyltransferase and methylesterase, PilK and ChpB; and a complex multidomain histidine

kinase, ChpA. However, the Chp system lacks a CheZ-like phosphatase. Rather, similar to *Sinorhizobium meliloti* (67), it has two CheY-like response regulators, PilG and PilH (51, 92). PilG is proposed to regulate activation of CyaB and pilus extension (55), while PilH has been proposed to be either a phosphate sink that limits downstream signalling in lieu of a phosphatase, as in *S. meliloti* (55, 91), or a separate response regulator controlling function of the T4aP retraction ATPase (93).

The Chp system also positively regulates levels of intracellular levels of cAMP by activating the major adenylate cyclase, CyaB (55). Deletion of *pilG* results in decreased cAMP, surface piliation, and twitching motility, while deletion of *pilH* has the opposite effect – increased cAMP and surface piliation – but decreased motility (55). Supplementation of a *pilG* mutant with extracellular cAMP restored surface piliation but not twitching motility (55), suggesting that PilG regulates pilus biogenesis and function by at least two pathways. A recent study showed that of the two proteins, PilH is the preferred target of ChpA phosphorylation (91). Decreased motility in the *pilH* background may reflect hyperphosphorylation of PilG, perturbation of the chemotactic response, and uncoordinated movement.

Important for *P. aeruginosa* virulence is a switch from planktonic to sessile physiological states when cells bind to biotic or abiotic surfaces. T4aP have been proposed to function as mechanosensors that signal

through the Chp system to regulate surface-associated virulence phenotypes, including biofilm formation and enzyme secretion (88, 89). The putative mechanosensory adhesin PilY1 participates in surface attachment, triggering the surface sensing signalling cascade via the PilMNOP alignment complex (31, 48, 88, 89). T4aP-mediated surface sensing stimulates Chp signalling and CyaB activity. A transcriptional regulator called virulence factor regulator (Vfr), binds cAMP and modulates the expression of >200 genes, including the type II secretion system (T2SS) and its effectors, and T4aP assembly components including the motor ATPases PilBTU, the inner membrane alignment subcomplex PilMNOP, the outer membrane secretin, PilQ, and the PilSR regulatory proteins (49). This circuitry allows for increased expression of components required for a sessile lifestyle only under appropriate conditions.

Other proteins affecting T4aP expression and function include FimL and FimV (39, 49, 50, 56). FimL is a polar, cytoplasmic cAMP regulatory protein that is required for surface piliation and motility (54, 56). It has 51% similarity to the amino-terminus of ChpA, containing histidine and threonine phosphotransfer sites, although its putative phosphoacceptor residues are replaced by glutamine (54). FimL is involved in regulation of cAMP levels, as decreased twitching motility and low intracellular cAMP in

mutants lacking *fimL* were rescued by deletion of *cpdA,* which encodes a cAMP phosphodiesterase (56, 136).

FimV is a large inner membrane protein with one transmembrane domain. Its periplasmic region contains a lysin motif (LysM) that binds peptidoglycan (PG) (141), and its cytoplasmic region contains three discontinuous tetratricopeptide repeat (TPR) motifs, involved in protein-protein or protein-carbohydrate interactions (142). TPR motifs are helical hairpins of ~34 amino acids, typically arranged in tandem repeats of 3-16 units forming a superhelix, although individual repeats can be separated from larger clusters (142). FimV homologs have been identified in other T4P-producing bacteria (53) although sequence similarity is low, with the most conserved features being the LysM motif, the single transmembrane segment, and a highly conserved cytoplasmic "FimV C-terminal domain" – TIGR03504 – encompassing a single TPR repeat and capping helix (173). FimV homologs are not limited to bacteria that produce T4P (174), suggesting they may have additional roles in bacterial physiology.

FimV homologs have been characterized in *Neisseria gonorrhoeae*, *N. meningitidis*, *Legionella pneumophila*, *Vibrio cholerae*, and *Shewanella putrifaciens* (53, 128-130, 132, 133, 174). However, their functions are not conserved across species. Deletion of FimV in *L. pneumophila* results in loss of twitching motility and cell elongation, while deletion of the *N. meningitidis* FimV homolog TspA had no effect on twitching motility or

surface piliation, but led to decreased host cell adhesion. The *V. cholerae* homolog of FimV, HubP, functions as a protein interaction hub, although its role is not limited to motility. Deletion of HubP alters the cellular distribution of the chemotactic and flagellar machinery, and the chromosomal origin, *oriCI* (128). HubP from *S. putrifaciens* is responsible for localization of the chemotactic machinery, but not the flagellar system (129). Yamaichi et al. (128) showed that localization of HubP was dependent on the LysM motif, a domain that is conserved among the FimV family of proteins (COG3170)(173). The studies of *L. pneumophila* FimV and *N. meningitidis* TspA (130, 132) did not address the role of the LysM motif or localization in function, but their mutant phenotypes might relate to mislocalization of motility or adhesion systems.

Wehbi et al. (125) showed that *P. aeruginosa fimV* mutants have decreased levels of the T4aP alignment subcomplex proteins, PilMNOP. Mutants with an in-frame deletion of the LysM motif had fewer PilQ multimers, suggesting that PG binding is important for optimal formation of the secretin. Interestingly, the cytoplasmic and periplasmic domains of FimV could reconstitute the function of full-length FimV when co-expressed, suggesting that the two fragments may have independent roles. Michel et al. (134) also showed that FimV is important for secretion of elastase via the T2SS when bacteria were grown on solid media. Importantly, FimV was identified in a transposon mutant screen as a

positive regulator of CyaB, the primary source of cAMP in *P. aeruginosa* (55).

Fulcher et al. (55) showed that twitching requires both cAMP-dependent and independent inputs. Supplementation of mutants lacking the Chp response regulator PilG with exogenous cAMP restored piliation but not motility. FimV also has a cAMP-independent role in twitching, as a mutant lacking FimV but expressing a constitutively active CyaB was also unable to twitch (173). FimL was recently proposed to link PilG to FimV in the mechanosensory pathway leading to CyaB activation (135), and FimV was necessary for localizing FimL and PilG to the cell poles. However, the proposed FimV-FimL-PilG interaction model fails to explain the cAMP-independent roles of FimV and PilG in twitching. Here, we examined the cAMP-independent role of FimV in the regulation of twitching motility. Using epistasis analyses, we show that FimV and PilG have distinct cAMP-independent roles in regulation of twitching motility. We show that many of the previously described phenotypes of mutants lacking *fimV* – decreased T2S, decreased PilMNOP and PilQ multimerization – are strictly cAMP-dependent. Loss of FimV also causes mislocalization of PilS, a membrane-bound sensor kinase that controls *pilA* transcription. Our data show that FimV plays a central, cAMP-independent role in twitching that is distinct from that of the Chp system.

RESULTS

FimV is required for Chp activation of CyaB

FimV, PilG, and FimL are all required for activation of CyaB, with FimL proposed to be a scaffold protein that links FimV to the Chp system through PilG (55, 56, 135, 175). However, while phenotypes associated with *fimL* deletion could be rescued by deletion of *cpdA* or increasing intracellular cAMP levels in other ways (56, 135, 136), provision of exogenous cAMP failed to restore motility in a *pilG* mutant (55). We investigated if the cAMP-independent function of PilG required FimV by comparing PilU levels – a proxy for cAMP levels (49, 173) – twitching, and piliation in *fimV*, *fimL*, and *pilG* single mutants or in double mutants also lacking *cpdA* (56) (Figure 3.1). Previously, we showed that a constitutively active form of CyaB (*cyaB-R456L*), originally identified in a *pilG* background (107), could increase intracellular cAMP levels in a *fimV* background (173). Here, we sought to determine if native CyaB was active in our mutants, so we deleted *cpdA* to prevent degradation of intracellular cAMP. To confirm that FimV and FimL were epistatic to PilG, we also examined *fimV pilH* and *fimL pilH* double mutants, that in the absence of PilH, are predicted to have hyperactive PilG, and hence higher levels of cAMP (55, 91).

A)

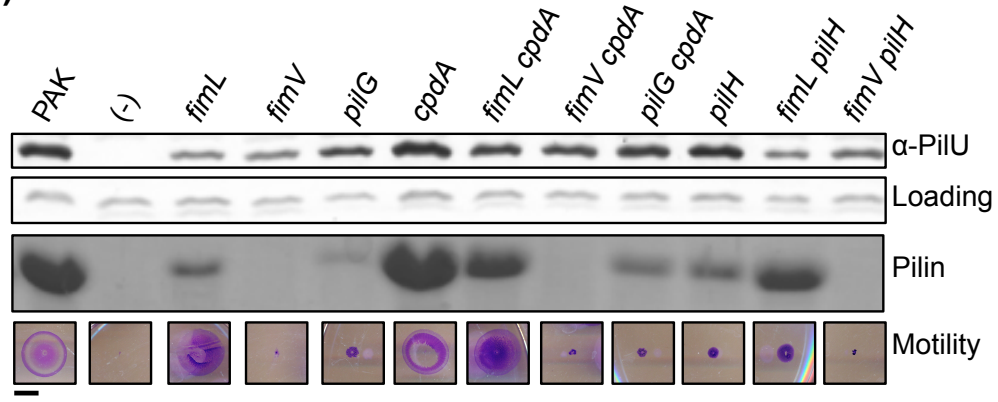
PAK
(-)
fimL
fimV
pilG
cpdA
fimL cpdA
fimV cpdA
pilG cpdA
pilH
fimL pilH
fimV pilH
α-PilU
Loading
Pilin
Motility

B)

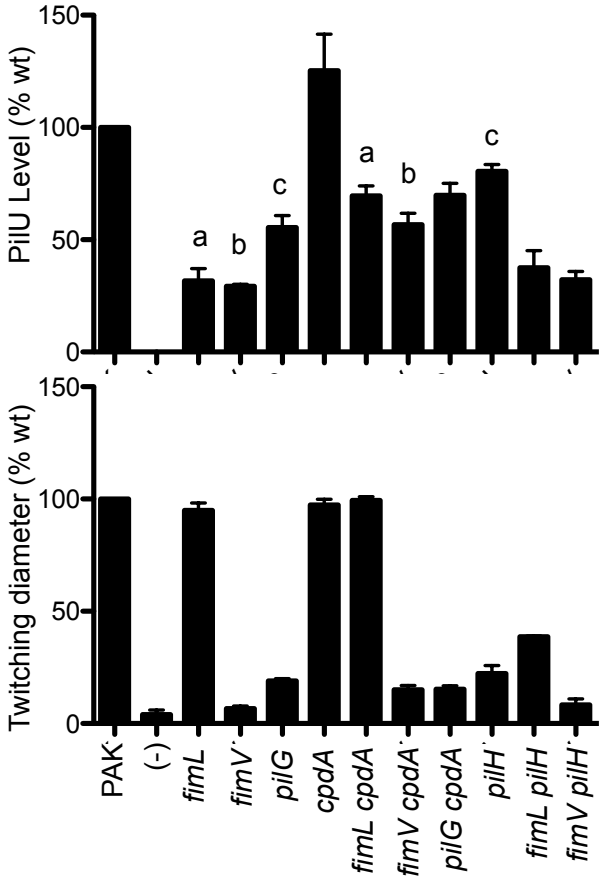
PilU Level (% wt)
150
100
50
0
a
b
c
a
b
c
Twitching diameter (% wt)
150
100
50
0
PAK
(-)
fimL
fimV
pilG
cpdA
fimL cpdA
fimV cpdA
pilG cpdA
pilH
fimL pilH
fimV pilH

Figure 3.1 – The Chp system requires FimV and FimL to activate CyaB. Cell lysates of the indicated strains were prepared as described in the Methods from cells grown on LB 1.5% (w/v) agar. Cell lysates were resolved on 12.5% SDS-PAGE and transferred to a nitrocellulose membrane. PilU was visualized by immunoblotting with anti-PilU antiserum. Levels of surface pilins were assessed by sheared surface protein preparation of strains grown on LB 1.5% agar supplemented with 0.1% (w/v) arabinose. The surface protein fractions were prepared as described in the Methods, and resolved by 12.5% SDS-PAGE and visualized by coomassie blue staining. Twitching motility was determined by stab inoculation of the indicated strains into LB 1% (w/v) agar. Strains were incubated for 16 h, and twitching zones were visualized by removing the agar layer and staining the bacteria with 1% (w/v) crystal violet. Scale bar denotes 1 cm. As a negative control for surface pilins and twitching, a *pilA* mutant was included. (B) Densitometric quantification of PilU levels, and quantification of twitching zones ± standard error. Data are representative of n=3 experiments. Bars labeled as ^{a,b,c} represent paired samples compared by student's t-test with $p < 0.05$.

As predicted (53, 55, 56, 93), *fimV*, *fimL*, and *pilG* mutants all had decreased levels of PilU, and decreased surface piliation (Figure 3.1). Both *pilG* and *fimV* were twitching deficient, while *fimL* twitched similar to wild type. The *cpdA* mutant had high levels of PilU, surface piliation, and wild type twitching, consistent with a high cAMP phenotype (55, 56). Deletion of *cpdA* in the *fimV*, *fimL*, or *pilG* backgrounds increased PilU levels relative to the corresponding single mutants (Figure 3.1). However, only the *fimL cpdA* mutant was motile, confirming that PilG and FimV have

cAMP-independent roles in T4P function. Furthermore, lack of twitching and piliation in the *fimV cpdA* mutant suggests that the cAMP-independent function of PilG requires FimV. Consistent with previous reports (55), the *pilH* mutant assembled surface pili and had high levels of PilU, but did not twitch. The *fimV pilH* and *fimL pilH* double mutants had PilU levels similar to those of *fimV* and *fimL* single mutants, suggesting that despite being hyperactive in the absence of *pilH*, PilG was unable to activate CyaB without FimV or FimL, confirming that both FimV and FimL are required for the Chp system to stimulate cAMP synthesis.

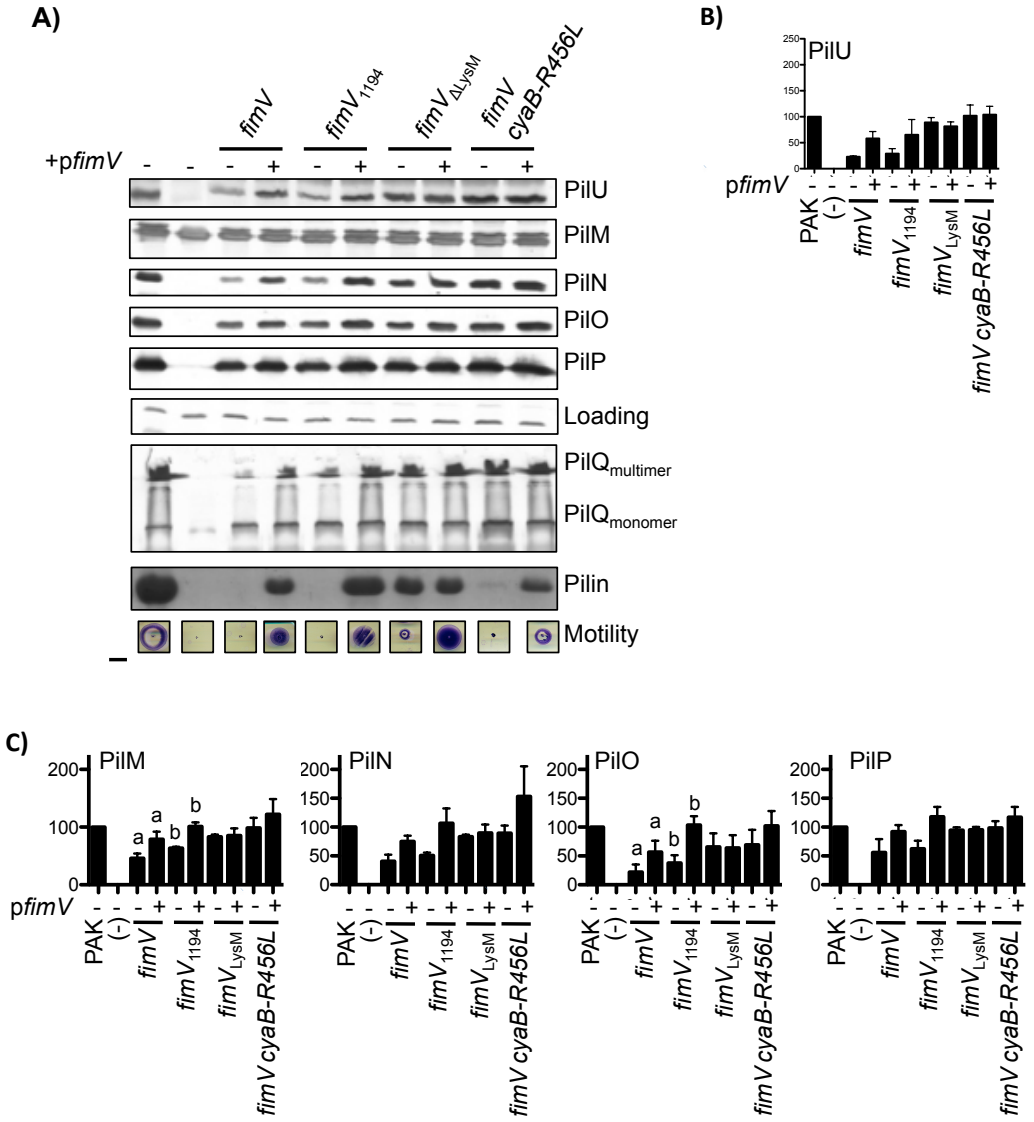

Figure 3.2 – FimV has cAMP-dependent and independent contributions to T4P function. *fimV, fimV*$_{1194}$*, fimV*$_{\text{LysM}}$, and *fimV cyaB-R456L* were transformed with arabinose-inducible expression vectors encoding full-length FimV (FimV) or as a control, with empty vector (pB). Cell lysates prepared as described in the Methods from cells grown on LB 1.5% agar supplemented with 0.1% (w/v) arabinose were resolved on 12.5% SDS-PAGE and transferred to a nitrocellulose membrane. Proteins were visualized by immunoblotting with antisera specific to PilU, or PilM,

PilN, PilO, PilP, or PilQ. Levels of surface pilins were assessed by sheared surface protein preparation of strains grown on LB 1.5% agar supplemented with 0.1% (w/v) arabinose. The surface protein fractions were prepared as described in the Methods, and resolved by 12.5% SDS-PAGE and visualized by coomassie blue staining. Twitching motility was determined by stab inoculation of the indicated strains into LB 1% (w/v) agar. Strains were incubated for 16 h, and twitching zones were visualized by removing the agar layer and staining the bacteria with 1% (w/v) crystal violet. Scale bar denotes 1 cm. (B) Densitometric quantification of PilU and (C) PilMNOP levels ± standard error. Data are representative of n=3 experiments. [a, b, c] paired samples compared by student's t-test with $p < 0.05$.

Decreased levels of PilMNOPQ and T2S in fimV is due to decreased cAMP

Wehbi et al. (125) showed previously that *fimV* mutants had reduced levels of PilMNOP, and that a $fimV_{\Delta LysM}$ mutant with an in-frame deletion of the LysM motif had decreased PilQ monomers and multimers. However, transcription of the *pilMNOPQ* operon is Vfr-dependent, thus it varies with cAMP levels (49). To determine if any of these phenotypes were also cAMP-independent, we examined levels of PilMNOPQ and PilU, and twitching motility in *fimV*, $fimV_{\Delta LysM}$, a mutant encoding only the cytoplasmic domain of FimV ($fimV_{1194}$), and a *fimV cyaB-R456L* mutant (173).

As predicted, the *fimV* mutant had low levels of PilU (~23% of wild type), reflecting low cAMP levels, while the *fimV cyaB-R456L* double mutant had increased levels of PilU relative to *fimV* (~102% relative to wild type) (Figure 3.2A, B). The $fimV_{1194}$ mutant had ~29% of wild type PilU, suggesting that expression of the cytoplasmic domain alone was insufficient to activate CyaB. Complementation of *fimV* and $fimV_{1194}$ with a construct expressing full-length FimV increased PilU levels to ~58% and ~65% of wild type, respectively. Surprisingly, the $fimV_{\mathrm{LysM}}$ mutant had ~89% of wild type PilU, suggesting that the LysM motif and thus PG binding was dispensable for CyaB activation.

The *fimV* mutant had decreased levels of PilMNOP, and no detectable PilQ multimers, and all were restored to wild type with full-length FimV. These data suggest that decreased cAMP in the *fimV* background was the cause of decreased levels of PilMNOP. In support of the link between PilMNOPQ and cAMP, the *fimV cyaB-R456L* double mutant had wild type levels of PilMNOP and multimeric PilQ. Despite restoration of PilMNOPQ expression, the *fimV cyaB-R456L* double mutant had no recoverable surface pili (Figure 3.2A) and could not twitch, confirming a cAMP-independent role(s) for FimV in pilus assembly and twitching motility. The $fimV_{1194}$ mutant had low levels of PilMNOP and no detectable PilQ multimers. These could be rescued by complementation with full length FimV. $fimV_{\Delta\mathrm{LysM}}$ had PilMNOPQ levels similar to *fimV*

complemented with full-length FimV, and could assemble surface pili (Figure 3.2C); however, twitching was ~37% of wild-type, less than *fimV* complemented with full length FimV (~63%). Impaired twitching in *fimV*$_{\Delta LysM}$ suggests that PG binding by FimV is important for its cAMP-independent function(s).

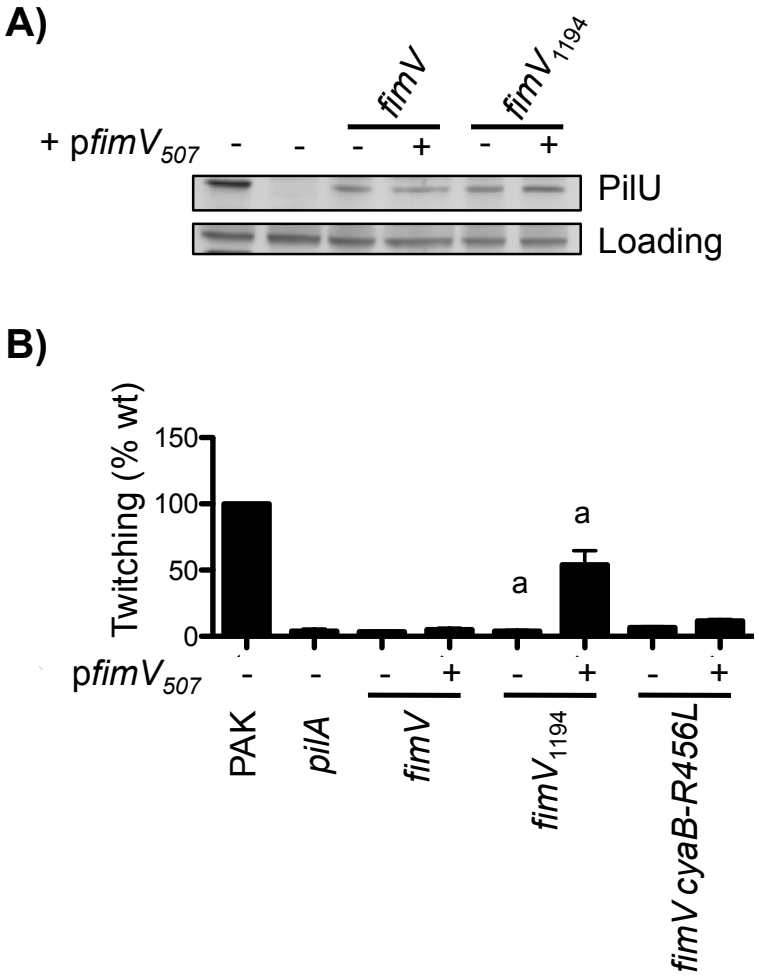

Figure 3.3 – The periplasmic domain of FimV is required for CyaB activation. *fimV,* and *fimV*$_{1194}$ were transformed with arabinose-inducible

expression vectors encoding the periplasmic domain (residues 1-507) of FimV ($FimV_{507}$) or as a control, with empty vector (pB). Cell lysates prepared as described in the Methods from cells grown on LB 1.5% agar supplemented with 0.1% (w/v) arabinose were resolved on 12.5% SDS-PAGE and transferred to a nitrocellulose membrane. PilU was visualized by immunoblotting with anti-PilU antiserum. (B) Twitching motility was determined by stab inoculation of the indicated strains into LB 1% (w/v) agar. Strains were incubated for 16 h, and twitching zones were visualized by removing the agar layer and staining the bacteria with 1% (w/v) crystal violet. Quantification of twitching zones ± standard error is shown. Data are representative of n=3 experiments. [a] paired samples compared by student's t-test with $p < 0.05$.

FimV's cytoplasmic domain is insufficient for CyaB activation

Wehbi et al. (125) showed that the *fimV*$_{1194}$ mutant that expresses only the cytoplasmic domain of FimV was unable to twitch, but that motility could be rescued by complementation with the periplasmic portion of FimV expressed from a plasmid ($pFimV_{507}$), suggesting that together the two FimV fragments could restore function without being physically connected. Given that other cAMP regulatory proteins such as FimL and PilG are cytoplasmic and interact with the C-terminal region of FimV (50, 56, 173), we hypothesized that the cytoplasmic region of FimV should be sufficient to regulate intracellular cAMP levels. We compared PilU levels in *fimV* or *fimV*$_{1194}$ strains complemented with empty vector or a construct encoding residues 1-507 of FimV ($pFimV_{507}$) (Figure 3.3A).

The *fimV* deletion mutant complemented with either empty vector or pFimV$_{507}$ had similar PilU levels, suggesting that the periplasmic domain alone is not sufficient to activate CyaB. *fimV*$_{1194}$ had PilU levels similar to *fimV*, suggesting that the cytoplasmic domain alone cannot activate CyaB. Surprisingly, expression of FimV$_{507}$ in the *fimV*$_{1194}$ background did not significantly increase PilU levels, suggesting that the cytoplasmic and periplasmic domains are unable to efficiently activate CyaB when they are not covalently linked to one another. However, CyaB activation is not strictly required for twitching motility, as both *fimL* and *cyaAB* mutants have low intracellular cAMP levels, but near wild-type motility (55, 56)

We next tested if the periplasmic region played a cAMP-independent role in twitching by complementing the *fimV cyaB-R456L* strain with pFimV$_{507}$. As shown previously (125), pFimV$_{507}$ restored ~50% of wild type twitching in *fimV*$_{1194}$ (Figure 3.3B). However, pFimV$_{507}$ failed to restore wild-type levels of twitching in *fimV cyaB-R456L*, suggesting that the cytoplasmic region of FimV plays a cAMP-independent role in twitching. Taken together, these data show that the cAMP-independent role of FimV is not limited to its periplasmic region.

FimV is required for PilS localization

The *V. cholerae* homolog of FimV, HubP, interacts with multiple proteins and has broad regulatory function (128). FimV is required for

localization of PilG and FimL (135), and the T4aP structural proteins PilMNOPQ (Carter et al., in preparation). We next tested if FimV was required for localization of PilS, another bipolar T4aP regulator (176, 177). PilS is the histidine sensor kinase component of the PilRS two-component system and monitors pilin inventories, regulating *pilA* transcription in response to changes in PilA levels in the inner membrane (57). PilS has 6 transmembrane helices, of which helices 5 and 6 are required for its localization (176).

In wild-type cells, a PilS-YFP fusion exhibited bipolar localization (Figure 3.4) as previously reported (176). However, in the absence of FimV, PilS-YFP was diffuse in the inner membrane. We examined PilS-YFP in $fimV_{\Delta LysM}$ to determine if binding to PG was required for PilS localization. Interestingly, PilS-YFP had a localization pattern similar to wild type cells, suggesting that PG-binding via the LysM motif was not critical for PilS localization by FimV. However, PilS was mislocalized in $fimV_{1194,}$ suggesting that another periplasmic element besides the LysM motif is required for PilS localization. We tested for direct FimV and PilS interactions using the BACTH system (152), but the results were negative in both directions (Figure 3.4B).

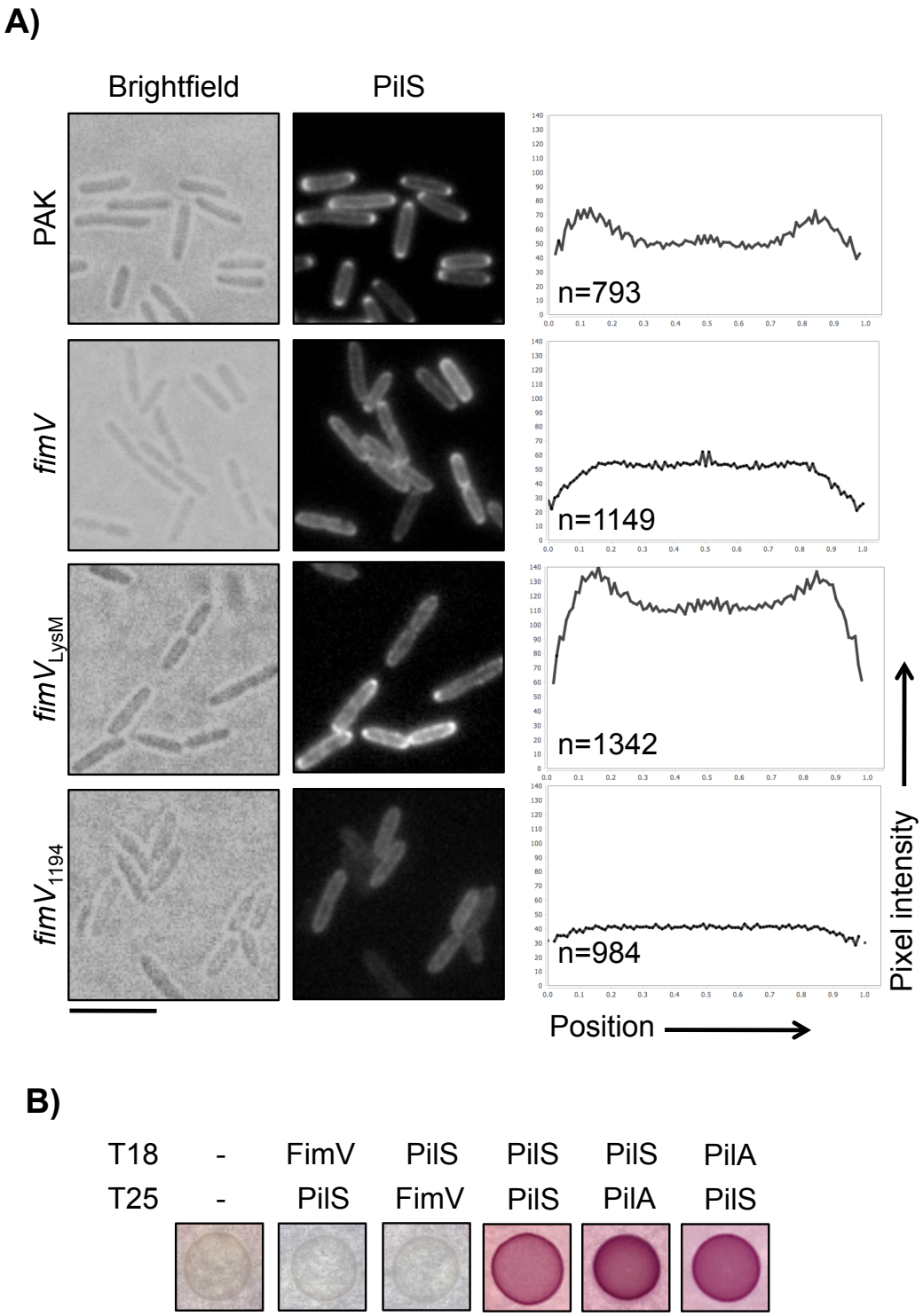

Figure 3.4 - FimV is required for PilS localization. (A) YFP was fused to the C-terminus of PilS and expressed in the wild type PAK, cells lacking

FimV (*fimV*), and mutants lacking the FimV LysM motif ($fimV_{\Delta LysM}$) or the periplasmic region of FimV ($fimV_{1194}$). Cells were stab inoculated into 1.0 borosilicate chambered coverglass containing LB 1% agar supplemented with 0.1% (w/v) arabinose. Slides were incubated at 37°C and imaged using a 60X oil immersion objective on an EVOS FL Auto. Pixel intensity profiles were generated of each cell on the YFP channel as stated in the methods. Scale bar denotes 5 μm. (B) Fusions of FimV or PilS to *B. pertussis* CyaB T18 or T25 fragments were expressed in *E.coli* BTH101 in a pairwise manner. Five µl of a liquid culture normalized to OD_{600} 0.6 was spotted onto MacConkey agar supplemented with 1% maltose and 0.5 mM IPTG. Plates were incubated at 30 °C for 24 h. Protein-protein interaction is visualized by pink growth on MacConkey agar indicating protein-protein interaction and reconstitution of *B. pertussis* CyaB function.

fimV deletion does not affect swimming motility

Since the *V. cholerae* and *S. putrefaciens* homologs of FimV affect flagellar localization and swimming motility (128), we tested whether deletion of *fimV* impaired swimming in *P. aeruginosa*. We saw no effect of FimV deletion on swimming motility (Figure 3.5), suggesting that FimV is not essential for flagellar function in *P. aeruginosa*. Consistent with reports that the flagellar system is negatively regulated by cAMP (49), the *cpdA* mutant was swimming impaired (40% relative to wild type). Deletion of *fimV* (~85%), *fimL* (~76%), and *pilG* (~75%) in the *cpdA* background reduced swimming slightly relative to the single mutants, most likely due to increased cAMP levels. Interestingly, despite having high cAMP levels

comparable with *cpdA (55)*, *pilH* had (~125% swimming motility relative to wildtype). This may be due to the significantly lower amount of surface pili for the *pilH* mutant versus the *cpdA* mutant, as pili might physically interfere with flagellar function.

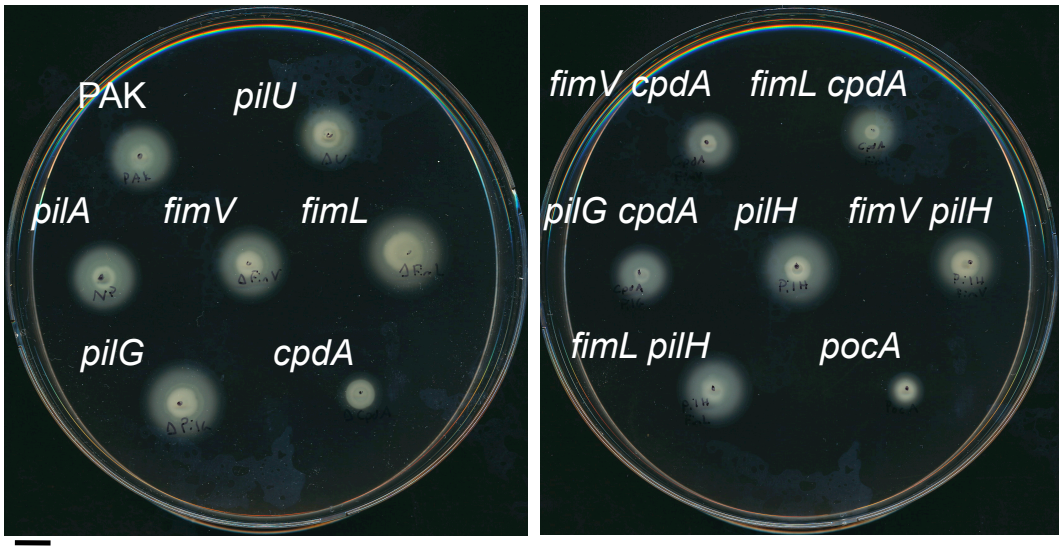

Figure 3.5 – FimV is not required for swimming motility. Cells grown overnight were resuspended and PBS and normalized to OD_{600} of 0.6. Two µl were spotted onto LB 0.3% agar and incubated overnight. As a control, a *pocA* mutant was included which has been shown to be swimming impaired (178). Representative swimming zones of the indicated strains. Scale bar = 1 cm. Graphical data displays average swimming diameter ± standard error, and is representative of n=3 independent trials.

DISCUSSION

PilG, FimL, and FimV were proposed to be components of a mechanosensory pathway that activates CyaB (135), with FimL functioning as a scaffold to connect PilG to FimV. Although deletion of *pilG*, *fimL*, or *fimV* leads to decreased cAMP, only the *fimL* mutant twitches following introduction of secondary mutations that restore intracellular cAMP levels (Figure 3.1) (55, 56), confirming that PilG and FimV have cAMP-independent roles in twitching (55, 173). These findings represent a gap in the FimV-FimL-PilG scaffold model, which does not account for the cAMP-independent regulation of twitching.

Twitching motility in the *fimL* background suggests that PilG and FimV must both function in its absence. In the case of PilG, although it was proposed to interact with FimL – and indirectly, FimV – at the cell poles, *fimL* deletion did not cause PilG mislocalization (135), implying that PilG has another interaction partner with which it can interact at the cell poles. It is possible that this other interaction partner mediates PilG effects on motility, independent of cAMP. In swimming cells, the PilG orthologue CheY interacts with FliM at the flagellar switch complex (81). However, the T4aP system lacks a functional equivalent of FliM. Possible interaction partners of PilG include PilM, PilC, or the retraction ATPases. PilU is an attractive possibility, as the piliated but non-motile phenotype of a *pilU* mutant phenocopies *pilG* mutants. PilC is also able to interact with PilT and PilU, and PilM can bind PilT (36), making them possible interaction

partners for PilG as well. Mislocalization of PilG in *fimV* may reflect the consequent mislocalization of one of these components, as Carter et al. provided evidence that deletion of *fimV* leads to mislocalization of structural components of the T4P assembly complex (Carter et al., in preparation).

Interestingly, the cAMP-independent role(s) of FimV appears to be distinct from that of PilG. FimV deletion mislocalizes a number of T4aP regulatory and structural proteins (135) (Carter et al., in preparation; Figure 3.4), while loss of PilG has not been shown to do so (135) (Figure S3.1). These data provide further evidence that FimV has a broader role in regulation of twitching than suggested by the FimL scaffold model (135). HubP from *V. cholerae* and *S. putrefaciens* are also responsible for localization of the flagellar chemotaxis machinery, and in the case of *V. cholerae*, the chromosomal partitioning machinery. It is possible that FimV performs a similar hub function in *P. aeruginosa.*

We showed previously (125) that the periplasmic and cytoplasmic regions of FimV could reconstitute FimV function when co-expressed. However, our data show that CyaB cannot be activated efficiently when the two halves of FimV are separated. The ability to twitch despite having low levels of intracellular cAMP is not surprising, as *fimL* and *cyaAB* mutants are both motile (55, 56). The cAMP-independent function of FimV was also not restricted to the periplasmic or cytoplasmic regions. The

model for *V. cholerae* HubP follows a similar model, where the LysM motif targets HubP and its interaction partners to the cell poles, and the cytoplasmic domain is responsible for multiple protein-protein interactions with the chromosomal origin, FlhG, and FlhF (128), regulators of flagellar assembly location and number (179, 180). It is possible that the two domains of FimV interact through their transmembrane domains and function similarly to HubP, to perform the same assembly-localization function in the T4P system.

Interestingly, septal PG binding was not required for CyaB activation although FimL, PilG, and CyaB are located at the cell poles (56, 135). While the LysM motif of HubP is required for its polar localization (128), there is no evidence that the same is true for FimV. It may be possible that deletion of the LysM motif alone does not mislocalize FimV, as it may have other interaction partners that tether it to the cell poles. Alternatively, FimV and CyaB may not need to co-localize to promote CyaB activity.

The LysM motif was also dispensable for localization of PilS to the cell poles. However, deletion of the entire periplasmic region led to PilS mislocalization (Figure 3.4). Although we did not observe a direct interaction between FimV and PilS, it is possible that they interact through other intermediaries, whose own localization relies on the presence of

FimV. Further, the localization patterns of $FimV_{\Delta LysM}$ and $FimV_{1194}$ have not yet been confirmed, so it is unknown if either retains polar localization.

Our data show that decreased levels of PilMNOP and PilQ multimers in *fimV* is cAMP-dependent. However, this is not a barrier to T4aP function, as strains lacking FimV remain susceptible to pilus-specific phage (125). Carter et al. (in preparation) showed that PilQ and PilO are mislocalized in $fimV_{\Delta LysM}$, raising the possibility that the surface pili assembled in $fimV_{\Delta LysM}$ are also mislocalized.

Although HubP has been shown in multiple species to be required for swimming motility, deletion of FimV did not decrease swimming motility (Figure 3.5). However, FimV likely affects flagellar function indirectly by modulating T4aP levels and/or cAMP levels, as deletion of *fimV* in the *cpdA* background increased swimming relative to *cpdA*. Based on the data in other species, we cannot rule out the possibility that FimV interacts with one or more regulators of flagellum function or positioning, but further studies are needed to test this.

In summary, our work resolved the cAMP-dependent and independent roles of FimV function. The cAMP-independent role of FimV may be related to localization of structural and regulatory components, as suggested by our findings and those of others (135) (Carter et al., in preparation). Importantly, PilG has also been shown to have a cAMP-independent role in regulating twitching, likely at the level of retraction (55).

As shown by Inclan et al., PilG localizes to the cell poles (135). It is possible that PilG regulates retraction specifically at the poles to allow for directional movement. However, additional studies are required to better resolve the cAMP-dependent and independent roles of PilG. Further characterization of the FimV protein-interaction network will be required in order to identify its full repertoire of direct and indirect interaction partners, and to determine how FimV localizes T4aP-related proteins.

Materials and Methods

Bacterial growth and culture conditions

Bacterial strains and plasmids are listed in **Table 1**. Unless otherwise stated, untransformed *P. aeruginosa* strains and all *E. coli* strains were grown on LB agar at 37 °C. Antibiotic selection was as follows unless stated otherwise: gentamicin, 15 µg/ml for *E. coli* and 30 µg/ml for *P. aeruginosa*; kanamycin, 50 µg/ml for *E. coli*; ampicillin, 100 µg/ml for *E. coli*. All *P. aeruginosa* strains containing a FimV complementation construct were grown on media supplemented with 0.1% (w/v) arabinose.

Mutant generation

Mutants were generated as previously described by Fulcher et al. (55). Briefly, mutants were generated by transforming the *fimL, fimV, cpdA,* and *pilH,* deletion cassettes into *E. coli* SM10. Knockout constructs were

transferred to *P. aeruginosa* PAK by biparental mating. *E. coli* SM10 was counterselected by plating on *Pseudomonas* isolation agar (Difco) supplemented with gentamicin (100 µg/ml). Gentamicin resistant colonies were then plated onto LB 1.5% agar supplemented with 8% (w/v) glucose and incubated for 24 h at 30 °C to resolve the plasmid. Sucrose-resistant colonies were then replica plated on LB 1.5% agar supplemented with 8% (w/v) glucose, and LB 1.5% agar supplemented with 30 µg/ml gentamicin. Glucose-tolerant and gentamicin-sensitive colonies were screened by PCR. The same method was used to generate all double mutants.

Immunoblotting

Western blotting of whole cell lysates was performed as previously described (28). In brief, whole cell lysates were prepared from strains were grown overnight on LB 1.5% agar, or in the case of plasmid transformed strains, LB 1.5% agar supplemented with 0.1% (w/v) arabinose. Cell growth was then resuspended in 1X PBS and normalized to an OD_{600} of 0.6. Cells were pelleted by centrifugation at 2.300 × g for 5min. Pellets were then resuspended in 175 µl of 1X SDS-PAGE loading dye. Cell lysates were resolved on 15% SDS-PAGE gels and transferred to nitrocellulose membranes. Membranes were blocked in 5% skim milk dissolved in PBS (pH 7.4) for 1 h, washed in PBS, and incubated with PBS-diluted antisera raised against the FimV periplasmic domain (1:1000),

PilU (1:5000), PilM (1:1000), PilN (1:1000), PilO (1:1000), PilP (1:1000), or PilQ (1:1000), or polyclonal anti-GFP antibody (Novus Biologicals; 1:5000) for 1 h, washed, incubated with alkaline phosphatase-conjugated goat-anti-rabbit secondary antibody (1:3000, Bio-Rad) for 1 h, and washed. Blots were developed using 5-bromo-4-chloro-3-indolylphosphate (BCIP) and nitro blue tetrazolium (NBT). Data are representative of n = 3 independent experiments.

Sheared surface protein preparation

Surface pili were analyzed as previously described (150). In brief, strains of interest were streaked in a grid-like pattern onto LB 1.5% agar, or in the case of plasmid-transformed strains, LB 1.5% agar supplemented with 0.1% (w/v) arabinose and grown overnight at 37 °C. Cells were gently scraped from the plates using a sterile coverslip and resuspended in 4.5 ml PBS (pH 7.4). Surface appendages were sheared by vortexing the cells for 30 s. The OD_{600} for each strain was measured, and an amount of cells equivalent to 4.5 ml of the sample with the lowest OD_{600} was pelleted by centrifugation at 16,100 x g for 5 min. When necessary, PBS was added to samples to a final volume of 4.5 ml prior to centrifugation. Supernatants were removed and centrifuged again at 16,100 x g for 20 min to remove remaining cells. Supernatants were collected and mixed with 5 *M* NaCl and 30% (w/v) polyethylene glycol (Sigma; molecular weight range ~8000)

to a final concentration of 0.5 *M* NaCl and 3% (w/v) polyethylene glycol, and incubated on ice for 30 min. Precipitated surface proteins were collected by centrifugation at 16,100 x g for 30 min. Supernatants were discarded and samples were centrifuged again at 16,100 x g for 2 min. Pellets were resuspended in 150 μl of 1X SDS-PAGE sample buffer (80 m*M* Tris, pH 6.8, 5.3% (v/v) 2-mercaptoethanol, 10% (v/v) glycerol, 0.02% (w/v) bromophenol blue, 2% (w/v) SDS). Samples were boiled for 10 min and resolved by 15% SDS-PAGE. Bands were visualized by staining with Coomassie brilliant blue (Sigma). Data are representative of n = 3 independent experiments.

Twitching assay

Twitching motility was tested as previously described (150). In brief, cells from an overnight culture were stab inoculated to the interface between LB 1% agar, or in the case of plasmid-transformed strains, LB 1% agar supplemented with 0.1% (w/v) arabinose and the underlying tissue culture-treated polystyrene petri dish, and incubated at 37 °C for 16 h (Thermo Fisher). Twitching zones were visualized by removing the agar and staining cells on the petri dish with 1% (w/v) crystal violet and washing with water to remove unbound dye. Twitching zones were measured by analyzing the diameter of each twitching zone in pixels using ImageJ software (NIH). Twitching zones were normalized to the twitching diameter

of wild type PAK in each individual experiment. Data are representative of n = 3 independent experiments.

Fluorescence microscopy

P. aeruginosa strains transformed with pBADGr::FimV-eYFP were grown overnight. Microscopy was performed using 8-well 1.0 borosilicate chambered coverglass (LabTek). Chamber slides were prepared by adding LB 1% agar supplemented with 0.1% (w/v) arabinose to create an agar layer ~3 mm in thickness and covering the bottom of the chamber. Agar was allowed to solidify with the lid off to prevent condensation. Bacteria was stab inoculated to the interface between the agar and coverglass. Slides were wrapped in foil to prevent photobleaching, and incubated at 37 °C for 1h in the dark. Cells were then imaged using an EVOS FL Auto with a monochrome camera for brightfield imaging and fluorescence imaging with a YFP LED light cube, through a 60X oil immersion objective, at room temperature. Representative fields were cropped from larger images and enlarged using ImageJ software (NIH) (151).

Fluorescence images were quantified using the MicrobeJ plugin for ImageJ. Brightfield and fluorescence images were arranged into a stack on ImageJ. Regions of interest corresponding to the bacteria were selected based on the brightfield image, and tresholding particles based

on length (0.5 μm-5 μm), width (0.2 μm-1.5 μm), and area (0.75 μm^2-max), and fit to rod-shaped bacteria. Pixel intensity profiles were generated by MicrobeJ using the profile option on the fluorescence image, using 1μm width, and 0.5μm extensions. Intensity profiles were plotted along a Y-axis of range 0-140, and the X-axis was partitioned into 100 bins. Pixel intensity profiles were generated for the YFP channel. Data are representative of at least 3 independent trials.

Bacterial two-hybrid assay

E. coli BTH101 cells were co-transformed with full length FimV and PilS fused to either the T18 or T25 fragments of *Bordetella pertussis* CyaB (152) by heat shock. Single colonies were resuspended in LB supplemented with 100 μg/ml ampicilin and 50 μg/ml kanamycin and grown for 8h. Five μl of each strain was then spot plated onto MacConkey agar supplemented with 100 μg/ml ampicilin and 50 μg/ml kanamycin, 1% (w/v) maltose, and 0.5 mM isopropyl β-D-thiogalactopyranoside (IPTG), and incubated at 30 °C for 16 h. Interactions were visualized by pink bacterial growth representing fermentation of maltose.

Swimming assay

Cells from overnight cultures were resuspended in PBS and standardized to OD_{600} 0.6. Two μl of resuspended cells were spotted onto

LB 0.3% agar and allowed to dry onto the surface of the agar. Plates were incubated at 30 °C for 16 h with the agar side down. Data are representative of n=3 independent experiments.

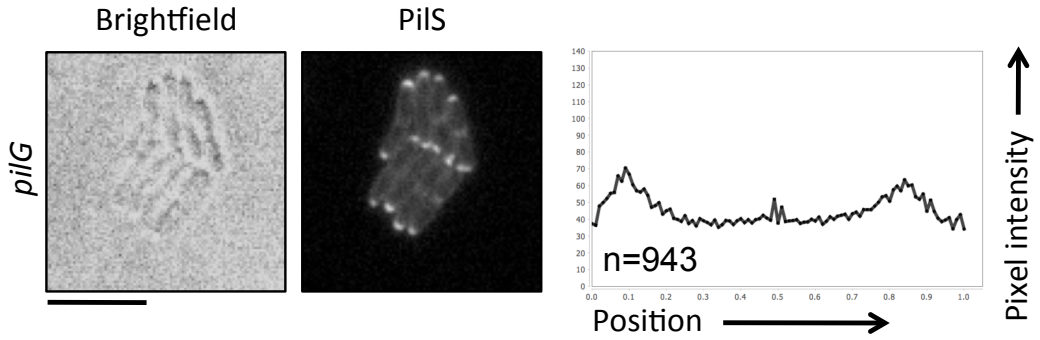

Figure S3.1 – PilS localization does not require PilG. . (A) YFP was fused to the C-terminus of PilS and expressed in cells lacking PilG (*pilG*). Cells were stab inoculated into 1.0 borosilicate chambered coverglass containing LB 1% agar supplemented with 0.1% (w/v) arabinose. Slides were incubated at 37°C and imaged using a 60X oil immersion objective on an EVOS FL Auto. Pixel intensity profiles were generated of each cell on the YFP channel as stated in the methods. Scale bar denotes 5 μm.

Table 3.1. Strains and plasmids used in this study

Strains	Genotype/Description	Source
P. aeruginosa		
PAK	Wild type *P. aeruginosa* strain K	(55)
NP	PAK with a deletion of *pilA*	(168)
pilU	PAK with a deletion of *pilU*	Wolfgang, MC
fimV	PAK with a deletion of *fimV*	(55)
$fimV_{LysM}$	PAK with an in-frame deletion of the LysM motif, nucleotides 519-690	This study
fimV cyaB-R456L	PAK with a deletion of *fimV* and an arginine to lysine substitution in *cyaB* at position 456	(173)
fimV1194	PAK with an FRT insertion at nucleotide position 1194 in *fimV*	This study
fimL	PAK with a deletion of *fimL*	This study
pilG	PAK with a deletion of *pilG*	(55)
cpdA	PAK with a deletion of *cpdA*	This study
cpdA fimV	PAK with deletions of *cpdA* and *fimV*	This study
cpdA fimL	PAK with deletions of *cpdA* and *fimL*	This study
cpdA pilG	PAK with deletions of *cpdA* and *pilG*	This study
pilH	PAK with a deletion of *pilH*	This study
pilH fimV	PAK with deletions of *pilH* and *fimV*	This study
pilH fimL	PAK with deletions of *pilH* and *fimL*	This study
E. coli		

DH5a	F-, Φ80*lac*ZΔM15, Δ(*lac*ZYA-*arg*F), U169, recA1, endA1, hsdR17(rk-, mk+), phoA, supE44, thi-1, gyrA96, relA1, λ-; General cloning strain	Invitrogen
BTH101	BTH101: F-, cya-99, araD139, galE15, galK16, rpsL1 (Str^r), hsdR2, mcrA1, mcrB1; Bacterial two-hybrid reporter strain	Euromedex
SM10		(181)
Plasmids		
pBADGr	Arabinose-inducuble expression construct	(169)
pBADGr::*fimV*	Arabinose-inducible expression construct encoding full length FimV	This study
pBADGr::*fimV507*	Arabinose-inducible expression construct encoding the periplasmic domain of FimV, residues 1-507	This study
pBADGr::*fimV-eYFP*	Arabinose-inducible expression construct encoding FimV with eYFP encoded in-frame at the C-terminus	This study
pUT18	IPTG-inducible expression vector encoding T18 fragment of *B. pertussis* CyaB	Euromedex
pKNT25	IPTG-inducible expression vector encoding T25 fragment of *B. pertussis* CyaB	Euromedex
pUT18::*fimV*	IPTG-inducible expression vector encoding T18 fragment of *B. pertussis* CyaB fused to the C-terminus of FimV	This study
pUT18C::*pilS*	IPTG-inducible expression vector encoding T18 fragment of *B. pertussis* CyaB fused to the N-terminus of PilS	(57)
pUT18C::*pilA*	IPTG-inducible expression vector encoding T18 fragment of *B. pertussis* CyaB fused to the N-terminus of PilA	(57)
pKNT25::*fimV*	IPTG-inducible expression vector encoding T25 fragment of *B. pertussis* CyaB fused to the C-terminus of FimV	This study

pKT25::*pilS*	IPTG-inducible expression vector encoding T25 fragment of *B. pertussis* CyaB fused to the N-terminus of PilS	(57)
pKT25::*pilA*	IPTG-inducible expression vector encoding T25 fragment of *B. pertussis* CyaB fused to the N-terminus of PilA	(57)
pEX18Gm::*fimL*	Suicide vector containing 1kb upstream and downstream from the *fimL* locus	This study
pEX18Gm::*cpdA*	Suicide vector containing 1kb upstream and downstream from the *cpdA* locus	This study
pEX18Gm::*pilH*	Suicide vector containing 1kb upstream and downstream from the *pilH* locus	This study
pEX18Ap-*fimV*-GmFRT	Suicide vector containing *fimV* amplified from PAO1 and disrupted at nucleotide position 1194 with an FRT-flanked gentamicin resistance cassette	(125)
pEX18Gm-*fimV*-ΔLysM	Suicide vector containing residues 1-1521 of *fimV* with a deletion of nucleotides 519-690	(125)

Table 3.2. Oligonucleotides used in this study

Primers	Sequence
eYFP-F	5' - AAG CTT ATG GTG AGC AAG GGC GAG GAG - 3'
eYFP-R	5' - AAG CTT ACT TGT ACA GCT CGT CCA TGC C - 3'
FimV-F	5' - TTAGTACTAAGGGATTACACTATGGTTCGGCT - 3'
$FimV_{507}$-R	5' GCG TCT AGA CTG TTC CTC GCC GG -3'
FimV YFP-F	5' - GCG GGT ACC ATG GTT CGG CTT CG -3'
FimV YFP-R	5' - GCG TCT AGA GGC CAG GCG CTC CA -3'
BTH FimV-F	5' - GCG TCT AGA AAT GGT TCG GCT TCG T - 3'
BTH FimV-R	5' GCG GGT ACC GCG GCC AGG CGC TCC AG - 3'
BTH PilG-F	5' - GCG TCT AGA AAT GGA ACA GCA ATC CGA CGG - 3'
BTH PilG-R	5' - TAA GGT ACC CGG GAA ACG GCG TCC ACC - 3'
BTH FimL-F	5' - GCG TCT AGA GAT GGT CAC AGG AGC CAC GTC CC - 3'
BTH FimL-R	5' - GCG GGT ACC GCG GCG GCC ACC GG - 3'
ko FimL F1	5’ CGC GAG CTC AAT GGG CGT GCC GTG CAT CA - 3’
ko FimL R1	5’- CGC GGA TCC CGG TCT AGT GCG CCT CCC -3’
ko FimL F2	5’- CGC GGA TCC TGG CCG GCG AGT TCC GCT -3’
ko FimL R2	5’- CGC AAG CTT GGA CCG TCA GCT CGC TGC TC - 3’
ko cpdA F1	5' - TC AAGCTT GGATCAGCTCGACGCCCGGCA - 3'
ko cpdA R1	5' - TCG GTA CCT CTT CGA AGT GGA CTA CGA CA - 3'

ko cpdA F2	5' - TAC GGT ACC AGG CGT CGG TGG CGG GAG T - 3'
ko cpdA R2	5' - TC GAATTC ACGACCCGCAGCGCGATTGC - 3'
ko pilH F1	5' - TTG AGC TCA GGT TGG CGC CCC - 3'
ko pilH R1	5' - TGA AGC TTG TTT ATA CGG CGA C - 3'

CHAPTER FOUR

PilG controls multiple aspects of *Pseudomonas aeruginosa* twitching motility

Preface

Chapter Four consists of the following manuscript for publication:

Buensuceso RNC, Khalil H, Farr S, Fulcher NB, Silversmith RE, Daniel-Ivad M, Chakraborty A, Wolfgang MC, Howell PL, Burrows LL. 2016. PilG controls multiple aspects of *Pseudomonas aeruginosa* twitching motility

Attributions: H.K. and S.F. generated the PilG-YFP fluorescent construct and PilG point mutant vectors. R.E.S. and N.B.F. performed kinase and β-galactosidase assays. M.D.I. helped with microscopy and structural modeling. A.C. generated expression construcs of PilG orthologs. R.N.C.B. performed western blots, twitching motility assays, phage sensitivity assay, microscopy, sheared surface protein preparations and SDS-PAGE. R.N.C.B. and L.L.B. performed bioinformatics analyses. Paper was written by R.N.C.B., M.C.W., P.L.H., and L.L.B.

PilG controls multiple aspects of *Pseudomonas aeruginosa* twitching motility

Running Title: PilG controls *Pseudomonas aeruginosa* twitching motility

Ryan N.C. Buensuceso[1], Hosam Khalil[1], Sarah Farr[1], Nanette B. Fulcher[2], Ruth E. Silversmith[3], Martin Daniel-Ivad[1], Amar Chakraborty[1], Matthew C. Wolfgang[2,3], P. Lynne Howell[4*] and Lori L. Burrows[1*].

[1]Department of Biochemistry and Biomedical Sciences, and the Michael G. DeGroote Institute for Infectious Diseases Research, McMaster University, Hamilton, ON; [2]Cystic fibrosis/Pulmonary Research and Treatment Center and [3]Department of Microbiology and Immunology, University of North Carolina School of Medicine, Chapel Hill, NC; and [4]Program in Molecular Structure and Function, Hospital for Sick Children, Toronto, ON and Department of Biochemistry, University of Toronto, Toronto, ON.

*Corresponding authors:

L.L. Burrows,

Tel: 905-525-9140 x22029 Fax: 905-522-9033 Email: burrowl@mcmaster.ca

P.L. Howell,

Tel: 416-813-5378 Fax: 416-813-5379 Email: howell@sickkids.ca

SUMMARY

Type IV pili (T4P) are major virulence factors of the opportunistic pathogen *Pseudomonas aeruginosa*, used for surface adhesion, and surface translocation by twitching motility. Twitching involves cycles of T4P extension, adhesion, and retraction, and is controlled by physical and chemical inputs. The Chp system is a putative chemotaxis phosphorelay that controls twitching and intracellular levels of the secondary messenger, cyclic AMP (cAMP). How Chp regulates pilus extension and retraction is unclear. Here we show that the CheY-like response regulator PilG localizes predominately to the leading pole of twitching cells, while PilH has diffuse localization. Levels of the PilB, PilT and PilU ATPases, are cAMP-dependent; therefore T4P extension but not dynamics are cAMP-dependent. Bacteriophage susceptibility showed PilG is not required for retraction, suggesting that PilG coordinates asymmetrical/pole-specific retraction for directed movement. Bioinformatic studies showed that Pseudomonads encode either a simple – possibly ancestral – version of the Chp system, or a complex form that also encode PilU, CyaB, and its activator FimL. Complementation of *P. aeruginosa* lacking *pilG* with PilG orthologs from other species showed that only closely related homologs restored cAMP-dependent and –independent functions. These data suggest that PilG and PilU may collaborate to favor pilus extension and

retraction at one pole of rod-shaped cells, allowing for directional movement across surfaces.

INTRODUCTION

Type IV pili (T4P) are long, filamentous protein polymers expressed by a broad range of bacteria and archaea that use them for surface attachment, DNA uptake, and twitching motility (2-5). Twitching motility is typically associated with bacteria expressing pili of the type IVa (T4aP) subfamily (7, 14, 15). During twitching motility, T4aP undergo repeated cycles of fiber extension (or assembly/biogenesis), attachment, and retraction (disassembly), pulling the cell towards the point of pilus attachment. Although T4aP have been well studied in a number of model organisms including *Pseudomonas aeruginosa*, *Neisseria* spp., and *Myxococcus xanthus,* species-specific differences in the regulation of twitching motility have been reported (16). While the terms assembly/extension/biogenesis and disassembly/retraction are used interchangeably, we will use extension and retraction throughout this manuscript.

T4P extension and retraction are powered by ATPases belonging to the secretion NTPase family (182). Typical T4aP systems have two ATPases, PilB and PilT, involved in pilus extension and retraction, respectively, although *P. aeruginosa* and some other species have PilB plus two or more PilT paralogues (27, 183). *P. aeruginosa* expresses PilB, PilT, and PilU; the latter has 39% sequence identity to PilT, but its function remains unclear (26, 27, 184-186). *P. aeruginosa pilU* mutants have at

least wild-type levels of surface pili, and remain susceptible to pilus-specific phages – a property that requires pilus retraction (27) – but lack appreciable twitching motility. Chiang et al. (35) showed previously that the localization pattern of the three ATPases differs. While PilB and PilT are bipolar (35), PilU is unipolar, and is localized more frequently to the lagging pole of twitching cells (Cynthia Whitchurch, personal communication).

In *P. aeruginosa*, twitching requires the input of a number of different cellular and environmental factors, including a putative chemotaxis system called Chp (50, 51). Similar to the canonical Che flagellar chemotaxis system, the Chp system includes a putative methyl-accepting chemotaxis protein (MCP) that may sense ligands (PilJ); two CheW-like putative adaptor proteins (PilI and ChpC); a multidomain CheA-like histidine kinase (ChpA); and putative adaptation methyltransferase and methylesterase enzymes (PilK and ChpB) (50, 51). There are two separate CheY-like single-domain response regulators, PilG and PilH, but no CheZ-like phosphatase. PilG and PilH are both targets of phosphotransfer from ChpA, although PilH has a higher rate of phosphorylation (91). Two hypotheses for the roles of PilG and PilH in regulating twitching motility have been advanced. Fulcher et al. hypothesized that both PilG and PilH are targets for ChpA phosphorylation, but that PilH might act as a phosphate sink to attenuate Chp signaling in

lieu of a phosphatase, similar to the organization in the flagellar chemotaxis system of *Sinorhizobium meliloti* (55, 67, 68, 91). This idea is consistent with previous reports (55, 93) that *pilH* mutants are motile but *pilG* mutants are not, suggesting that PilG is the authentic response regulator. Bertrand et al. (93) proposed another model, where PilG and PilH control pilus extension and retraction respectively. In their model, PilG and PilH control PilB and PilT activities, respectively, explaining the hyperpiliated but reduced motility phenotype of *pilH* mutants. Here we provide evidence that the PilG is the response regulator of the Chp system.

Recently, Fulcher et al. (55) showed that in addition to controlling twitching motility, the Chp system of *P. aeruginosa* regulates levels of intracellular cyclic AMP (cAMP). Many *P. aeruginosa* virulence-related phenotypes – including twitching motility – are regulated by a cAMP-binding transcription factor called Vfr (virulence factor regulator), a homologue of *E. coli* CRP (cAMP receptor protein). Vfr controls expression of ~200 virulence genes, including many involved in T4aP biogenesis, including the minor pilin operon *fimU-pilVWXY1E*, the alignment subcomplex genes *pilNOPQ*, *pilU, and vfr* itself (49, 110, 187, 188). *P. aeruginosa* has two adenylate cyclases, CyaA and CyaB, with the latter being the main source of intracellular cAMP (49, 106). PilG is proposed to activate CyaB in a complex with FimL and the bitopic inner membrane protein FimV, with FimL serving as a scaffold that connects

PilG and FimV (135). Deletion of *pilG* decreased CyaB function, reduced levels of intracellular cAMP, and abrogated piliation and twitching motility. Supplementation of the growth medium with cAMP restored piliation but not twitching motility in the *pilG* background, suggesting that PilG had separate roles in cAMP-dependent pilus biogenesis and cAMP-independent pilus retraction. Interestingly, the piliated but non-motile phenotype of the cAMP-supplemented *pilG* mutant resembles that of a *pilU* mutant (27), suggesting a possible functional connection. However, because many of the genes required for T4P biogenesis are cAMP-dependent, mutants deficient in cAMP biogenesis resemble mutants unable to extend pili. Consequently, low levels of cAMP in many T4P-deficient mutants make extension/retraction dynamics difficult to assess.

In this study, we examined the roles of PilG in twitching motility. Bioinformatic analyses of available *Pseudomonas* genomes (189) revealed intriguing links between the Chp system, PilU, and components of the cAMP regulatory circuit. We show that Pseudomonads can be divided into ‘simple’ or ‘complex’ species based on the presence or absence of specific genes, but that PilG orthologues from the simple Pseudomonads are capable of complementing both cAMP-dependent and independent functions of PilG in a complex species *pilG* mutant. Using a strain expressing a CyaB R456L variant that no longer requires PilG for its activity (107), we confirmed the previous finding that PilG controls

twitching motility in a cAMP-independent manner (55). Both PilU and PilG localized predominately to the leading poles of actively twitching cells, consistent with roles in controlling directionality, while PilH was diffuse in the cytoplasm, in keeping with its hypothesized role as a phosphate sink.

RESULTS

PilB, PilT, and PilU ATPase protein levels are cAMP-dependent

Fulcher et al. (55) showed that specific Chp mutants have reduced levels of intracellular cAMP due to loss of CyaB activation. Supplementation of the growth media with cAMP restored piliation but not twitching in a *pilG* mutant, suggesting that pilus biogenesis was a cAMP-dependent phenotype, while pilus fiber extension/retraction dynamics necessary for twitching were cAMP-independent (55). To determine whether the pilus biogenesis defect in the *pilG* background was associated with altered levels of the motor ATPases, we examined the levels of PilB, PilT and PilU by western blot. Levels of PilB, PilT, and PilU were decreased in the *pilG* and *cyaAB* backgrounds compared to wildtype. Levels of PilU were most sensitive to decreased levels of intracellular cAMP, as they decreased to ~20% compared to wildtype in *cyaAB* (Fig 4.1A). Deletion of *pilH* had no effect on ATPase levels. To determine if the inability of a cAMP-supplemented *pilG* mutant to twitch was due to decreased levels of the retraction ATPases, we used a CyaB point mutant

(R456L) that is active in the absence of PilG (107). The point mutation was introduced into wild type, *pilG*, and *pilH* backgrounds, allowing for constitutive activation of CyaB and synthesis of cAMP in the absence of upstream regulators. The *cyaB-R456L* mutant had levels of PilB, PilT, and PilU similar to wild type. In the *pilG cyaB-R456L* background, levels of PilB, PilT, and PilU were increased to 98%, 102%, and 84% of wild type respectively. The increased cAMP in the *pilG cyaB-R456L* background did not restore twitching, confirming previous findings (55). Taken together, these data suggest that the inability of a cAMP-supplemented *pilG* mutant to twitch is not due to decreased levels of the motor ATPases, and may instead be related to how efficiently they mediate pilus extension and retraction.

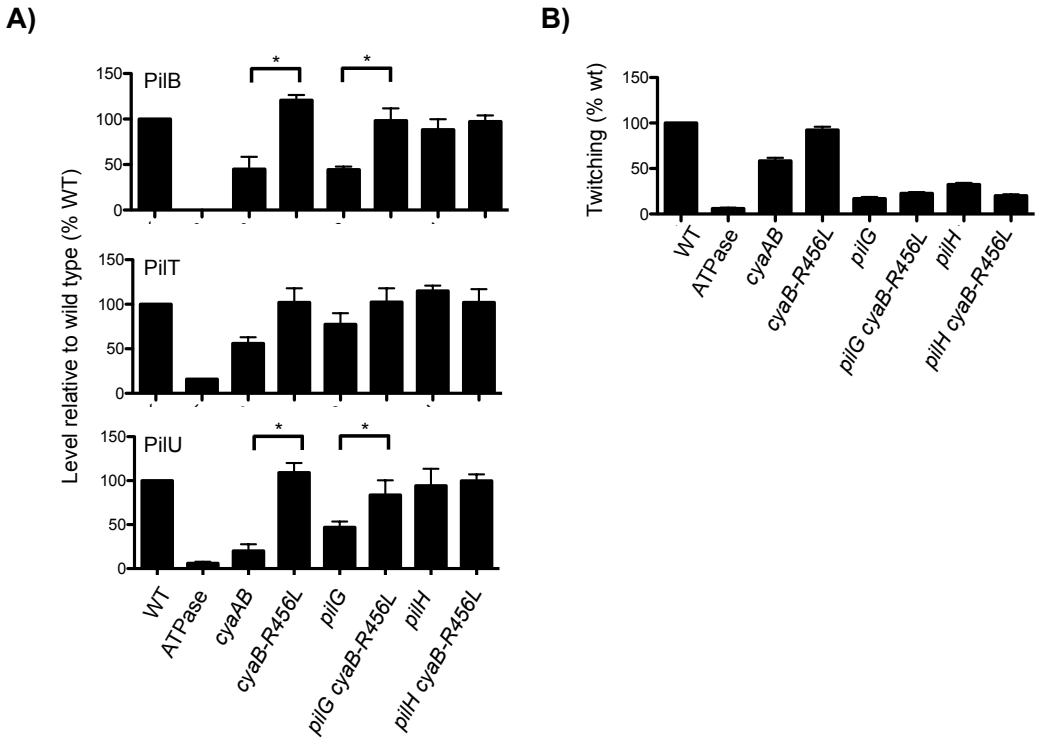

Figure 4.1 – Levels of PilB, PilT, and PilU are cAMP dependent.
(A) Cell lysates of the indicated strains were prepared as described in the Methods from cells grown on LB 1.5% (w/v) agar. Cell lysates were resolved on 12.5% SDS-PAGE and transferred to a nitrocellulose membrane. ATPases were visualized by immunoblotting with anti-PilB, PilT, or PilU antisera. Densitometry was performed on 3 independent western blots for each ATPase. (B) Twitching motility was determined by stab inoculation of the indicated strains into LB 1% (w/v) agar. Strains were incubated for 16 h, and twitching zones were visualized by removing the agar layer and staining the bacteria with 1% (w/v) crystal violet. As a negative control for surface pilins and twitching, a *pilA* mutant was included. Data are representative of n=3 experiments.

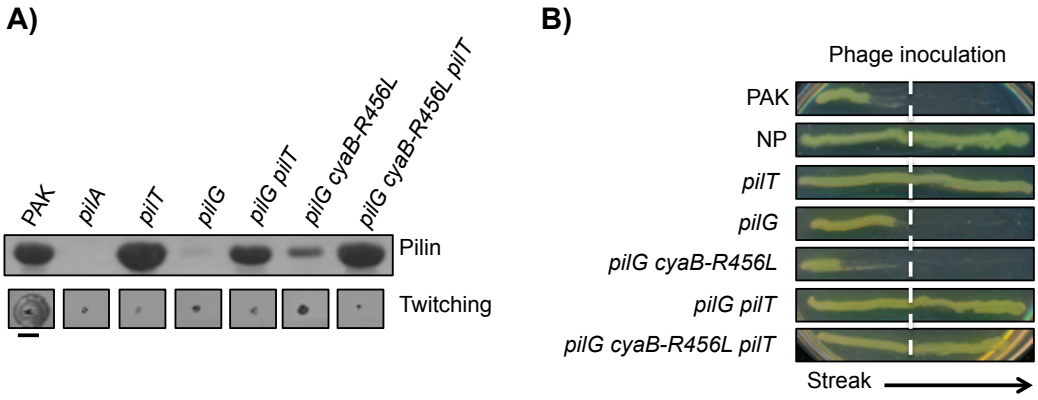

Figure 4.2 – PilG is dispensable for T4P retraction. (A) Levels of surface pilins were assessed by sheared surface protein preparation of strains grown on LB 1.5% agar. The surface protein fractions were prepared as described in the Methods, and resolved by 12.5% SDS-PAGE and visualized by coomassie blue staining. Twitching motility was determined by stab inoculation of the indicated strains into LB 1% (w/v) agar. Strains were incubated for 16 h, and twitching zones were visualized by removing the agar layer and staining the bacteria with 1% (w/v) crystal violet. Scale bar denotes 1 cm. As a negative control for surface pilins and twitching, a *pilA* mutant was included. Data are representative of n=3 experiments. (B) Phage sensitivity assay. Bacteriophage PO4 was spot inoculated onto LB/1.5% agar. Indicated strains were inoculated through the spot inoculation of phage. Dashed white line indicates approximate position of phage inoculation.

PilG contributes to the extension/retraction balance

Given that the lack of twitching in a *pilG* mutant was not due to a lack of ATPases, we next examined the extension/retraction dynamics in the absence of *pilG* by comparing levels of surface piliation (Figure 4.2A). To do this, we deleted *pilT* in a *pilG* background to isolate the T4P

extension phenotype. We also examined a *pilG cyaB-R456L pilT* triple mutant to determine the contribution of cAMP to surface piliation in the absence of *pilG*. As expected, *pilG* had little recoverable surface pili, though there was some recovery in *pilG cyaB-R456L*. These data confirmed that increased cAMP promotes T4P assembly (55). The large difference in the amount of surface pilins between *pilG cyaB-R456L* and wild type suggested that there was a defect in either extension or retraction in the absence of *pilG*. To clarify this, we introduced *pilT* mutations into these backgrounds to isolate the T4P extension phenotype. The *pilG cyaB-R456L pilT* mutant had levels of surface pilin levels similar to the *pilT* mutant, suggesting that it had normal levels of T4P extension. The *pilG pilT* mutant had less surface pilins relative to *pilT*, suggesting that it had an extension defect likely due to decreased intracellular cAMP.

Importantly, although none of the strains twitched, the increases in the amount of recoverable surface pili that were observed after disruption of *pilT* in the *pilG* or *pilG cyaB-R456L* backgrounds suggested that those mutants were still capable of pilus retraction when PilT was present. We verified ongoing pilus retraction by testing sensitivity to a pilus-specific phage, PO4 (Figure 4.2B). Phage PO4 attaches to host T4aP, and upon pilus retraction, is brought in close enough proximity to the cell surface for transduction of phage DNA and eventual cell lysis. PO4 is unable to transduce its DNA into retraction-deficient strains, leading to phage

resistance. Both *pilG* and *pilG cyaB-R456L* mutants were phage sensitive, confirming that they are retraction competent. These data suggest that PilG coordinates twitching motility, but is not essential for pilus retraction. Notably, *pilG cyaB-R456L* phenocopied a *pilU* mutant, which is capable of pilus assembly and retraction, but is unable to twitch (27).

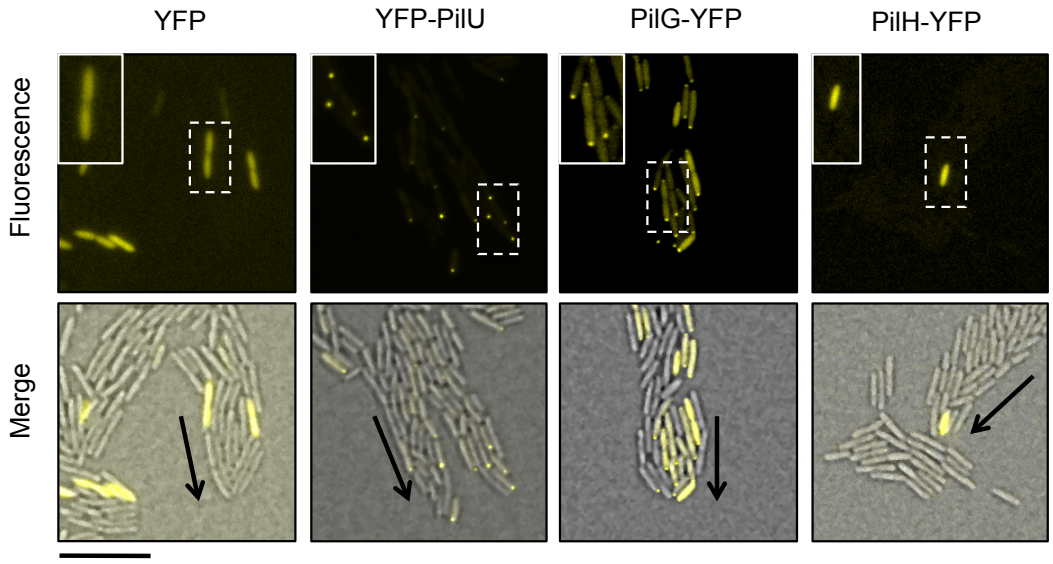

Figure 4.3 – Localization patterns of PilG and PilH fluorescent fusions. Wildtype PAK cells were transformed with expression constructs encoding YFP-PilU or response regulator-YFP fusion proteins, by electroporation. Transformed cells were resuspended in LB and mixed with resuspended and untransformed wild type PAK at ratios of 2:1 to 1:2. The mixed cultures were pelleted by centrifugation, and a sample of the cell pellet was stab inoculated into chambered coverglass slides containing LB 1% agar. Slides were incubated in the dark for 2 h, and then imaged using a 60X oil immersion objective on an EVOS FL Auto

microscope. Scale bar indicates 10 μm distance. Arrows indicate direction of twitching.

PilG localizes to the leading poles of twitching cells, while PilH is diffuse

In the two-response regulator system of *S. meliloti*, only the response regulator believed to be involved in downstream signaling is polarly localized (190). To see if the PilG/PilH system was similar, we examined their localization in twitching cells. C-terminal fusions of either PilG or PilH to YFP were expressed in twitching cells. PilH-YFP was diffuse in the cytoplasm, while PilG-YFP showed a mixed pattern of polar and diffuse localization (Figure 4.3). In cells at the periphery of twitching colonies, there was a pronounced polar focus of PilG-YFP. Other cells had foci at both poles, often with a more intense focus at the leading pole. PilG's localization pattern suggests that it is potentially dynamic, and is consistent with a role in control of directional motility. PilH's diffuse localization is consistent with its proposed role as a phosphate sink (67).

Evolutionary links between PilU, the Chp system, and the cAMP regulatory circuit

Based on the similar phenotype of *pilG cyaB-R456L* and regulation of PilU levels through PilG, we explored other potential links between PilU and PilG function. Bioinformatic analyses of available *Pseudomonas* genomes (189) showed that *pilG* homologs were present in all species,

but *pilU* was present only in strains of *P. aeruginosa*, *P. fulva*, *P. stutzeri*, and *P. mendocina*, which we term 'complex' species. Strains of *P. entomophila*, *P. putida*, *P. brassicacearum*, *P. fluorescens*, and *P. syringae*, which we term 'simple' species, lack a *pilU* homolog. Further, only complex species have *chp* gene clusters that include genes encoding the putative adaptation proteins PilK (methyltransferase) and ChpB (methylesterase), as well as the ChpD and ChpE proteins of unknown function (Figure 4.4A). In addition to simpler *chp* clusters lacking *pilK* and *chpBDE* homologs, species lacking *pilU* had an ~1.5 kb shorter version of the *chpA* kinase gene. In *P. aeruginosa*, *chpA* encodes a complex signal transduction protein that is predicted to phosphorylate PilG and PilH. It has 9 potential sites of phosphorylation, 6 histidine phosphotransfer (Hpt) domains, a serine phosphotransfer domain (Spt), a threonine phosphotransfer domain (Tpt), and a CheY-like receiver domain (50). Simple ChpA orthologs generally lacked regions between Tpt and Hpt2, regions flanking Hpt4, and Hpt6. Although *P. putida* lacks Hpt5, it is present in other simple species (Figure S1). Hpt2, which in *P. aeruginosa* is the primary source of phosphoryl groups for PilG (91), was present in each species we examined.

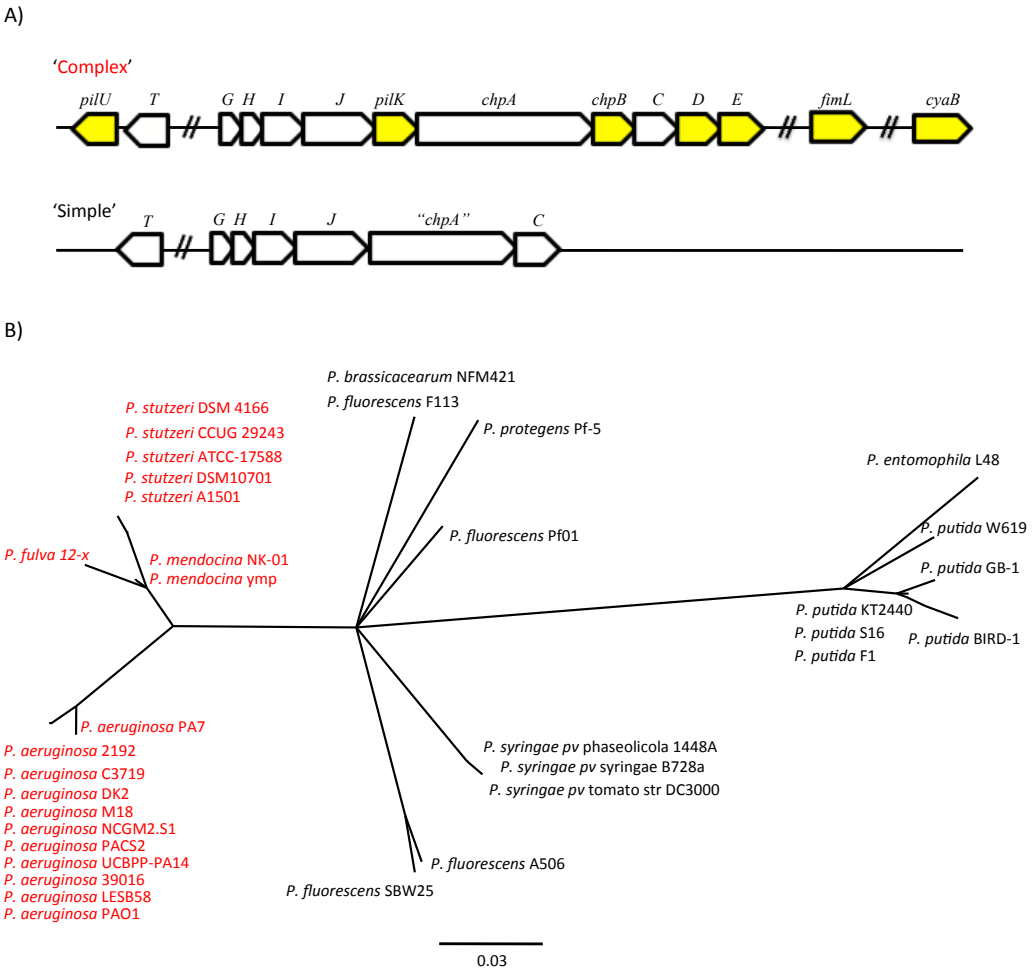

Figure 4.4 – PilU is genetically linked to the Chp system. (A) Schematic of complex and simple Pil-Chp clusters found in *Pseudomonas* genomes annotated on the Pseudomonas Genome Database. Genes marked in yellow are unique to the full-length cluster. (B) Unrooted phylogenetic tree based on MUSCLE alignment of PilG ortholog amino acid sequences. Complex species are shown in red. Scale bar indicated distance in substitutions per site.

Only complex species encoded the adenylate cyclase CyaB, as well as regulatory components FimL and FimX (56, 191). A comparative genome search for other genes that are present in complex species but absent in simple species produced a list of 56 additional genes with the same distribution pattern (Table S1). None were obviously associated with motility, although some were previously identified as belonging to the cAMP-dependent Vfr regulon (Table S1, genes labeled in red) (49).

Although simple species lack components of the cAMP regulatory circuit, they encode PilG orthologs with ~75-88% sequence similarity to those from complex species. A PilG phylogenetic tree showed that orthologs from complex species form a distinct clade compared with those from simple species (Figure 4.4B), and that among the latter, *P. entomophila* and *P. putida* formed a separate cluster. These observations suggested that the PilG orthologs in complex species could have specific sequence differences that related to gain-of-function in regulation of CyaB activity and cAMP production.

'Simple' cluster PilG orthologs can complement a P. aeruginosa pilG mutant

To determine if PilG from simple species were capable of complementing both cAMP-dependent and independent pathways, we

expressed PilG from *P. fluorescens* ($PilG_{Pf}$) or *P. putida* ($PilG_{Pp}$) – representing phylogenetically closest and furthest simple orthologs – in *P. aeruginosa pilG* and *pilG cyaB-R456L* mutants, and examined their PilU levels, surface piliation, and twitching motility (Figure 4.5). Transformation of *pilG* or *pilG cyaB-R456L* with $PilG_{Pf}$ or $PilG_{Pp}$ could restore PilU levels and surface piliation. However, complementation with $PilG_{Pp}$ was less efficient at restoring twitching than $PilG_{Pf}$. Thus, PilG homologs from simple species can at least partly restore both cAMP-dependent and independent functions in *P. aeruginosa*.

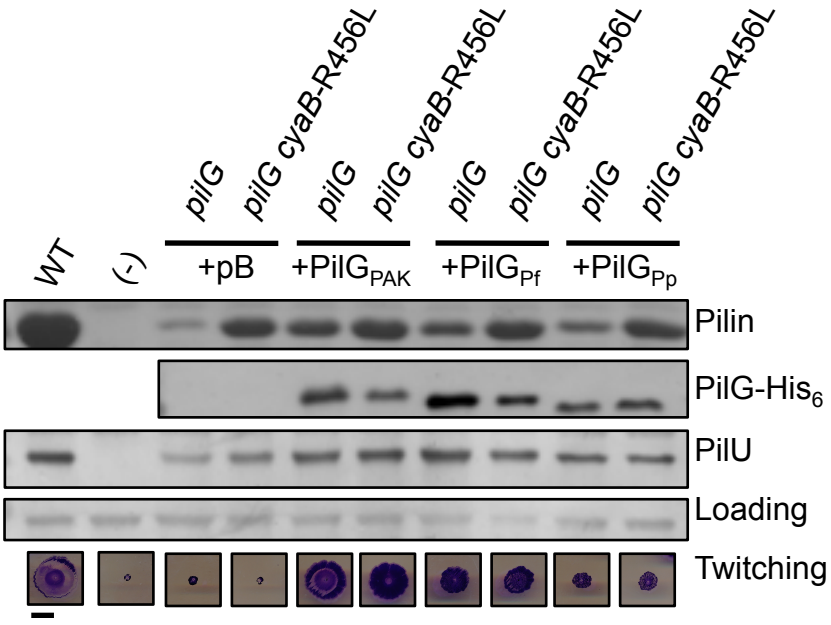

Figure 4.5 – 'Simple' cluster PilG orthologs restore twitching and piliation in a *pilG* mutant. PAK *pilG* and *cyaB-R456L pilG* were transformed with *P. aeruginosa* PilG ($PilG_{Pa}$), *P. fluorescens* ($PilG_{Pf}$) or *P.*

putida ($PilG_{Pp}$) orthologs, or pBADGr (pB). WT PAK was transformed with empty vector (pBADGr) as a vector control. (-) denotes the negative control, either a *pilA* mutant or *pilU* mutant. Levels of surface pilins were assessed by sheared surface protein preparation of strains grown on LB 1.5% agar. The surface protein fractions were prepared as described in the Methods, and resolved by 12.5% SDS-PAGE and visualized by coomassie blue staining. PilU levels were determined by preparing cell lysates of the indicated strains as described in the Methods from cells grown on LB 1.5% (w/v) agar. Cell lysates were resolved on 12.5% SDS-PAGE and transferred to a nitrocellulose membrane and immunoblotted with anti-PilU antiserum. Twitching motility was determined by stab inoculation of the indicated strains into LB 1% (w/v) agar. Strains were incubated for 16 h, and twitching zones were visualized by removing the agar layer and staining the bacteria with 1% (w/v) crystal violet. Scale bar denotes 1 cm.

Characterization of PilG point mutants

Although ChpA is predicted to be the kinase that would phosphorylate PilG and PilH, this hypothesis has not yet been tested experimentally. Using a high-confidence Phyre2 model of PilG generated on an RcsC template (192), we identified the predicted phosphoacceptor residue, Asp58 (Figure 4.6A), and converted it to Glu, Asn or Ala by site-directed mutagenesis. All the HisX6 tagged mutant proteins were stable in both wild type and the *pilG* mutant (Figure 4.6B). Using a purified C-terminal fragment of ChpA, an *in vitro* radioactive phosphotransfer assay

was performed as described in the Methods. Only wild-type PilG was phosphorylated by ChpA (Figure 4.6C).

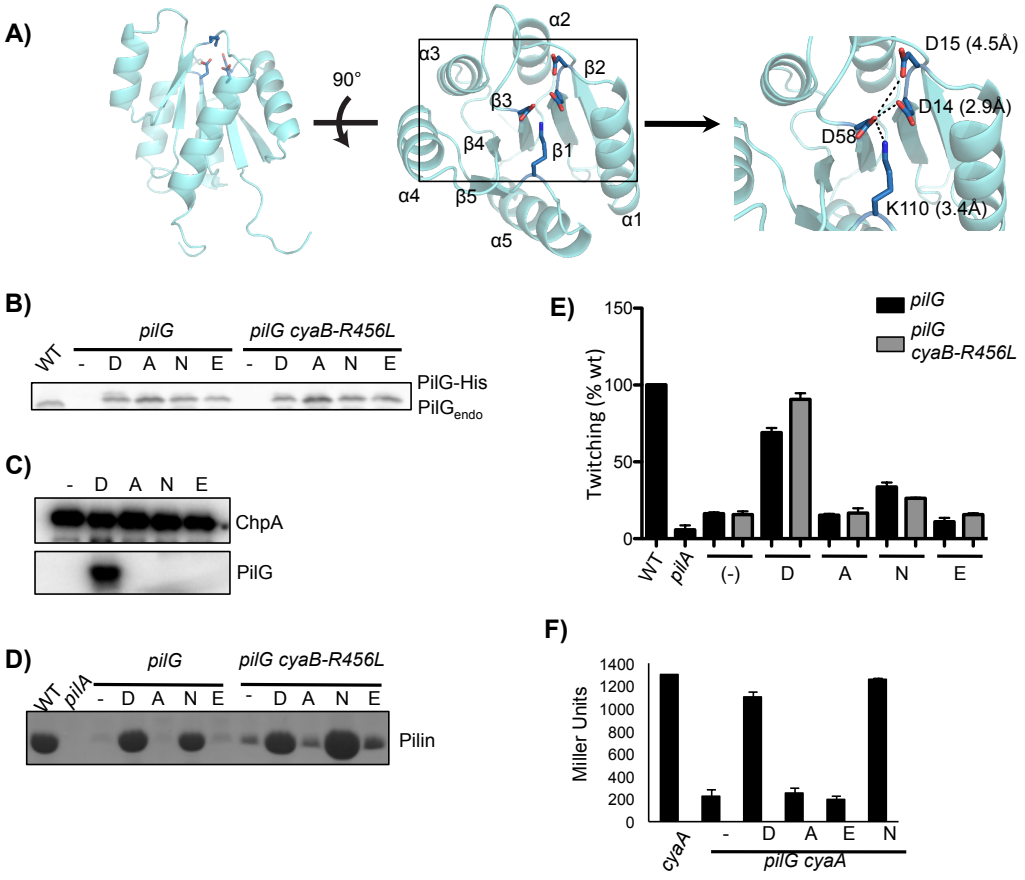

Figure 4.6 – PilG D58N is constitutively active.

(A) Model of PilG structure. Phyre was used to model PilG using the RcsC aspartate phosphotransferase (PDB: 2AYX) as a template. The phosphoacceptor site is indicated with a black box. Right panel: Enlarged view of phosphoacceptor site. The phosphoacceptor residue, D58, is indicated. Neighboring residues in close proximity to D58 as well as side chain distances are indicated. (B) PilG point mutants are stably expressed in *P. aeruginosa*. PAK *pilG* and *pilG cyaB-R456L* were transformed with

pBADGr expression plasmids encoding wildtype PilG (D), PilG point mutants D58A (A), D58N (N) or D58E (E), or empty vector (-). As a control, we included wildtype (WT) PAK. Whole cell lysates were probed by western Blot using anti-PilG antisera. (C) Phosphorylation of PilG point mutants. Purified $ChpA_{1668-2328}$ was incubated with ^{32}P ATP and purified PilG, PilG D58A, D58N, D58E, or incubated alone as a control (-). ChpA and phospho-PilG were resolved by SDS-PAGE and imaged by autoradiography. Top panel: purified ChpA binding to ^{32}P ATP. Bottom panel: phosphorylated PilG, bound to ^{32}P. (D) Sheared surface protein fractions were prepared as outlined in the Methods. Surface pilns were resolved by 15% SDS-PAGE and visualized by Coomassie staining. NP, non-piliated. (E) Motility of *pilG* or *pilG cyaB-R456L* expressing PilG, PilG D58A, PilG D58N, or PilG D58E was determined by twitching motility assay. Twitching assay was performed by stab inoculation into LB/1% agar and incubated overnight at 37°C. twitching zones were visualized by crystal violet staining. (F) CyaB activation by PilG point mutants. PAK *cyaA::lac*P1-*lacZ* cells were transformed with pMMB (-), pMMB *piG*, pMMB *pilG*-D58A, pMMB *pilG*-D58E, or pMMB *pilG*-D58N. Activity is from samples with roughly equivalent levels of PilG protein as determined by immunoblot with anti-PilG antibody (not shown). Induction of *pilG* expression with 50 mM IPTG yielded about the same level of PilG for all constructs except PilGD58E, which required 150 mM IPTG. All data are representative of n=3 independent experiments.

To determine if phosphorylation was required for PilG's cAMP-dependent and independent functions, we tested the ability of the mutant proteins to complement *pilG* and *pilG cyaB-R456L* mutants. Complementation with wild type PilG *in trans* restored twitching in *pilG* to

~70% and to 90% in *pilG cyaB-R456L* compared to the parent strain transformed with the vector control, (Figure 4.6E). Neither PilG D58A nor PilG D58E restored piliation (Figure 4.6D) or twitching (Figure 4.6E) in either *pilG* or *pilG cyaB-R456L.* Interestingly – since it was not phosphorylated by ChpA – the PilG D58N mutant restored piliation to both *pilG* and *pilG cyab-R456L,* and twitching to ~33% in *pilG* and 26% in *pilG cyaB-R456L* relative to wild type (Figure 4.6E). Consistent with their effects on twitching motility, wild type PilG and PilG D58N restored surface piliation in both *pilG* and *pilG cyaB-R456L* (Figure 4.6D). Because PilG is required for CyaB activity, we examined the effect of the PilG point mutations on intracellular cAMP levels. Wild type or mutant PilG variants were used to complement a *cyaA pilG* double mutant (in which only CyaB contributes to cAMP synthesis) expressing a β-galactosidase reporter responsive to intracellular cAMP levels (55). PilG and PilG D58N restored the production of cAMP to levels commensurate with the *cyaA* mutant control (Figure 6F). The ability of the PilG D58N mutant to restore function *in vivo* is likely due to the spontaneous deamidation of Asn58 to Asp, as reported previously for a D57N mutant of CheY (64). However, these results suggest that phosphorylation of PilG is require for both cAMP-dependent and independent functions of PilG.

DISCUSSION

Two forms of the Chp system

Whitchurch et al. (50) reported that homologs of the *P. aeruginosa chp* genes were found in a number of other species, and that *P. fluorescens*, *P. putida*, and *P. syringae* lacked PilK and ChpB homologs. The subsequent increase in the number of available *Pseudomonas* genomes over the last decade allowed us to broaden that analysis. The *chp* clusters fall into two broad classes, which we termed simple and complex. The simple cluster encodes a shorter form of ChpA and lacks genes encoding orthologs of the putative methyltransferase PilK and putative methylesterase ChpB, as well as ChpD and ChpE, suggesting that it may have reduced capacity to adapt to changes in signal strength or type. A total of 60 genes unique to complex species were identified using comparative genomics (Table S1); they include *cyaB* and *fimL* involved in the cAMP regulatory circuit; *fimX,* encoding a cyclic-di-GMP binding protein required for twitching motility; and the T4P ATPase-encoding gene, *pilU*. Among those genes are 11 whose expression was decreased in a *vfr* mutant (Table S1, genes highlighted in red) (49). A functional link between the Chp system and cAMP production by CyaB has been established (55), and these observations suggest that the Chp system may have a broader role in regulation than previously appreciated. Luo and colleagues (89) recently described a model in which they propose that Chp signaling is

part of a hierarchical pathway involving cAMP, cyclic-di-GMP, and the minor pilins. Their data suggest that PilJ may signal via direct interactions with the sensor kinase FimS of the FimS-AlgR two-component system to positively regulate transcription of the *fimU-pilVWXY1* minor pilin operon. PilY1 and the minor pilins would then regulate their own production through PilJ, FimS-AlgR, and Vfr (193). More recently, Persat et al. (88) suggested that PilJ may interact with PilA subunits that have undergone force-induced conformational changes due to retraction under tension, and that these interactions could lead to upregulation of cAMP production and surface-associated virulence. These data suggest that the Chp system is integral to the expression of *P. aeruginosa* virulence phenotypes.

The complex *P. aeruginosa* ChpA protein has 9 potential sites of phosphorylation, including six Hpt domains, one Ser phosphotransfer domain, one Thr phosphotransfer domain, and a CheY-like pseudoreceiver (REC) domain (50). Leech and Mattick (90) showed that ChpA's Hpt2 and Hpt3 and REC domains are required for twitching. Silversmith et al. proposed that Hpt2 and Hpt3 are the dominant sources of phosphoryl transfer to PilG and PilH (91). Hpt6 is unique to complex versions of ChpA, suggesting that it might be involved in phosphotransfer to other regulatory components that are specific to complex species. These might include ChpB, whose homologue CheB is regulated by CheA phosphorylation (194), or FimX, whose REC domain controls its unipolar

localization (54, 120). Phosphotransfer from ChpA to multiple components could be involved in the coordinate activation of cAMP- and cyclic-di-GMP-dependent pathways in complex species. An alternate model proposed by Luo and colleagues (89) suggests that Chp-dependent regulation of the minor pilin operon may have downstream effects on cyclic-di-GMP levels. In *Xanthomonas axonopodis* pv. citri, the regulatory protein PilZ interacts with FimX to regulate pilus extension (118). PilZ is present in all complex species, but also in the simple species *P. syringae*, *P. brassicacerum* and *P. fluorescens* that lack FimX, suggesting that there are species-dependent variations in regulation of pilus expression and function.

Both complex and simple species encode PilG orthologs, with amino acid identities of at least 71% Our data show that simple PilG orthologs, even from distantly related species such as *P. putida*, can at least partly regulate both cAMP-dependent and independent pathways in *P. aeruginosa*, a complex species. This finding argues against the idea that the more elaborate Chp clusters in complex species are the result of gain-of-function evolution following acquisition of the *cyaB* gene and associated regulatory elements such as FimL. Comparison of high confidence models of PilG, $PilG_{Pf}$, and $PilG_{Pp,}$ generated using the Phyre2 server (192) revealed no obvious clustering of amino acid substitutions to any particular face of the protein that might account for functional differences due to changes in potential interaction interfaces (data not

shown). These data suggest that the ability of the Chp pathway to regulate cAMP production was likely not an original ability of the complex cluster Pseudomonads, and was acquired later.

PilG is the response regulator of the Chp system

Based on mutant phenotypes, PilG and PilH were previously hypothesized to function as response regulators controlling pilus extension and retraction, respectively (93). Fulcher et al. (55) subsequently proposed that PilH may function as a phosphate sink to control the levels of PilG phosphorylation, similar to the diffusely-localized CheY1 protein in the flagellar chemotaxis system of *S. meliloti* (67). Our data suggest that PilG is dispensable for T4P retraction as mutants lacking *pilG* are phage sensitive. Decreased surface piliation in *pilG* is due to decreased intracellular cAMP, as *pilG cyaB-R456L pilT* but not *pilG pilT* has levels of surface pilins similar to wild type. However, lack of twitching motility in *pilG* and *pilG cyaB-R456L* confirm that PilG is required for twitching motility independent of its role in cAMP regulation. Interestingly, non-phosphorylatable PilG localizes to the cell poles, suggesting that phosphorylation is not necessary for polar localization (135). Consistent with this, bacterial two-hybrid data suggests that both wild type and PilG D58A both interact with FimL, which has been shown previously to have unipolar localization (56). PilG was proposed to interact with FimL, which

in turn interacted with FimV (135). Only deletion of *fimV* mislocalized PilG suggesting that it has a second interaction partner which is likely related to its cAMP-independent function.

The relatively high level of function of PilG D58N in the absence of phosphorylation (Figure 4.6) was somewhat unexpected. A D57N mutation of *E. coli* CheY was previously shown to be active due to phosphorylation at S56, which was dependent on the activity of CheA (60), and a S56A D57N double mutant was inactive. Due to the *in vitro* nature of the kinase assay, we cannot exclude the possibility that PilG or any of the PilG point mutants might be phosphorylated at another residue *in vivo*. However, PilG D58A and PilG D58E, which have the same residues that could serve as alternate sites of phosphorylation, are inactive. Instead, the partial function of the PilG D58N point mutant is likely due to spontaneous deamidation of N58 *in vivo*, as reported previously for a D57N mutant of CheY (64). Interestingly, PilG D58A had the same localization pattern as wild-type PilG (135), suggesting that as in *E. coli*, response regulator localization is independent of phosphorylation (195). Our data confirm that phosphorylation of PilG is required to activate CyaB and to regulate motility, although the nature of phospho-PilG's interaction partner(s) is currently unknown. PilG is 28% identical to CheY, but the T4P system lacks homologs of the flagellar switch complex, suggesting that PilG acts through a different mechanism to regulate motility. CheY becomes

delocalized in *E. coli* lacking *cheA* (195), but PilG-YFP localized to the cell poles in mutants lacking *chpA* (135). These data suggest that PilG interacts with one or more as yet unidentified components to coordinate cAMP-dependent and independent functions.

PilG controls both extension and retraction

PilG modulates both extension and retraction of T4P (55). Pilus biogenesis is cAMP-dependent, as demonstrated by the difference in piliation of a *pilG pilT* double mutant and a *pilG pilT cyaB-R456L* triple mutant relative to *pilT* (Figure 4.3). PilG activation of CyaB increases intracellular cAMP levels, thereby promoting transcription of Vfr-dependent T4P genes, including those encoding the PilMNOPQ proteins that form the assembly complex, and the minor pilins FimU, PilVWX and PilE plus the putative adhesin PilY1, involved in control of pilus extension (49, 196, 197). PilG also increases levels of the extension ATPase PilB through its activation of CyaB (Figure 4.2A). Together, these increases in expression would lead to more T4P assembly systems in the cell envelope, and thus increased piliation. Activation of CyaB by PilG is proposed to be through FimL and FimV (135). Pilus retraction does not require PilG, as both *pilG* and *pilG cyaB-R456L* mutants are susceptible to pilus-specific phage (Fig 4.2B). Localization of PilG to a single pole may bias retraction over extension at one pole of the cell. Lack of PilG may result in an imbalance

between retraction and extension at the poles, leading to retraction of T4P along opposing vectors at both poles, preventing directional movement.

Although PilT and PilU ATPase levels are positively regulated by cAMP, both proteins function downstream of PilB, as pilus disassembly can only occur following pilus assembly. The presence of *pilG* in simple species that lack *pilU* and *cyaB* suggests that the ancestral function of PilG was likely spatial and/or temporal coordination of pilus retraction. We hypothesize that hyperactivation of PilG caused by deletion of *pilH* and the resulting increases in cAMP and T4P expression, also results in extension of pili at both poles instead of mostly at the leading pole, impairing directional movement. These data suggest that twitching motility requires optimal levels of phosphorylated PilG.

In summary, our data show that the *P. aeruginosa* Chp system regulates T4P function by modulating expression of assembly system components – and thus pilus extension – in a cAMP dependent manner, while coordinating twitching motility in a cAMP-independent manner. The signals to which the Chp system responds, and how Chp signaling is coordinated with that of factors such as FimX and PilZ that control pilus extension in response to cyclic-di-GMP levels, remain to be clarified. This regulatory complexity is consistent with the ability of *Pseudomonas* and related environmental bacteria to adapt to a wide range of growth environments.

The role of PilU in twitching

Because PilU orthologs appear to be unique to complex species, we initially hypothesized that PilU function was linked to the Chp system and the cAMP-regulatory circuit. Expression of PilU – but not PilB or PilT – is decreased ~11-fold in a *vfr* mutant (49). Here we showed that expression of all three ATPases was cAMP-dependent. A potential role for PilU in coordination of motility is supported by its unipolar localization in twitching cells (35) (Cynthia Whitchurch, personal communication) and the ability of a *pilU* mutant to both extend and retract pili without net motility; these phenotypes are shared by *pilG* mutants supplemented with cAMP, either in the medium or by constitutive activation of CyaB (27, 55, 107). This result demonstrates the need to separate cAMP-dependent and independent effects when examining pilus function, which depends on the ability to repeatedly extend and retract in a coordinated manner.

As the *pilG cyaB-R456L* mutant phenocopies a *pilU* mutant, we hypothesize that the two are functionally connected. The bioinformatic analysis suggests that this could be in part through the cAMP regulatory circuit. Inclan et al. showed that PilG localization is dependent on FimV, however there is no evidence to suggest a direct interaction (135). We propose that PilG will colocalize with other members of the cAMP regulatory circuit, and in this way, play a role in coordinating asymmetrical

pilus function through PilU, which has unipolar distribution (35). In their absence, simultaneous pilus extension and retraction at both cell poles likely leads to a loss of directed movement. Similarly, uncoordinated retraction of pili along multiple vectors was proposed to be responsible for loss of motility in *pocA* mutants of *P. aeruginosa*, which express non-polar pili (178).

Studies in *M. xanthus* showed that ATPase localization during T4P-mediated motility can be influenced by its Chp-like Frz chemotaxis system (100). Although the Frz system is not required for the initial polar localization of the *M. xanthus* ATPases, signaling through the Frz system leads to GTPase signaling that re-sorts polar localization of PilB and PilT (198). Based on the homology between the Frz and Chp systems, Whitchurch et al. (50) proposed previously that they play similar roles. However, Whitchurch et al. showed that PilU remains localized to a single cell pole during short reversals (Cynthia Whitchurch, personal communication). One possibility is that PilU prevents PilT binding at one of the poles, thereby promoting retraction at the leading pole of the cell and directional movement.

PilG has several important roles in regulating twitching. The model proposed by Inclan et al. does not explain the cAMP-independent role of PilG, as its interaction partner, FimL, only participates in cAMP-dependent control (56, 135). Our data show that decreased T4P extension in *pilG* is

due to decreased intracellular cAMP, which leads to decreased transcription of multiple T4P structural components (49). In the absence of PilG, our data suggest that there is an imbalance between T4P extension and retraction when intracellular cAMP is high. Whether the cAMP-independent function of PilG intersects with PilU is unknown, but it will be interesting to see the roles of both of them in regulating twitching. Taken together, our data suggest that PilG has a cAMP-independent role in controlling the balance between T4P extension and retraction, and this may be an ancestral function of PilG homologs.

METHODS

Bacterial strains and growth conditions

The bacterial strains and plasmids used in this study are listed in Table I. Unless otherwise specified, bacteria were grown on LB 1.5% (w/v) agar at 37°C. Antibiotic selection was as follows: Gentamicin (Gm), 15 μg ml^{-1} (*E. coli*), or 30 μg ml^{-1} (*P. aeruginosa*).

Western blotting

Western blotting of whole cell lysates was performed as previously described (28). In brief, whole cell lysates were resolved on 12.5% SDS-PAGE gels and transferred to nitrocellulose membranes. Membranes were blocked in 5% skim milk (w/v) dissolved in PBS (pH 7.4), washed in PBS,

incubated in the appropriate rabbit antisera diluted in PBS (anti-PilB 1:2000; anti-PilT 1:500; anti-PilU 1:5000; anti-PilG 1:1000), washed, incubated with alkaline phosphatase-conjugated goat anti-rabbit secondary antibody (1:3000; Bio-Rad), and washed in PBS. Blots were developed using BCIP (5-bromo-4-chloro-3-indolylphosphate) and NBT (nitro-blue tetrazolium) as per manufacturer's instructions.

Twitching motility assays

Twitching motility was tested as described previously (150). In brief, cells from an overnight culture were stab inoculated to the interface between LB 1% (w/v) agar and the underlying polystyrene petri dish, and incubated at 37 °C for 16 h. Twitching zones were visualized by removing the agar and staining cells on the petri dish with 1% (w/v) crystal violet followed by washing excess crystal violet with tap water.

Electroporation

Cells from overnight solid media cultures were washed three times with sterile milliQ H_2O and resuspended in sterile milliQ H_2O. Using 0.2 cm electroporation cuvettes, 100 μl cell suspension was pulsed at 2.5 V. Electroporated cells were resuspended in 500 μl LB and incubated at 37 °C for 3 h. Following recovery, cells were plated on selective media and grown at 37 °C overnight.

Sheared surface protein preparation

Surface pili and flagella were analyzed as described previously (150). In brief, strains of interest were streaked in a grid pattern onto LB 1.5% (w/v) agar in 15 cm diameter petri dishes, and grown at 37°C overnight. Cells were gently scraped from the plates using a sterile coverslip and resuspended in 4.5 ml PBS (pH 7.4). Surface appendages were removed by vortexing of resuspended cells for 30 s. An amount of cells normalized by OD_{600} were pelleted by centrifugation at 16,100 × g for 5 min. Supernatant was collected and centrifuged again at 16,100 × g for 20 min to remove remaining cells. Supernatants were collected, mixed with 1/10 volume of each of 5 M NaCl and 30% w/v polyethylene glycol (Sigma; molecular weight range ~8000), and incubated on ice for 90 min. Precipitated surface protein was collected by centrifugation at 16,100 × g for 30 min. Supernatants were discarded and samples were centrifuged again at 16,100 × g for 2 min. Pellets were resuspended with 150 ml of 1X SDS-PAGE sample buffer (80mM Tris, pH 6.8, 5.3% v/v 2-mercaptoethanol, 10% v/v glycerol, 0.02% w/v bromophenol blue, 2% w/v SDS). Samples were boiled for 10 min and resolved by 15% SDS-PAGE gels. Bands were visualized by staining with Coomassie brilliant blue (Sigma).

Phage sensitivity

Five µl of bacteriophage PO4 was spot inoculated onto LB 1.5% (w/v) agar. Strains were inoculated in a straight line through the phage inoculum. Plates were then incubated at 37 °C overnight.

Fluorescence microscopy

P. aeruginosa (PAK) strains expressing YFP tagged protein (PilU, PilG and PilH) were grown overnight on solid LB media supplemented with gentamicin at 37 ^{o}C. Transformed and untransformed PAK cells were resuspended in LB and normalized to OD_{600} = 0.8. Cells containing empty vector were mixed with cells carrying fluorescent fusions at ratios of 2:1 to 1:2. Cell mixtures were pelleted by centrifugation, and a sample of the pellet was stab inoculated into 1.0 borosilicate chambered coverglass slides (Lab-Tek) containing LB 1% (w/v) agar. Cells were incubated in the dark for 2 h at 37 ^{o}C. Cells were visualized with an EVOS FL Auto (Life Technologies) using a 60x oil immersion objective. For fluorescence microscopy, a YFP LED light cube (excitation λ =500-524 nm, emission λ = 524-527 nm) was used. Images were acquired and edited using EVOS FL Auto Cell Imaging System (Life Technologies) and ImageJ (NIH).

Comparative gene analysis

Complex species were identified by searching the Pseudomonas Genome Database for putative orthologs of the Chp genes. Species encoding putative orthologs of *P. aeruginosa* PilGHIJK and ChpABCDE were classified as complex species. Species lacking components of the cluster were classified as simple species.

The comparative search tool was then used to identify all annotated genes present in complex species genomes, and not in the simple species.

Plasmid construction

pBADGr::*pilG*$_{Pa}$ was generated by amplifying the PilG coding region of *P. aeruginosa* strain PAK using the indicated primers. *pilG*$_{Pa}$ was ligated into pBADGr at the EcoRI and XbaI sites using T4 DNA ligase (Thermo Scientific) as per manufacturer's instructions.

A pUC57 construct encoding PilG (GI: 229593123) from *P. fluorescens* SBW25 (PilG$_{Fl}$) was synthesized by GenScript USA. *pilG*$_{Pf}$ was excised from pUC57::*pilG*$_{Pf}$ by digestion with EcoRI and XbaI, and subcloned into pBADGr.

β-galactosidase assay

The β-galactosidase activity was assayed as described previously (49). Bacteria were grown to mid-logarithmic phase in LB broth or LB broth

containing 30 μg ml^{-1} carbenicillin containing 50 mM isopropyl β-D-1-thiogalactopyranoside (IPTG) or 150 mM PilG D58E.

Kinase assay

DNA encoding *P. aeruginosa* PilG or ChpA residues 1668-2328 was obtained by PCR using PAK genomic DNA as template. The fragments was inserted between the NdeI/BamHI (for PilG) or NdeI/HindIII (for $ChpA_{1668-2328}$) sites of pET28a (Merck Millipore) to encode the desired protein with an N-terminal, thrombin-cleavable his_6-tag. Plasmids encoding PilG mutants D58A, D58N, and D58E were made by site directed mutagenesis (Quikchange, Agilent Technologies) of the wild type pET28-PilG plasmid. For protein expression and purification, plasmids were transformed into *Escherichia coli* BL21(DE3). Expression cultures were grown at 37˚C to an absorbance at 600 nm of 0.4. Expression was then induced with 0.5 mM IPTG and allowed to proceed for 16 h at room temperature. The his_6-tagged proteins were purified by standard Ni-NTA affinity protocols (Qiagen), followed by thrombin cleavage of the His_6-tag, and gel filtration chromatography (Superdex 75 1660, GE Biosciences). 1.4 mM ChpA construct (PAK $ChpA_{1668-2328}$, which comprises Hpt6, the dimerization domain, the catalytic comain, and the CheW-like domain) and 30 mM [γ-^{32}P]-ATP were incubated at room temperature for 15 min either in the absence of PilG (-) or in the presence of 19 mM wild type PilG, PilG

D58A, PilG D58N, or PilG D58E. Reactions were quenched with 2x SDS sample buffer and a fixed volume separated on an 18% polyacrylamide SDS gel. The gel was dried and analyzed by phosphorimaging.

ACKNOWLEDGEMENTS

This work was supported by Canadian Institutes of Health Research grant MOP 93585 to LLB and PLH. MCW and NBF were supported by National Institutes of Health grant AI069116. RES was supported by National Institutes of Health grant R01GM050860.

Table 4.1. Strains and plasmids used in this study

Strain or Plasmid	Description	Source
E. coli		
E. coli DH5α	F- φ80*lac*ZΔM15 Δ(*lac*ZYA-*arg*F)U169 *rec*A1 *end*A1 *hsd*R17(rk-, mk+) *pho*A *sup*E44 *thi*-1 *gyr*A96 *rel*A1 λ-	Invitrogen
E. coli SM10	thi-1 thr leu tonA lacY supE recA RP4-2-Tcr::Mu, Km^r; mobilizes plasmids into *P. aeruginosa* via conjugation	(181)
P. aeruginosa		
PAK	PAK wildtype, laboratory strain	Boyd, J.
PAK NP	Tet^r cassette inserted into *pilA*	(168)
PAK *pilG*	Deletion of *pilG*	(55)
PAK *cyaAB*	Deletion of *cyaA* and *cyaB*	(55)
PAK *pilG cyaB*-R456L	deletion of *cyaA* and *cyaB*, R to L substition of codon 456	This study
PAK *pilT*	FRT scar at position 540 of *pilT*	(26)
PAK *pilG pilT cyaB*-R456L	Deletion of *pilG*, FRT scar at positio 540 of *pilT*, and R to L substition of codon 456	This study
PAK *pilG pilT*	Deletion of *pilG* and FRT scar at position 540 of *pilT*	This study
PAK *pilH*	Deletion of *pilH*	(55)
Plasmid		
pMarkiC	pUCP20 carrying YFP	This study
pMarkiC *pilG*	pUCP20 containing PilG with C-terminal YFP	This study
pMarkiC *pilH*	pUCP20 containing PilH C-terminal YFP	This study
pUCP20Gm-*yfp*	YFP construct	(35)
pUCP20Gm-*yfp-piU*	YFP-PilU fusion construct	(35)
pBADGr	Broad host range arabinose inducible vector used for complementation; gentamicin resistance marker	(169)

pBADGr *pilG*	Comeplementation construct carrying PilG	This study
pBADGr *pilG* D58A	Complementation construct carrying PilG D58A	This study
pBADGr *pilG* D58N	Complementation construct carrying PilG D58N	This study
pBADGr *pilG* D58E	Complementation construct carrying PilG D58E	This study
pEX18Gm	Suicide vector with Gmr cassette	(199)
pEX18Gm *cyaB* R456L	Allele exchange vector containing *cyaB* codon 456 flanked by upstream and downstream 1kb	(173)
pEX18Ap *pilT::FRT*	Suicide vector containing pilT disrupted with FRT-flanked gentamicin cassette at position 540	(169)

Table 4.2. Oligonucleotides used in this study

Primers	
PilG D58A Fwd	5' - GAACATCATTTTCGTCGCCATCATGATGCCGCGC - 3'
PilG D58A Rev	5' - GCGCGGCATCATGATGGCGACGAAAATGATGTTC - 3'
PilG D58N Fwd	5' - GAACATCATTTTCGTCAACATCATGATGCCGCGC - 3'
PilG D58N Rev	5' - GCGCGGCATCATGATGTTGACGAAAATGATGTTC - 3'
PilG D58E Fwd	5' - GAACATCATTTTCGTCGAGATCATGATGCCGCGC - 3'
PilG D58E Rev	5' - GCGCGGCATCATGATCTCGACGAAAATGATGTTC - 3'
PilG Fwd (for cloning into pBADGr)	5' - GCGGAATTCATGGAACAGCAATCCGACGGTTTGAAAGTGATGGTG - 3'
PilG-His Rev (for cloning into pBADGr)	5' - GCGTCTAGATCAGTGGTGATGGTGATGATGGGAAACGGCGTCCACCGG - 3'

Table S4.1 – List of PAO1 genes shared among 'complex' species and absent from 'simple' species

Locus Tag	Gene Name	Product Name
PA0347	*glpQ*	glycerophosphoryl diester phosphodiesterase, periplasmic
PA0391[1]		hypothetical protein
PA0412	*pilK*	methyltransferase PilK
PA0414	*chpB*	probable methylesterase
PA0573		hypothetical protein
PA0657		probable ATPase
PA0664		hypothetical protein
PA0745		probable enoyl-CoA hydratase/isomerase
PA0780	*pruR*	proline utilization regulator
PA0951		probable ribonuclease
PA0952		hypothetical protein
PA1191		hypothetical protein
PA1505	*moaA2*	molybdopterin biosynthetic protein A2
PA1595		hypothetical protein
PA1822	*fimL*	FimL
PA1825		hypothetical protein

PA2024		probable ring-cleaving dioxygenase
PA2184		conserved hypothetical protein
PA2632		hypothetical protein
PA2779		hypothetical protein
PA2829		hypothetical protein
PA2992		hypothetical protein
PA2994	*nqrF*	Na+-translocating NADH:quinone oxidoreductase, subunit Nqr6
PA2995	*nqrE*	Na+-translocating NADH:quinone oxidoreductase subunit Nqr5
PA2996	*nqrD*	Na+-translocating NADH:uniquinone oxidoreductase subunit Nqr4
PA2997	*nqrC*	Na+-translocating NADH:ubiquinone oxidoreductase subunit Nrq3
PA2998	*nqrB*	Na+-translocating NADH:ubiquinone oxidoreductase subunit Nrq2
PA2999	*nqrA*	Na+-translocating NADH:ubiquinone oxidoreductase subunit Nrq1
PA3051		hypothetical protein
PA3052		hypothetical protein
PA3091		hypothetical protein

PA3217	*cyaB*	CyaB
PA3270		hypothetical protein
PA3276		hypothetical protein
PA3289		hypothetical protein
PA3306		hypothetical protein
PA3967		hypothetical protein
PA4048		hypothetical protein
PA4325		hypothetical protein
PA4369		hypothetical protein
PA4396		probable two-component response regulator
PA4404		hypothetical protein
PA4611		hypothetical protein
PA4616		probable c4-dicarboxylate-binding protein
PA4713		hypothetical protein
PA4737		hypothetical protein
PA4870		conserved hypothetical protein
PA4929		hypothetical protein
PA4959	*fimX*	FimX
PA5027		hypothetical protein
PA5073		hypothetical protein
PA5137		hypothetical protein

PA5190		probable nitroreductase
PA5207		probable phosphate transporter
PA5208		conserved hypothetical protein
PA5291		probable choline transporter
PA5305		conserved hypothetical protein
PA5307		hypothetical protein
PA5518		probable potassium efflux transporter

[1]Expression of genes in red text was decreased in a *vfr* mutant (49)

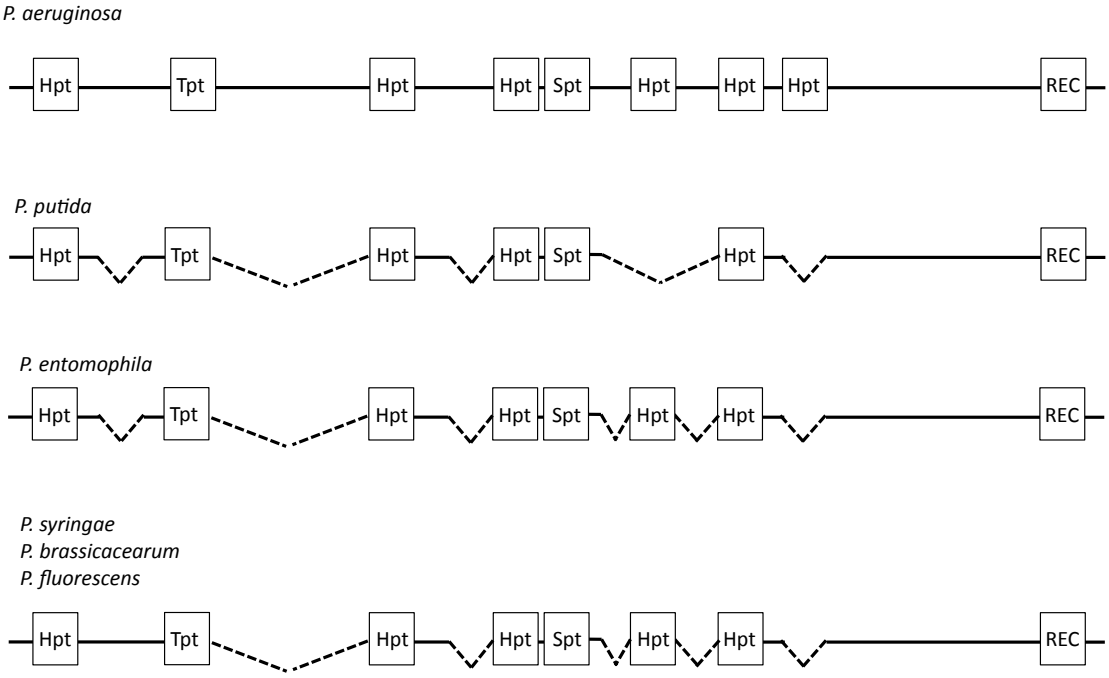

Figure S4.1 – ChpA orthologs in 'simple' Chp cluster species have fewer predicted phosphotransfer domains. Schematic depicting predicted histidine phosphotransfer domains (Hpt), threonine phosphotransfer domains (Tpt), serine phosphotransfer domains (Spt), and CheY-like receiver domains (REC). Dashed lines represent regions not present in the ChpA coding region relative to the *P. aeruginosa* coding region.

CHAPTER FIVE

Conclusions and Future Directions

Summary of contributions to the field

This thesis describes studies aimed at clarifying the role of the Chp chemotaxis system and the inner membrane protein FimV in the regulation of twitching in *P. aeruginosa*. Our investigations of FimV showed that it has a cAMP-independent role in regulating twitching in *P. aeruginosa* that is distinct from the previously identified cAMP-independent role of the Chp system (55). We clarified which of the previously reported phenotypes associated with *fimV* deletion – decreased T2S (134) and decreased PilMNOPQ (125) – were due to decreased intracellular cAMP levels (Chapter 2 and 3), and determined the structure of a domain critical to both aspects of FimV function (Chapter 2). Our study of the Chp response regulator PilG suggests that it may regulate T4aP function by altering the balance between extension and retraction at the leading poles of moving bacteria (Chapter 4). Together, these data and newer models of T4aP regulation help provide clarity about the organization of the T4aP regulatory circuit, which is important for understanding its role in *P. aeruginosa* physiology and virulence.

The C-terminal region of FimV

The most conserved regions of FimV orthologs are the periplasmic LysM motif, and the C-terminal domain. While LysM motifs are known to be involved in polar targeting (128, 129), the role of the C-terminal domain

was unknown. We demonstrated a role for the C-terminal domain in FimV function, and determined the structure for this highly conserved region found in multiple FimV homologs.

FimV, FimL, and the Chp system were all identified as regulators of CyaB function (54-56), although the original study did not explain if or how they work together to do so. Inclan et al. (135) later proposed that FimV interacts with FimL to connect it to the Chp system. In Chapter 2, we showed that this critical interaction occurs through the conserved FimV C-terminal domain (Figure 2.6). Consistent with the proposed model, a C-terminally truncated form, $FimV_{689}$, failed to restore either the cAMP-dependent or independent functions of FimV (Figure 2.4). These two studies were the first to provide evidence showing how FimV, FimL, and the Chp system work in concert to activate CyaB. Complementation studies using $FimV_{689}$ also showed that the cAMP-independent and cAMP-dependent functions of FimV were not localized to the periplasmic and cytoplasmic regions of FimV, respectively, as previously hypothesized (125).

No experimentally-derived structural information was available for FimV and its homologs prior to our study. The structure we determined encompasses the highly conserved 'FimV C-terminal domain', the first for this region of FimV and its orthologs. The structure confirmed the presence of a single TPR motif and capping helix, which at least in the

case of FimV, is sufficient for a protein-protein interaction with FimL. Interestingly, sequence alignment of the conserved domain in FimV orthologs showed that the most highly conserved residues do not correspond to the published TPR consensus sequence (126). The conserved TPR residues were identified from sequence alignment of TPR sequences form eukaryotic proteins (126). Alignment of TPR sequences from bacterial proteins with solved structures showed loose conservation with the published TPR consensus sequence (126) (Figure 5.1). The TPR in the FimV C-terminal domain may represent a specialized subset of TPRs unique to the FimV family. The differences between the FimV C-terminal TPR and the published TPR consensus sequence suggest that sequence conservation alone is a poor predictor of a TPR motif. The high sequence variability among TPRs makes it a rich area for further study.

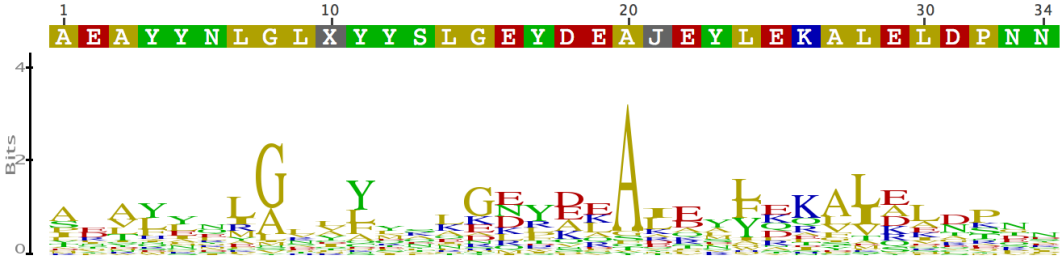

Figure 5.1 – Alignment of bacterial TPRs. Conservation of TPRs among bacterial proteins. TPR sequences from bacterial proteins with solved structures were used to generate a consensus logo. Aligned sequences included: *Bacillus thuringiensis* NprR TPR1-7 (5DBK), *E. coli* LapB TPR1-6 (4ZLH), *B. fragilis* BF2334 TPR1-4 (4I17), *Magnetobacterium bavaricum*

MamA TPR1-5 (3VTY), *Cytophaga hutchinsonii* Q11TI6_CYTH3 TPR1-7 (3U4T), *P. aeruginosa* PilF TPR1-6 (2H01), *T. thermophilus* TTC0263 TPR1-5 (2PL2), *E. coli* NlpI TPR1-4 (1XNF), *B. subtilis* YrrB TPR1-6 (2Q7F), and *E. coli* NrfG TPR1-4 (2E2E).

The cAMP-independent role of FimV in regulation of twitching motility

FimV is involved in twitching (53), T2S (134), control of PilMNOPQ levels (125), and importantly, activation of CyaB (55). While PilMNOPQ transcription was shown previously to be cAMP-dependent (49), cAMP deficiency could not explain the lack of twitching in the *fimV* background, as *cyaAB* mutants are still capable of twitching motility (55), suggesting that FimV has a cAMP-independent role in twitching. Our study is the first to directly address and resolve its cAMP-dependent and –independent functions (Chapter 3).

The activating point mutations of CyaB identified by Topal et al. (107) in a *pilG* background allowed us to resolve cAMP-dependent and –independent phenotypes of *fimV*. Restoration of intracellular cAMP in *fimV* restores T2S (Figure 2.5) and PilMNOPQ levels (Figure 3.2), confirming that they are cAMP-dependent phenotypes, and that the same activating point mutations in CyaB render it independent of both FimV and PilG. Our study and those of Carter et al. (in preparation) and Inclan et al. (135) provide evidence that at least part of the cAMP-independent role of FimV is to localize T4aP structural and regulatory proteins (Figure 3.4). Our data

are the first to show that FimV is linked to T4aP regulatory machinery outside of the Chp-cAMP regulatory circuit. Phylogenetic analysis by Inclan et al. (135) confirmed that FimV is expressed in T4aP-encoding species that lack the Pil-Chp system, as well as FimL or CyaB.

The model of FimV function proposed by Inclan et al. – where FimV interacts with FimL and indirectly through FimL, with PilG – does not account for its cAMP-independent roles. The HubP family of FimV orthologs serve as polar protein organization centres, required for localization of the flagellar chemotactic cluster and regulation of flagellar number in *Vibrio* and *Shewenella* (128, 129, 131). We did not test whether *P. aeruginosa* FimV interacts with the flagellar positioning and number regulators FlhF or FlhG, as *fimV* deletion did not impair swimming motility (Figure 3.5). Together, our data support a new role for FimV as a protein hub for parts of the pilus-specific Chp chemotactic cluster (135), as well as T4aP structural (Carter et al., in preparation) and regulatory components (Figure 3.4). One of the major goals moving forward will be to identify FimV's complete repertoire of interaction partners.

The role of PilG in twitching

PilG is a critical activator of CyaB, but also has cAMP-independent effects on twitching (55), although their underlying mechanism is unclear. We provided evidence that PilG is potentially involved in regulating the

balance between extension and retraction at the leading pole of cells (Chapter 4).

When provided with extracellular cAMP, *pilG* mutants are still unable to twitch despite restoration of surface pili (55), suggesting a retraction-related role for PilG. Our data elaborates on this idea by isolating not only the cAMP-dependent phenotype of *pilG*, but the T4aP extension phenotype as well. We confirmed that PilG controls pilus extension in a cAMP-dependent manner, and suggest that it mediates the balance between extension and retraction in a cAMP-independent manner, likely at the leading poles of twitching cells.

PilG and PilH have been proposed to either control PilB and PilT respectively, or function as a response regulator (PilG) and phosphate sink (PilH) pair. Subcellular localization patterns of PilG and PilH mirror the localization patterns of CheY2 (polar) and CheY1 (diffuse) in *S. meliloti* (190). Recent phosphokinetic characterization of the ChpA-PilG/PilH system (91) shows preferential phosphorylation of PilH, supporting the RR/phosphate sink model. Our analysis of the Chp cluster suggested that the Chp system has an ancestral function in controlling T4P retraction, supporting our hypothesis that PilG is involved in regulating the extension/retraction balance. The response regulators from the characterized flagellar systems interact with the flagellar switch complex, leading to a change in the direction of flagellar rotation. The T4aP system

lacks a functional analog of FliM but recent evidence suggests that the T4aP motor is likely rotary, with PilB or PilT docking onto PilC, and ATP hydrolysis causing PilC to rotate either clockwise (PilB-mediated) or counter clockwise (PilT-mediated) (36). PilG may function by affecting the ability of PilB or PilT to dock onto the platform protein at the leading pole.

Importantly, our findings suggest a model where PilG and FimV function overlaps in terms of cAMP regulation, but the cAMP-independent functions of each are distinct. Whereas FimV likely has hub properties, we have no evidence to date that *pilG* deletion mislocalizes any of the T4aP structural or regulatory components. These data have major implications on the proposed mechanosensory models that include the FimV-FimL-PilG scaffold model (135) and the hierarchical second messenger cascade (89). The cAMP-independent function of FimV and PilG, and the continued localization of PilG in *fimL* cannot be explained by FimV-FimL-PilG model. The latter model did not account for FimV at all (89), which clearly has an important role in CyaB activation, and localization of PilG, and likely the T4aP assembly complex itself. FimV may have a central role in the larger regulatory model, being required for localization of many components of the regulatory pathway, including the T4aP itself. Based on new FimV-related data, new regulatory models will have to include FimV as a hub for several regulatory proteins. It is possible that further study of the FimV

interaction network will reveal a connection to the c-di-GMP circuit and the regulation of biofilm formation.

Taken together, the studies presented in this thesis as well as concurrent work from other groups, provide the foundation for a model of T4aP regulation that integrates cAMP-dependent and independent functions, not accounted for in other studies of FimV function (135).

Future directions

The FimV interaction network

The next major step in understanding the role of FimV will be to characterize its interaction network. FimV is required for localization of T4aP structural components to the cell pole (Carter et al., in preparation), interactions with cAMP regulatory and chemotactic proteins (135), and T4aP regulatory proteins (Figure 3.4). How FimV localizes all these proteins is unclear. In *V. cholerae*, HubP mediates localization of the chemotactic cluster through interactions with cellular partitioning proteins, ParA1 and ParB (128). To test if this model is conserved in *P. aeruginosa*, potential interactions of FimV and the ParA and ParB homologs, Soj and Spo0J will be examined using the BACTH assay, and co-purification and mass spectrometry to identify other interaction partners, while fluorescence microscopy can be used to verify its role in protein localization.

Our data show that the *fimV*$_{\Delta LysM}$ mutant is twitching impaired, but can assembly surface pili (Figure 3.2) despite partial mislocalization of T4aP assembly complexes (Carter et al., in preparation). Although pili can be assembled, it is likely that mislocalized assembly complexes also lead to mislocalized surface pili. To test this idea, pili localization in *fimV* and *fimV*$_{\Delta LysM}$ backgrounds will be determined by transmission electron microscopy. A fusion of *fimV*$_{\Delta LysM}$ to a fluorescent protein will be made to determine if PG-binding is required for FimV localization.

The roles of PilG

PilG interacts with FimL, but deletion of *fimV* – but not *fimL* – mislocalized PilG, suggesting that PilG has another binding partner that tethers it to the cell pole (135). It is possible that this unidentified binding partner represents its connection to the cAMP-independent pathway.

To gain insight into how PilG exerts its cAMP-independent effects, interaction studies will be performed between PilG and the cytoplasmic components of the T4aP assembly complex, including the alignment subcomplex proteins PilMNO, and the ATPases PilBTU. Associations with PilG will be tested using BACTH and fluorescence microscopy in various T4aP assembly complex deletion mutants.

The localization pattern of PilG suggests that it biases type IV pilus function to one pole at a time. To determine if PilG consistently marks the

leading poles of twitching cells, fusions of PilG to photostable fluorescent fusions will be made. Localization will be tested in real-time to determine PilG localization before, during, and after reversals in direction.

The function of PilU

One of the major unanswered questions surrounding T4aP function in *P. aeruginosa* concerns the function of the ATPase, PilU. Mutants lacking PilU are nonmotile, produce at least wild-type levels of surface pili, and are phage sensitive (27). Recent evidence also suggests that PilU localizes to the old pole and remains there during reversals in twitching direction (Cynthia Whitchurch, personal communication). The phenotypes of *pilU* mutants are similar to those of a cAMP-supplemented PilG mutant (55), suggesting that they could be functionally linked. PilU is also found only in Pseudomonads with CyaB and FimL (Figure 4.4), hinting at a connection to activation of virulence via the mechanosensing pathway proposed by the Gitai lab (88). To investigate this potential link, we will co-express PilG and PilU fusions to fluorescent proteins and determine their localization relative to each other before, during, and after cellular reversals.

It is also possible that PilU and PilG do not function with one another. As PilU and PilT are both capable of binding to PilC and are predicted to be structurally similar, it is possible that PilU functions by

competing with PilT for docking onto PilC. Although PilT was shown to localize to both poles (35), these experiments were not performed in the context of actively twitching cells. To explore this idea, fluorescent fusions of PilU and PilT will be co-expressed in twitching cells, and fluorescent signals can be quantified during twitching.

There is very little information about PilU function and regulation. Phosphoproteomic analysis showed that the functional equivalent of PilB in *T. thermophilus* is phosphorylated (200), and phosphorylation negatively regulates piliation and twitching. Another AAA ATPase, p97, is regulated by phosphorylation on a patch of C-terminal tyrosine residues (201). PilU has a C-terminal patch of tyrosines that may also be a target for phosphorylation (Tyr322, Tyr325, Tyr332). We have started to examine the possibility that these residues are important for function by mutating the residues to alanine or phenylalanine and examine functionality and localization of the non-phosphorylatable mutant. These data will help to characterize the role of PilU in twitching.

Significance and Conclusions

T4aP are important virulence factors for *P. aeruginosa*. Their function relies on a complex signalling pathway that integrates mechanosensing, cAMP signalling, chemosensing, and localization. Some proteins, including FimV and PilG, are involved in multiple regulatory

systems and based on their phylogenetic distribution, may represent examples of regulatory integration of older and newer circuits. Our study is the first to resolve the cAMP-independent and –dependent roles of FimV, and to contrast this with the cAMP-independent role of PilG. Prior to these and concurrent studies, regulation of twitching by FimV and its connection to the Chp system were not well studied. The data presented here help to resolve the signalling pathways controlling twitching – in particular, our understanding of FimV function. Moving forward, these data will help to inform a new model of twitching regulation that will better integrate the different regulatory pathways. A better understanding of these pathways will uncover new methods to control T4aP function and virulence.

REFERENCES

1. **Berry JL, Pelicic V.** 2015. Exceptionally widespread nanomachines composed of type IV pilins: the prokaryotic Swiss Army knives. FEMS Microbiol Rev **39:**134-154.
2. **Albers SV, Pohlschroder M.** 2009. Diversity of archaeal type IV pilin-like structures. Extremophiles : life under extreme conditions **13:**403-410.
3. **Averhoff B, Friedrich A.** 2003. Type IV pili-related natural transformation systems: DNA transport in mesophilic and thermophilic bacteria. Arch Microbiol **180:**385-393.
4. **Bradley DE.** 1980. A function of *Pseudomonas aeruginosa* PAO polar pili: twitching motility. Can J Microbiol **26:**146-154.
5. **Pelicic V.** 2008. Type IV pili: e pluribus unum? Mol Microbiol **68:**827-837.
6. **Burrows LL.** 2005. Weapons of mass retraction. Mol Microbiol **57:**878-888.
7. **Burrows LL.** 2012. *Pseudomonas aeruginosa* twitching motility: type IV pili in action. Annu Rev Microbiol **66:**493-520.
8. **O'Toole GA, Kolter R.** 1998. Flagellar and twitching motility are necessary for *Pseudomonas aeruginosa* biofilm development. Mol Microbiol **30:**295-304.
9. **Heiniger RW, Winther-Larsen HC, Pickles RJ, Koomey M, Wolfgang MC.** 2010. Infection of human mucosal tissue by Pseudomonas aeruginosa requires sequential and mutually dependent virulence factors and a novel pilus-associated adhesin. Cell Microbiol **12:**1158-1173.
10. **Cursino L, Galvani CD, Athinuwat D, Zaini PA, Li Y, De La Fuente L, Hoch HC, Burr TJ, Mowery P.** 2011. Identification of an operon, Pil-Chp, that controls twitching motility and virulence in *Xylella fastidiosa*. Molecular plant-microbe interactions : MPMI **24:**1198-1206.
11. **Weiss RL.** 1971. The structure and occurrence of pili (fimbriae) on *Pseudomonas aeruginosa*. J Gen Microbiol **67:**135-143.
12. **Obritsch MD, Fish DN, MacLaren R, Jung R.** 2005. Nosocomial infections due to multidrug-resistant *Pseudomonas aeruginosa*: epidemiology and treatment options. Pharmacotherapy **25:**1353-1364.
13. **Govan JR, Deretic V.** 1996. Microbial pathogenesis in cystic fibrosis: mucoid *Pseudomonas aeruginosa* and *Burkholderia cepacia*. Microbiol Rev **60:**539-574.
14. **Inoue T, Tanimoto I, Ohta H, Kato K, Murayama Y, Fukui K.** 1998. Molecular characterization of low-molecular-weight

component protein, Flp, in *Actinobacillus actinomycetemcomitans* fimbriae. Microbiol Immunol **42:**253-258.

15. **Skerker JM, Shapiro L.** 2000. Identification and cell cycle control of a novel pilus system in *Caulobacter crescentus*. Embo J **19:**3223-3234.
16. **Mattick JS.** 2002. Type IV pili and twitching motility. Annu Rev Microbiol **56:**289-314.
17. **Semmler AB, Whitchurch CB, Mattick JS.** 1999. A re-examination of twitching motility in *Pseudomonas aeruginosa*. Microbiology **145 (Pt 10):**2863-2873.
18. **Comolli JC, Hauser AR, Waite L, Whitchurch CB, Mattick JS, Engel JN.** 1999. *Pseudomonas aeruginosa* gene products PilT and PilU are required for cytotoxicity in vitro and virulence in a mouse model of acute pneumonia. Infect Immun **67:**3625-3630.
19. **D'Argenio DA, Gallagher LA, Berg CA, Manoil C.** 2001. Drosophila as a model host for *Pseudomonas aeruginosa* infection. J Bacteriol **183:**1466-1471.
20. **Han X, Kennan RM, Davies JK, Reddacliff LA, Dhungyel OP, Whittington RJ, Turnbull L, Whitchurch CB, Rood JI.** 2008. Twitching motility is essential for virulence in *Dichelobacter nodosus*. J Bacteriol **190:**3323-3335.
21. **Koo J, Lamers RP, Rubinstein JL, Burrows LL, Howell PL.** 2016. Structure of the *Pseudomonas aeruginosa* Type IVa Pilus Secretin at 7.4 A. Structure **24:**1778-1787.
22. **Koo J, Tammam S, Ku SY, Sampaleanu LM, Burrows LL, Howell PL.** 2008. PilF is an outer membrane lipoprotein required for multimerization and localization of the *Pseudomonas aeruginosa* Type IV pilus secretin. J Bacteriol **190:**6961-6969.
23. **Bitter W, Koster M, Latijnhouwers M, de Cock H, Tommassen J.** 1998. Formation of oligomeric rings by XcpQ and PilQ, which are involved in protein transport across the outer membrane of *Pseudomonas aeruginosa*. Mol Microbiol **27:**209-219.
24. **Takhar HK, Kemp K, Kim M, Howell PL, Burrows LL.** 2013. The platform protein is essential for type IV pilus biogenesis. J Biol Chem **288:**9721-9728.
25. **Nunn D, Bergman S, Lory S.** 1990. Products of three accessory genes, *pilB*, *pilC*, and *pilD*, are required for biogenesis of *Pseudomonas aeruginosa* pili. J Bacteriol **172:**2911-2919.
26. **Whitchurch CB, Hobbs M, Livingston SP, Krishnapillai V, Mattick JS.** 1991. Characterisation of a *Pseudomonas aeruginosa* twitching motility gene and evidence for a specialised protein export system widespread in eubacteria. Gene **101:**33-44.

27. **Whitchurch CB, Mattick JS.** 1994. Characterization of a gene, *pilU*, required for twitching motility but not phage sensitivity in *Pseudomonas aeruginosa*. Mol Microbiol **13:**1079-1091.
28. **Ayers M, Sampaleanu LM, Tammam S, Koo J, Harvey H, Howell PL, Burrows LL.** 2009. PilM/N/O/P proteins form an inner membrane complex that affects the stability of the *Pseudomonas aeruginosa* type IV pilus secretin. J Mol Biol **394:**128-142.
29. **Martin PR, Watson AA, McCaul TF, Mattick JS.** 1995. Characterization of a five-gene cluster required for the biogenesis of type 4 fimbriae in *Pseudomonas aeruginosa*. Mol Microbiol **16:**497-508.
30. **Nunn DN, Lory S.** 1991. Product of the *Pseudomonas aeruginosa* gene *pilD* is a prepilin leader peptidase. Proc Natl Acad Sci U S A **88:**3281-3285.
31. **Nguyen Y, Sugiman-Marangos S, Harvey H, Bell SD, Charlton CL, Junop MS, Burrows LL.** 2015. *Pseudomonas aeruginosa* minor pilins prime type IVa pilus assembly and promote surface display of the PilY1 adhesin. J Biol Chem **290:**601-611.
32. **Burrows LL.** 2013. A new route for polar navigation. Mol Microbiol **90:**919-922.
33. **Scheurwater EM, Burrows LL.** 2011. Maintaining network security: how macromolecular structures cross the peptidoglycan layer. FEMS Microbiol Lett **318:**1-9.
34. **Friedrich C, Bulyha I, Sogaard-Andersen L.** 2014. Outside-in assembly pathway of the type IV pilus system in *Myxococcus xanthus*. J Bacteriol **196:**378-390.
35. **Chiang P, Habash M, Burrows LL.** 2005. Disparate subcellular localization patterns of *Pseudomonas aeruginosa* Type IV pilus ATPases involved in twitching motility. J Bacteriol **187:**829-839.
36. **McCallum M, Tammam S, Little DJ, Robinson H, Koo J, Shah M, Calmettes C, Moraes TF, Burrows LL, Howell PL.** 2016. PilN binding modulates the structure and binding partners of the *Pseudomonas aeruginosa* Type IVa Pilus protein PilM. J Biol Chem **291:**11003-11015.
37. **Mancl JM, Black WP, Robinson H, Yang Z, Schubot FD.** 2016. Crystal Structure of a Type IV Pilus Assembly ATPase: Insights into the Molecular Mechanism of PilB from *Thermus thermophilus*. Structure **24:**1886-1897.
38. **Sampaleanu LM, Bonanno JB, Ayers M, Koo J, Tammam S, Burley SK, Almo SC, Burrows LL, Howell PL.** 2009. Periplasmic domains of *Pseudomonas aeruginosa* PilN and PilO form a stable heterodimeric complex. J Mol Biol **394:**143-159.

39. **Leighton TL, Buensuceso RN, Howell PL, Burrows LL.** 2015. Biogenesis of *Pseudomonas aeruginosa* type IV pili and regulation of their function. Environ Microbiol **17:**4148-4163.
40. **Leighton TL, Yong DH, Howell PL, Burrows LL.** 2016. Type IV Pilus Alignment Subcomplex Proteins PilN and PilO Form Homo- and Heterodimers in Vivo. J Biol Chem **291:**19923-19938.
41. **Tammam S, Sampaleanu LM, Koo J, Manoharan K, Daubaras M, Burrows LL, Howell PL.** 2013. PilMNOPQ from the *Pseudomonas aeruginosa* type IV pilus system form a transenvelope protein interaction network that interacts with PilA. J Bacteriol **195:**2126-2135.
42. **Leighton TL, Dayalani N, Sampaleanu LM, Howell PL, Burrows LL.** 2015. Novel Role for PilNO in Type IV Pilus Retraction Revealed by Alignment Subcomplex Mutations. J Bacteriol **197:**2229-2238.
43. **Alm RA, Hallinan JP, Watson AA, Mattick JS.** 1996. Fimbrial biogenesis genes of *Pseudomonas aeruginosa*: *pilW* and *pilX* increase the similarity of type 4 fimbriae to the GSP protein-secretion systems and *pilY1* encodes a gonococcal PilC homologue. Mol Microbiol **22:**161-173.
44. **Alm RA, Mattick JS.** 1995. Identification of a gene, *pilV*, required for type 4 fimbrial biogenesis in *Pseudomonas aeruginosa*, whose product possesses a pre-pilin-like leader sequence. Mol Microbiol **16:**485-496.
45. **Russell MA, Darzins A.** 1994. The *pilE* gene product of *Pseudomonas aeruginosa*, required for pilus biogenesis, shares amino acid sequence identity with the N-termini of type 4 prepilin proteins. Mol Microbiol **13:**973-985.
46. **Rudel T, Scheurerpflug I, Meyer TF.** 1995. *Neisseria* PilC protein identified as type-4 pilus tip-located adhesin. Nature **373:**357-359.
47. **Orans J, Johnson MD, Coggan KA, Sperlazza JR, Heiniger RW, Wolfgang MC, Redinbo MR.** 2010. Crystal structure analysis reveals *Pseudomonas* PilY1 as an essential calcium-dependent regulator of bacterial surface motility. Proc Natl Acad Sci U S A **107:**1065-1070.
48. **Siryaporn A, Kuchma SL, O'Toole GA, Gitai Z.** 2014. Surface attachment induces *Pseudomonas aeruginosa* virulence. Proc Natl Acad Sci U S A **111:**16860-16865.
49. **Wolfgang MC, Lee VT, Gilmore ME, Lory S.** 2003. Coordinate regulation of bacterial virulence genes by a novel adenylate cyclase-dependent signaling pathway. Dev Cell **4:**253-263.
50. **Whitchurch CB, Leech AJ, Young MD, Kennedy D, Sargent JL, Bertrand JJ, Semmler AB, Mellick AS, Martin PR, Alm RA, Hobbs M, Beatson SA, Huang B, Nguyen L, Commolli JC,**

Engel JN, Darzins A, Mattick JS. 2004. Characterization of a complex chemosensory signal transduction system which controls twitching motility in *Pseudomonas aeruginosa*. Mol Microbiol **52:**873-893.

51. **Darzins A.** 1994. Characterization of a *Pseudomonas aeruginosa* gene cluster involved in pilus biosynthesis and twitching motility: sequence similarity to the chemotaxis proteins of enterics and the gliding bacterium *Myxococcus xanthus*. Mol Microbiol **11:**137-153.
52. **Darzins A.** 1995. The *Pseudomonas aeruginosa* pilK gene encodes a chemotactic methyltransferase (CheR) homologue that is translationally regulated. Mol Microbiol **15:**703-717.
53. **Semmler AB, Whitchurch CB, Leech AJ, Mattick JS.** 2000. Identification of a novel gene, *fimV*, involved in twitching motility in *Pseudomonas aeruginosa*. Microbiology **146 (Pt 6):**1321-1332.
54. **Whitchurch CB, Beatson SA, Comolli JC, Jakobsen T, Sargent JL, Bertrand JJ, West J, Klausen M, Waite LL, Kang PJ, Tolker-Nielsen T, Mattick JS, Engel JN.** 2005. *Pseudomonas aeruginosa fimL* regulates multiple virulence functions by intersecting with Vfr-modulated pathways. Mol Microbiol **55:**1357-1378.
55. **Fulcher NB, Holliday PM, Klem E, Cann MJ, Wolfgang MC.** 2010. The *Pseudomonas aeruginosa* Chp chemosensory system regulates intracellular cAMP levels by modulating adenylate cyclase activity. Mol Microbiol **76:**889-904.
56. **Inclan YF, Huseby MJ, Engel JN.** 2011. FimL regulates cAMP synthesis in *Pseudomonas aeruginosa*. PLoS One **6:**e15867.
57. **Kilmury SL, Burrows LL.** 2016. Type IV pilins regulate their own expression via direct intramembrane interactions with the sensor kinase PilS. Proc Natl Acad Sci U S A **113:**6017-6022.
58. **Capra EJ, Laub MT.** 2012. Evolution of two-component signal transduction systems. Annu Rev Microbiol **66:**325-347.
59. **West AH, Stock AM.** 2001. Histidine kinases and response regulator proteins in two-component signaling systems. Trends Biochem Sci **26:**369-376.
60. **Appleby JL, Bourret RB.** 1999. Activation of CheY mutant D57N by phosphorylation at an alternative site, Ser-56. Mol Microbiol **34:**915-925.
61. **Bourret RB, Hess JF, Simon MI.** 1990. Conserved aspartate residues and phosphorylation in signal transduction by the chemotaxis protein CheY. Proc Natl Acad Sci U S A **87:**41-45.
62. **Galperin MY.** 2010. Diversity of structure and function of response regulator output domains. Curr Opin Microbiol **13:**150-159.
63. **Scharf BE, Fahrner KA, Turner L, Berg HC.** 1998. Control of direction of flagellar rotation in bacterial chemotaxis. Proc Natl Acad Sci U S A **95:**201-206.

64. **Wolanin PM, Webre DJ, Stock JB.** 2003. Mechanism of phosphatase activity in the chemotaxis response regulator CheY. Biochemistry **42:**14075-14082.
65. **Boyd JM, Lory S.** 1996. Dual function of PilS during transcriptional activation of the *Pseudomonas aeruginosa* pilin subunit gene. J Bacteriol **178:**831-839.
66. **Jimenez-Pearson MA, Delany I, Scarlato V, Beier D.** 2005. Phosphate flow in the chemotactic response system of *Helicobacter pylori*. Microbiology **151:**3299-3311.
67. **Sourjik V, Schmitt R.** 1998. Phosphotransfer between CheA, CheY1, and CheY2 in the chemotaxis signal transduction chain of *Rhizobium meliloti*. Biochemistry **37:**2327-2335.
68. **Amin M, Kothamachu VB, Feliu E, Scharf BE, Porter SL, Soyer OS.** 2014. Phosphate sink containing two-component signaling systems as tunable threshold devices. PLoS Comput Biol **10:**e1003890.
69. **Wadhams GH, Armitage JP.** 2004. Making sense of it all: bacterial chemotaxis. Nat Rev Mol Cell Biol **5:**1024-1037.
70. **Taylor BL, Zhulin IB, Johnson MS.** 1999. Aerotaxis and other energy-sensing behavior in bacteria. Annu Rev Microbiol **53:**103-128.
71. **Krell T, Lacal J, Munoz-Martinez F, Reyes-Darias JA, Cadirci BH, Garcia-Fontana C, Ramos JL.** 2011. Diversity at its best: bacterial taxis. Environ Microbiol **13:**1115-1124.
72. **Kim KK, Yokota H, Kim SH.** 1999. Four-helical-bundle structure of the cytoplasmic domain of a serine chemotaxis receptor. Nature **400:**787-792.
73. **Khursigara CM, Wu X, Zhang P, Lefman J, Subramaniam S.** 2008. Role of HAMP domains in chemotaxis signaling by bacterial chemoreceptors. Proc Natl Acad Sci U S A **105:**16555-16560.
74. **Briegel A, Li X, Bilwes AM, Hughes KT, Jensen GJ, Crane BR.** 2012. Bacterial chemoreceptor arrays are hexagonally packed trimers of receptor dimers networked by rings of kinase and coupling proteins. Proc Natl Acad Sci U S A **109:**3766-3771.
75. **Kirby JR.** 2009. Chemotaxis-like regulatory systems: unique roles in diverse bacteria. Annu Rev Microbiol **63:**45-59.
76. **Grebe TW, Stock J.** 1998. Bacterial chemotaxis: the five sensors of a bacterium. Curr Biol **8:**R154-157.
77. **Hulko M, Berndt F, Gruber M, Linder JU, Truffault V, Schultz A, Martin J, Schultz JE, Lupas AN, Coles M.** 2006. The HAMP domain structure implies helix rotation in transmembrane signaling. Cell **126:**929-940.

78. **Gegner JA, Dahlquist FW.** 1991. Signal transduction in bacteria: CheW forms a reversible complex with the protein kinase CheA. Proc Natl Acad Sci U S A **88:**750-754.
79. **Gegner JA, Graham DR, Roth AF, Dahlquist FW.** 1992. Assembly of an MCP receptor, CheW, and kinase CheA complex in the bacterial chemotaxis signal transduction pathway. Cell **70:**975-982.
80. **Surette MG, Levit M, Liu Y, Lukat G, Ninfa EG, Ninfa A, Stock JB.** 1996. Dimerization is required for the activity of the protein histidine kinase CheA that mediates signal transduction in bacterial chemotaxis. J Biol Chem **271:**939-945.
81. **Bren A, Eisenbach M.** 1998. The N terminus of the flagellar switch protein, FliM, is the binding domain for the chemotactic response regulator, CheY. J Mol Biol **278:**507-514.
82. **Bren A, Welch M, Blat Y, Eisenbach M.** 1996. Signal termination in bacterial chemotaxis: CheZ mediates dephosphorylation of free rather than switch-bound CheY. Proc Natl Acad Sci U S A **93:**10090-10093.
83. **Yonekawa H, Hayashi H, Parkinson JS.** 1983. Requirement of the *cheB* function for sensory adaptation in *Escherichia coli*. J Bacteriol **156:**1228-1235.
84. **Kehry MR, Dahlquist FW.** 1982. The methyl-accepting chemotaxis proteins of *Escherichia coli*. Identification of the multiple methylation sites on methyl-accepting chemotaxis protein I. J Biol Chem **257:**10378-10386.
85. **Springer WR, Koshland DE, Jr.** 1977. Identification of a protein methyltransferase as the *cheR* gene product in the bacterial sensing system. Proc Natl Acad Sci U S A **74:**533-537.
86. **Baker MD, Wolanin PM, Stock JB.** 2006. Signal transduction in bacterial chemotaxis. Bioessays **28:**9-22.
87. **Kearns DB, Robinson J, Shimkets LJ.** 2001. *Pseudomonas aeruginosa* exhibits directed twitching motility up phosphatidylethanolamine gradients. J Bacteriol **183:**763-767.
88. **Persat A, Inclan YF, Engel JN, Stone HA, Gitai Z.** 2015. Type IV pili mechanochemically regulate virulence factors in *Pseudomonas aeruginosa*. Proc Natl Acad Sci U S A **112:**7563-7568.
89. **Luo Y, Zhao K, Baker AE, Kuchma SL, Coggan KA, Wolfgang MC, Wong GC, O'Toole GA.** 2015. A hierarchical cascade of second messengers regulates *Pseudomonas aeruginosa* surface behaviors. MBio **6**.
90. **Leech AJ, Mattick JS.** 2006. Effect of site-specific mutations in different phosphotransfer domains of the chemosensory protein ChpA on *Pseudomonas aeruginosa* motility. J Bacteriol **188:**8479-8486.

91. **Silversmith RE, Wang B, Fulcher NB, Wolfgang MC, Bourret RB.** 2016. Phosphoryl Group Flow within the *Pseudomonas aeruginosa* Pil-Chp Chemosensory System: DIFFERENTIAL FUNCTION OF THE EIGHT PHOSPHOTRANSFERASE AND THREE RECEIVER DOMAINS. J Biol Chem **291:**17677-17691.
92. **Darzins A.** 1993. The *pilG* gene product, required for *Pseudomonas aeruginosa* pilus production and twitching motility, is homologous to the enteric, single-domain response regulator CheY. J Bacteriol **175:**5934-5944.
93. **Bertrand JJ, West JT, Engel JN.** 2010. Genetic analysis of the regulation of type IV pilus function by the Chp chemosensory system of *Pseudomonas aeruginosa*. J Bacteriol **192:**994-1010.
94. **DeLange PA, Collins TL, Pierce GE, Robinson JB.** 2007. PilJ localizes to cell poles and is required for type IV pilus extension in Pseudomonas aeruginosa. Curr Microbiol **55:**389-395.
95. **Li Y, Bustamante VH, Lux R, Zusman D, Shi W.** 2005. Divergent regulatory pathways control A and S motility in *Myxococcus xanthus* through FrzE, a CheA-CheY fusion protein. J Bacteriol **187:**1716-1723.
96. **Inclan YF, Vlamakis HC, Zusman DR.** 2007. FrzZ, a dual CheY-like response regulator, functions as an output for the Frz chemosensory pathway of *Myxococcus xanthus*. Mol Microbiol **65:**90-102.
97. **Ward MJ, Zusman DR.** 1999. Motility in *Myxococcus xanthus* and its role in developmental aggregation. Curr Opin Microbiol **2:**624-629.
98. **Sun H, Zusman DR, Shi W.** 2000. Type IV pilus of *Myxococcus xanthus* is a motility apparatus controlled by the *frz* chemosensory system. Curr Biol **10:**1143-1146.
99. **Jakovljevic V, Leonardy S, Hoppert M, Sogaard-Andersen L.** 2008. PilB and PilT are ATPases acting antagonistically in type IV pilus function in *Myxococcus xanthus*. J Bacteriol **190:**2411-2421.
100. **Bulyha I, Schmidt C, Lenz P, Jakovljevic V, Hone A, Maier B, Hoppert M, Sogaard-Andersen L.** 2009. Regulation of the type IV pili molecular machine by dynamic localization of two motor proteins. Mol Microbiol **74:**691-706.
101. **Borlee BR, Goldman AD, Murakami K, Samudrala R, Wozniak DJ, Parsek MR.** 2010. *Pseudomonas aeruginosa* uses a cyclic-di-GMP-regulated adhesin to reinforce the biofilm extracellular matrix. Mol Microbiol **75:**827-842.
102. **Ryan RP, Fouhy Y, Lucey JF, Dow JM.** 2006. Cyclic di-GMP signaling in bacteria: recent advances and new puzzles. J Bacteriol **188:**8327-8334.

103. **Ryan RP.** 2013. Cyclic di-GMP signalling and the regulation of bacterial virulence. Microbiology **159:**1286-1297.
104. **McDonough KA, Rodriguez A.** 2012. The myriad roles of cyclic AMP in microbial pathogens: from signal to sword. Nat Rev Microbiol **10:**27-38.
105. **Yahr TL, Vallis AJ, Hancock MK, Barbieri JT, Frank DW.** 1998. ExoY, an adenylate cyclase secreted by the *Pseudomonas aeruginosa* type III system. Proc Natl Acad Sci U S A **95:**13899-13904.
106. **Smith RS, Wolfgang MC, Lory S.** 2004. An adenylate cyclase-controlled signaling network regulates *Pseudomonas aeruginosa* virulence in a mouse model of acute pneumonia. Infect Immun **72:**1677-1684.
107. **Topal H, Fulcher NB, Bitterman J, Salazar E, Buck J, Levin LR, Cann MJ, Wolfgang MC, Steegborn C.** 2012. Crystal structure and regulation mechanisms of the CyaB adenylyl cyclase from the human pathogen *Pseudomonas aeruginosa*. J Mol Biol **416:**271-286.
108. **Linder JU, Schultz JE.** 2003. The class III adenylyl cyclases: multi-purpose signalling modules. Cell Signal **15:**1081-1089.
109. **Nikolskaya AN, Mulkidjanian AY, Beech IB, Galperin MY.** 2003. MASE1 and MASE2: two novel integral membrane sensory domains. J Mol Microbiol Biotechnol **5:**11-16.
110. **West SE, Sample AK, Runyen-Janecky LJ.** 1994. The *vfr* gene product, required for *Pseudomonas aeruginosa* exotoxin A and protease production, belongs to the cyclic AMP receptor protein family. J Bacteriol **176:**7532-7542.
111. **Fuchs EL, Brutinel ED, Klem ER, Fehr AR, Yahr TL, Wolfgang MC.** 2010. In vitro and in vivo characterization of the *Pseudomonas aeruginosa* cyclic AMP (cAMP) phosphodiesterase CpdA, required for cAMP homeostasis and virulence factor regulation. J Bacteriol **192:**2779-2790.
112. **Wolfe AJ, Visick KL.** 2008. Get the message out: cyclic-Di-GMP regulates multiple levels of flagellum-based motility. J Bacteriol **190:**463-475.
113. **Simm R, Morr M, Kader A, Nimtz M, Romling U.** 2004. GGDEF and EAL domains inversely regulate cyclic di-GMP levels and transition from sessility to motility. Mol Microbiol **53:**1123-1134.
114. **Tal R, Wong HC, Calhoon R, Gelfand D, Fear AL, Volman G, Mayer R, Ross P, Amikam D, Weinhouse H, Cohen A, Sapir S, Ohana P, Benziman M.** 1998. Three *cdg* operons control cellular turnover of cyclic di-GMP in *Acetobacter xylinum*: genetic organization and occurrence of conserved domains in isoenzymes. J Bacteriol **180:**4416-4425.

115. **Galperin MY, Nikolskaya AN, Koonin EV.** 2001. Novel domains of the prokaryotic two-component signal transduction systems. FEMS Microbiol Lett **203:**11-21.
116. **Alm RA, Bodero AJ, Free PD, Mattick JS.** 1996. Identification of a novel gene, *pilZ*, essential for type 4 fimbrial biogenesis in *Pseudomonas aeruginosa*. J Bacteriol **178:**46-53.
117. **Amikam D, Galperin MY.** 2006. PilZ domain is part of the bacterial c-di-GMP binding protein. Bioinformatics **22:**3-6.
118. **Guzzo CR, Salinas RK, Andrade MO, Farah CS.** 2009. PILZ protein structure and interactions with PILB and the FIMX EAL domain: implications for control of type IV pilus biogenesis. J Mol Biol **393:**848-866.
119. **Jain R, Behrens AJ, Kaever V, Kazmierczak BI.** 2012. Type IV pilus assembly in *Pseudomonas aeruginosa* over a broad range of cyclic di-GMP concentrations. J Bacteriol **194:**4285-4294.
120. **Huang B, Whitchurch CB, Mattick JS.** 2003. FimX, a multidomain protein connecting environmental signals to twitching motility in *Pseudomonas aeruginosa*. J Bacteriol **185:**7068-7076.
121. **Qi Y, Chuah ML, Dong X, Xie K, Luo Z, Tang K, Liang ZX.** 2011. Binding of cyclic diguanylate in the non-catalytic EAL domain of FimX induces a long-range conformational change. J Biol Chem **286:**2910-2917.
122. **Rao F, Yang Y, Qi Y, Liang ZX.** 2008. Catalytic mechanism of cyclic di-GMP-specific phosphodiesterase: a study of the EAL domain-containing RocR from *Pseudomonas aeruginosa*. J Bacteriol **190:**3622-3631.
123. **Kuchma SL, Ballok AE, Merritt JH, Hammond JH, Lu W, Rabinowitz JD, O'Toole GA.** 2010. Cyclic-di-GMP-mediated repression of swarming motility by *Pseudomonas aeruginosa*: the *pilY1* gene and its impact on surface-associated behaviors. J Bacteriol **192:**2950-2964.
124. **Kuchma SL, Griffin EF, O'Toole GA.** 2012. Minor pilins of the type IV pilus system participate in the negative regulation of swarming motility. J Bacteriol **194:**5388-5403.
125. **Wehbi H, Portillo E, Harvey H, Shimkoff AE, Scheurwater EM, Howell PL, Burrows LL.** 2010. The peptidoglycan-binding protein FimV promotes assembly of the *Pseudomonas aeruginosa* type IV pilus secretin. J Bacteriol **193:**540-550.
126. **Lamb JR, Tugendreich S, Hieter P.** 1995. Tetratrico peptide repeat interactions: to TPR or not to TPR? Trends Biochem Sci **20:**257-259.
127. **D'Andrea LD, Regan L.** 2003. TPR proteins: the versatile helix. Trends Biochem Sci **28:**655-662.

128. **Yamaichi Y, Bruckner R, Ringgaard S, Moll A, Cameron DE, Briegel A, Jensen GJ, Davis BM, Waldor MK.** 2012. A multidomain hub anchors the chromosome segregation and chemotactic machinery to the bacterial pole. Genes Dev **26:**2348-2360.
129. **Rossmann F, Brenzinger S, Knauer C, Dorrich AK, Bubendorfer S, Ruppert U, Bange G, Thormann KM.** 2015. The role of FlhF and HubP as polar landmark proteins in *Shewanella putrefaciens* CN-32. Mol Microbiol **98:**727-742.
130. **Oldfield NJ, Bland SJ, Taraktsoglou M, Dos Ramos FJ, Robinson K, Wooldridge KG, Ala'Aldeen DA.** 2007. T-cell stimulating protein A (TspA) of *Neisseria meningitidis* is required for optimal adhesion to human cells. Cell Microbiol **9:**463-478.
131. **Takekawa N, Kwon S, Nishioka N, Kojima S, Homma M.** 2016. HubP, a Polar Landmark Protein, Regulates Flagellar Number by Assisting in the Proper Polar Localization of FlhG in *Vibrio alginolyticus*. J Bacteriol **198:**3091-3098.
132. **Coil DA, Anne J.** 2010. The role of *fimV* and the importance of its tandem repeat copy number in twitching motility, pigment production, and morphology in *Legionella pneumophila*. Arch Microbiol **192:**625-631.
133. **Coil DA, Vandersmissen L, Ginevra C, Jarraud S, Lammertyn E, Anne J.** 2008. Intragenic tandem repeat variation between *Legionella pneumophila* strains. BMC Microbiol **8:**218.
134. **Michel GP, Aguzzi A, Ball G, Soscia C, Bleves S, Voulhoux R.** 2011. Role of *fimV* in type II secretion system-dependent protein secretion of *Pseudomonas aeruginosa* on solid medium. Microbiology **157:**1945-1954.
135. **Inclan YF, Persat A, Greninger A, Von Dollen J, Johnson J, Krogan N, Gitai Z, Engel JN.** 2016. A scaffold protein connects type IV pili with the Chp chemosensory system to mediate activation of virulence signaling in *Pseudomonas aeruginosa*. Mol Microbiol **101:**590-605.
136. **Nolan LM, Beatson SA, Croft L, Jones PM, George AM, Mattick JS, Turnbull L, Whitchurch CB.** 2012. Extragenic suppressor mutations that restore twitching motility to *fimL* mutants of *Pseudomonas aeruginosa* are associated with elevated intracellular cyclic AMP levels. Microbiologyopen **1:**490-501.
137. **Belete B, Lu H, Wozniak DJ.** 2008. *Pseudomonas aeruginosa* AlgR regulates type IV pilus biosynthesis by activating transcription of the *fimU-pilVWXY1Y2E* operon. J Bacteriol **190:**2023-2030.
138. **Lauer P, Albertson NH, Koomey M.** 1993. Conservation of genes encoding components of a type IV pilus assembly/two-step protein export pathway in *Neisseria gonorrhoeae*. Mol Microbiol **8:**357-368.

139. **Tammam S, Sampaleanu LM, Koo J, Sundaram P, Ayers M, Chong PA, Forman-Kay JD, Burrows LL, Howell PL.** 2011. Characterization of the PilN, PilO and PilP type IVa pilus subcomplex. Mol Microbiol **82:**1496-1514.
140. **Wolfgang M, van Putten JP, Hayes SF, Dorward D, Koomey M.** 2000. Components and dynamics of fiber formation define a ubiquitous biogenesis pathway for bacterial pili. Embo J **19:**6408-6418.
141. **Buist G, Steen A, Kok J, Kuipers OP.** 2008. LysM, a widely distributed protein motif for binding to (peptido)glycans. Mol Microbiol **68:**838-847.
142. **Blatch GL, Lassle M.** 1999. The tetratricopeptide repeat: a structural motif mediating protein-protein interactions. Bioessays **21:**932-939.
143. **Karpenahalli MR, Lupas AN, Soding J.** 2007. TPRpred: a tool for prediction of TPR-, PPR- and SEL1-like repeats from protein sequences. BMC Bioinformatics **8:**2.
144. **Das AK, Cohen PW, Barford D.** 1998. The structure of the tetratricopeptide repeats of protein phosphatase 5: implications for TPR-mediated protein-protein interactions. Embo J **17:**1192-1199.
145. **Cerveny L, Straskova A, Dankova V, Hartlova A, Ceckova M, Staud F, Stulik J.** 2013. Tetratricopeptide repeat motifs in the world of bacterial pathogens: role in virulence mechanisms. Infect Immun **81:**629-635.
146. **Adebali O, Ortega DR, Zhulin IB.** 2015. CDvist: a webserver for identification and visualization of conserved domains in protein sequences. Bioinformatics **31:**1475-1477.
147. **Powell S, Forslund K, Szklarczyk D, Trachana K, Roth A, Huerta-Cepas J, Gabaldon T, Rattei T, Creevey C, Kuhn M, Jensen LJ, von Mering C, Bork P.** 2014. eggNOG v4.0: nested orthology inference across 3686 organisms. Nucleic Acids Res **42:**D231-239.
148. **Katoh K, Standley DM.** 2013. MAFFT multiple sequence alignment software version 7: improvements in performance and usability. Mol Biol Evol **30:**772-780.
149. **Tamura K, Stecher G, Peterson D, Filipski A, Kumar S.** 2013. MEGA6: Molecular Evolutionary Genetics Analysis version 6.0. Mol Biol Evol **30:**2725-2729.
150. **Kus JV, Tullis E, Cvitkovitch DG, Burrows LL.** 2004. Significant differences in type IV pilin allele distribution among *Pseudomonas aeruginosa* isolates from cystic fibrosis (CF) versus non-CF patients. Microbiology **150:**1315-1326.
151. **Schneider CA, Rasband WS, Eliceiri KW.** 2012. NIH Image to ImageJ: 25 years of image analysis. Nat Methods **9:**671-675.

152. **Karimova G, Pidoux J, Ullmann A, Ladant D.** 1998. A bacterial two-hybrid system based on a reconstituted signal transduction pathway. Proc Natl Acad Sci U S A **95:**5752-5756.
153. **Kapust RB, Tozser J, Fox JD, Anderson DE, Cherry S, Copeland TD, Waugh DS.** 2001. Tobacco etch virus protease: mechanism of autolysis and rational design of stable mutants with wild-type catalytic proficiency. Protein Eng **14:**993-1000.
154. **Otwinowski Z, Minor W.** 1997. Processing of X-ray diffraction data collected in oscillation mode. Method Enzymol **276:**307-326.
155. **Adams PD, Grosse-Kunstleve RW, Hung LW, Ioerger TR, McCoy AJ, Moriarty NW, Read RJ, Sacchettini JC, Sauter NK, Terwilliger TC.** 2002. PHENIX: building new software for automated crystallographic structure determination. Acta Crystallogr D Biol Crystallogr **58:**1948-1954.
156. **McCoy AJ, Grosse-Kunstleve RW, Adams PD, Winn MD, Storoni LC, Read RJ.** 2007. Phaser crystallographic software. J Appl Crystallogr **40:**658-674.
157. **Emsley P, Cowtan K.** 2004. Coot: model-building tools for molecular graphics. Acta Crystallogr D Biol Crystallogr **60:**2126-2132.
158. **Davis IW, Leaver-Fay A, Chen VB, Block JN, Kapral GJ, Wang X, Murray LW, Arendall WB, 3rd, Snoeyink J, Richardson JS, Richardson DC.** 2007. MolProbity: all-atom contacts and structure validation for proteins and nucleic acids. Nucleic Acids Res **35:**W375-383.
159. **Lewenza S, Falsafi RK, Winsor G, Gooderham WJ, McPhee JB, Brinkman FS, Hancock RE.** 2005. Construction of a mini-Tn5-*luxCDABE* mutant library in *Pseudomonas aeruginosa* PAO1: a tool for identifying differentially regulated genes. Genome Res **15:**583-589.
160. **Holm L, Rosenstrom P.** 2010. Dali server: conservation mapping in 3D. Nucleic Acids Res **38:**W545-549.
161. **Hasegawa H, Holm L.** 2009. Advances and pitfalls of protein structural alignment. Curr Opin Struct Biol **19:**341-348.
162. **Lunelli M, Lokareddy RK, Zychlinsky A, Kolbe M.** 2009. IpaB-IpgC interaction defines binding motif for type III secretion translocator. Proc Natl Acad Sci U S A **106:**9661-9666.
163. **Lapouge K, Smith SJ, Walker PA, Gamblin SJ, Smerdon SJ, Rittinger K.** 2000. Structure of the TPR domain of p67phox in complex with Rac.GTP. Mol Cell **6:**899-907.
164. **Dasgupta N, Ramphal R.** 2001. Interaction of the antiactivator FleN with the transcriptional activator FleQ regulates flagellar number in *Pseudomonas aeruginosa*. J Bacteriol **183:**6636-6644.

165. **Ensminger AW, Yassin Y, Miron A, Isberg RR.** 2012. Experimental evolution of *Legionella pneumophila* in mouse macrophages leads to strains with altered determinants of environmental survival. PLoS Pathog **8:**e1002731.
166. **Bansal PK, Nourse A, Abdulle R, Kitagawa K.** 2009. Sgt1 dimerization is required for yeast kinetochore assembly. J Biol Chem **284:**3586-3592.
167. **Krachler AM, Sharma A, Kleanthous C.** 2010. Self-association of TPR domains: Lessons learned from a designed, consensus-based TPR oligomer. Proteins **78:**2131-2143.
168. **Watson AA, Mattick JS, Alm RA.** 1996. Functional expression of heterologous type 4 fimbriae in *Pseudomonas aeruginosa*. Gene **175:**143-150.
169. **Asikyan ML, Kus JV, Burrows LL.** 2008. Novel proteins that modulate type IV pilus retraction dynamics in *Pseudomonas aeruginosa*. J Bacteriol **190:**7022-7034.
170. **Adams PD, Afonine PV, Bunkoczi G, Chen VB, Davis IW, Echols N, Headd JJ, Hung LW, Kapral GJ, Grosse-Kunstleve RW, McCoy AJ, Moriarty NW, Oeffner R, Read RJ, Richardson DC, Richardson JS, Terwilliger TC, Zwart PH.** 2010. PHENIX: a comprehensive Python-based system for macromolecular structure solution. Acta Crystallogr D Biol Crystallogr **66:**213-221.
171. **Chen VB, Arendall WB, 3rd, Headd JJ, Keedy DA, Immormino RM, Kapral GJ, Murray LW, Richardson JS, Richardson DC.** 2010. MolProbity: all-atom structure validation for macromolecular crystallography. Acta Crystallogr D Biol Crystallogr **66:**12-21.
172. **Chang YW, Rettberg LA, Treuner-Lange A, Iwasa J, Sogaard-Andersen L, Jensen GJ.** 2016. Architecture of the type IVa pilus machine. Science **351:**aad2001.
173. **Buensuceso RN, Nguyen Y, Zhang K, Daniel-Ivad M, Sugiman-Marangos SN, Fleetwood AD, Zhulin IB, Junop MS, Howell PL, Burrows LL.** 2016. The Conserved Tetratricopeptide Repeat-Containing C-Terminal Domain of *Pseudomonas aeruginosa* FimV Is Required for Its Cyclic AMP-Dependent and -Independent Functions. J Bacteriol **198:**2263-2274.
174. **Siewering K, Jain S, Friedrich C, Webber-Birungi MT, Semchonok DA, Binzen I, Wagner A, Huntley S, Kahnt J, Klingl A, Boekema EJ, Sogaard-Andersen L, van der Does C.** 2014. Peptidoglycan-binding protein TsaP functions in surface assembly of type IV pili. Proc Natl Acad Sci U S A **111:**E953-961.
175. **Fuchs EL, Brutinel ED, Jones AK, Fulcher NB, Urbanowski ML, Yahr TL, Wolfgang MC.** 2010. The *Pseudomonas aeruginosa* Vfr regulator controls global virulence factor expression through cyclic

AMP-dependent and -independent mechanisms. J Bacteriol **192:**3553-3564.

176. **Boyd JM.** 2000. Localization of the histidine kinase PilS to the poles of *Pseudomonas aeruginosa* and identification of a localization domain. Mol Microbiol **36:**153-162.
177. **Boyd JM, Koga T, Lory S.** 1994. Identification and characterization of PilS, an essential regulator of pilin expression in *Pseudomonas aeruginosa*. Mol Gen Genet **243:**565-574.
178. **Cowles KN, Moser TS, Siryaporn A, Nyakudarika N, Dixon W, Turner JJ, Gitai Z.** 2013. The putative Poc complex controls two distinct *Pseudomonas aeruginosa* polar motility mechanisms. Mol Microbiol **90:**923-938.
179. **Schuhmacher JS, Rossmann F, Dempwolff F, Knauer C, Altegoer F, Steinchen W, Dorrich AK, Klingl A, Stephan M, Linne U, Thormann KM, Bange G.** 2015. MinD-like ATPase FlhG effects location and number of bacterial flagella during C-ring assembly. Proc Natl Acad Sci U S A **112:**3092-3097.
180. **Kusumoto A, Shinohara A, Terashima H, Kojima S, Yakushi T, Homma M.** 2008. Collaboration of FlhF and FlhG to regulate polar-flagella number and localization in *Vibrio alginolyticus*. Microbiology **154:**1390-1399.
181. **Simon V, Schumann W.** 1987. In vivo formation of gene fusions in *Pseudomonas putida* and construction of versatile broad-host-range vectors for direct subcloning of Mu d1 and Mu d2 fusions. Appl Environ Microbiol **53:**1649-1654.
182. **Kaiser D.** 2000. Bacterial motility: how do pili pull? Current biology : CB **10:**R777-780.
183. **Kurre R, Hone A, Clausen M, Meel C, Maier B.** 2012. PilT2 enhances the speed of gonococcal type IV pilus retraction and of twitching motility. Mol Microbiol **86:**857-865.
184. **Turner LR, Lara JC, Nunn DN, Lory S.** 1993. Mutations in the consensus ATP-binding sites of XcpR and PilB eliminate extracellular protein secretion and pilus biogenesis in *Pseudomonas aeruginosa*. J Bacteriol **175:**4962-4969.
185. **Park HS, Wolfgang M, Koomey M.** 2002. Modification of type IV pilus-associated epithelial cell adherence and multicellular behavior by the PilU protein of *Neisseria gonorrhoeae*. Infect Immun **70:**3891-3903.
186. **Wolfgang M, Park HS, Hayes SF, van Putten JP, Koomey M.** 1998. Suppression of an absolute defect in type IV pilus biogenesis by loss-of-function mutations in *pilT*, a twitching motility gene in *Neisseria gonorrhoeae*. Proc Natl Acad Sci U S A **95:**14973-14978.
187. **Beatson SA, Whitchurch CB, Sargent JL, Levesque RC, Mattick JS.** 2002. Differential regulation of twitching motility and elastase

production by Vfr in *Pseudomonas aeruginosa*. J Bacteriol **184:**3605-3613.

188. **Albus AM, Pesci EC, Runyen-Janecky LJ, West SE, Iglewski BH.** 1997. Vfr controls quorum sensing in *Pseudomonas aeruginosa*. J Bacteriol **179:**3928-3935.
189. **Winsor GL, Lam DK, Fleming L, Lo R, Whiteside MD, Yu NY, Hancock RE, Brinkman FS.** 2011. *Pseudomonas* Genome Database: improved comparative analysis and population genomics capability for *Pseudomonas* genomes. Nucleic Acids Res **39:**D596-600.
190. **Riepl H, Maurer T, Kalbitzer HR, Meier VM, Haslbeck M, Schmitt R, Scharf B.** 2008. Interaction of CheY2 and CheY2-P with the cognate CheA kinase in the chemosensory-signalling chain of *Sinorhizobium meliloti*. Mol Microbiol **69:**1373-1384.
191. **Kazmierczak BI, Lebron MB, Murray TS.** 2006. Analysis of FimX, a phosphodiesterase that governs twitching motility in *Pseudomonas aeruginosa*. Mol Microbiol **60:**1026-1043.
192. **Kelley LA, Sternberg MJ.** 2009. Protein structure prediction on the Web: a case study using the Phyre server. Nat Protoc **4:**363-371.
193. **Okkotsu Y, Tieku P, Fitzsimmons LF, Churchill ME, Schurr MJ.** 2013. *Pseudomonas aeruginosa* AlgR phosphorylation modulates rhamnolipid production and motility. J Bacteriol **195:**5499-5515.
194. **Lupas A, Stock J.** 1989. Phosphorylation of an N-terminal regulatory domain activates the CheB methylesterase in bacterial chemotaxis. J Biol Chem **264:**17337-17342.
195. **Sourjik V, Berg HC.** 2000. Localization of components of the chemotaxis machinery of *Escherichia coli* using fluorescent protein fusions. Mol Microbiol **37:**740-751.
196. **Ayers M, Howell PL, Burrows LL.** 2010. Architecture of the type II secretion and type IV pilus machineries. Future Microbiol **5:**1203-1218.
197. **Giltner CL, Habash M, Burrows LL.** 2010. *Pseudomonas aeruginosa* minor pilins are incorporated into type IV pili. J Mol Biol **398:**444-461.
198. **Bulyha I, Lindow S, Lin L, Bolte K, Wuichet K, Kahnt J, van der Does C, Thanbichler M, Sogaard-Andersen L.** 2013. Two small GTPases act in concert with the bactofilin cytoskeleton to regulate dynamic bacterial cell polarity. Dev Cell **25:**119-131.
199. **Hoang TT, Karkhoff-Schweizer RR, Kutchma AJ, Schweizer HP.** 1998. A broad-host-range Flp-FRT recombination system for site-specific excision of chromosomally-located DNA sequences: application for isolation of unmarked Pseudomonas aeruginosa mutants. Gene **212:**77-86.

200. **Wu WL, Liao JH, Lin GH, Lin MH, Chang YC, Liang SY, Yang FL, Khoo KH, Wu SH.** 2013. Phosphoproteomic analysis reveals the effects of PilF phosphorylation on type IV pilus and biofilm formation in *Thermus thermophilus* HB27. Mol Cell Proteomics **12:**2701-2713.
201. **Ewens CA, Kloppsteck P, Forster A, Zhang X, Freemont PS.** 2010. Structural and functional implications of phosphorylation and acetylation in the regulation of the AAA+ protein p97. Biochem Cell Biol **88:**41-48.